Jan Kuckenberg

Early detection and discrimination of biotic and abiotic stresses in *Triticum aestivum* and *Malus domestica* by means of chlorophyll fluorescence

Institut für Nutzpflanzenwissenschaften und Ressourcenschutz (INRES)

Bereich Pflanzen- und Gartenbauwissenschaften

Early detection and discrimination of biotic and abiotic stresses in *Triticum aestivum* and *Malus domestica* by means of chlorophyll fluorescence

Inaugural-Dissertation

zur

Erlangung des Grades

Doktor der Agrarwissenschaften

(Dr.agr.)

der

Hohen Landwirtschaftlichen Fakultät

der

Rheinischen Friedrich-Wilhelms-Universität

zu Bonn

vorgelegt am 16.01.2008

von

Dipl.-Ing. agr. Jan Kuckenberg

aus

Leverkusen

Referent: Prof. Dr. G. Noga

Korreferent: PD Dr. E.-C. Oerke

Tag der mündlichen Prüfung: 07.04.2008

„Diese Dissertation ist auf dem Hochschulschriftenserver der ULB Bonn

http://hss.ulb.uni-bonn.de/diss_online elektronisch publiziert."

2008

Early detection and discrimination of biotic and abiotic stresses in *Triticum aestivum* and *Malus domestica* by means of chlorophyll fluorescence

The key objective of this work was to assess the potential of selected chlorophyll fluorescence techniques for detection of temporal and spatial changes in leaf and plant response to economically important stress factors as a basis for implementing these techniques in 'Precision Farming'. Early detection and visualisation of fluorescence patterns upon infection with leaf rust (*Puccinia triticina*) and powdery mildew (*Blumeria graminis*) was studied at the single leaf level on wheat (*Triticum aestivum* L.) by means of Pulse-Amplitude-Modulated (PAM) fluorescence imaging. The necessity of previous dark-adaptation of plant material for reliable stress detection was investigated. The approach of 'multipoint' scanning Laser-Induced Fluorescence (LIF) was applied for detection and discrimination of biotic (leaf rust and powdery mildew*)* and abiotic (nitrogen deficiency) stress factors in the light at wheat leaf and canopy level. In order to avoid misinterpretation of fluorescence signals in 'Precision Farming', the effect of enhanced UV-B radiation on LIF and PAM parameters was studied in detail in apple (*Malus domestica* Borkh.) leaves. An additional objective of this thesis was to investigate the capability of LIF and light-remission techniques for detecting senescence-induced heterogeneities in apple (cvs 'Jonagold' and 'Golden Delicious') peel chlorophyll content and internal fruit quality characteristics under shelf life conditions.

1. PAM fluorescence imaging enabled pre-symptomal pathogen detection and visualisation of spatial differences during proceeding *Blumeria graminis* and *Puccinia triticina* infections at the individual wheat leaf level. The initial infection of both fungi caused an increase in ground fluorescence (Fo) and a decrease in photochemical efficiency (Fv/Fo, Fv/Fm). Among the evaluated fluorescence parameters, Fv/Fo displayed the most pronounced response to both kinds of infection. However, the detection of pathogen infection appeared less effective if fluorescence images were taken on leaves without previous dark adaptation.

2. The 'multipoint' scanning LIF technique revealed spatial differences in fluorescence values at leaf and canopy level. The results of cross-validation analysis indicated that with this approach, samples with pathogen infections may be miss-recognised as N-deficiency and vice versa. However, considering standard deviations of F690 and F730 recordings in addition to their mean values significantly improved the identification accuracy of N-deficiency and leaf rust infection at both leaf and canopy level.

3. Short-term UV-B stress affected neither chlorophyll content nor Red/NIR-light reflection of apple leaves, but could be well detected by PAM and LIF technique. Significantly reduced fluorescence intensities and F686/F740 fluorescence ratio as well as a high spatial heterogeneity of photosynthetic performance after UV-B stress have to be taken into account for applying these techniques in 'Precision Farming'. However, the disturbance in photosynthetic functionality was followed by a continuous recovery process as indicated by restoring fluorescence parameters. The rate of recovery was dependent on UV-B dose.

4. Changes in ground colour of apple fruit could be successfully monitored by LIF and light-remission techniques, whereas among the investigated parameters Normalised-Differenced-Vegetation-Index (NDVI) and fluorescence emission at 730nm showed the strongest correlation with peel chlorophyll content. The 'multipoint' fluorescence scanning mode of LIF technique provided also detailed information on fruit colour heterogeneities. The correlation degree between remission and fluorescence parameters with internal fruit parameters and maturity could be significantly improved by taking into respect differences in pigment content and flesh characteristics on the sunlit and shaded apple sides.

Früherkennung und Unterscheidung biotischen und abiotischen Stresses bei *Triticum aestivum* and *Malus domestica* mittels Chlorophyllfluoreszenz-basierender Verfahren

Zielsetzung dieser Arbeit war es, das Potenzial ausgewählter Chlorophyllfluoreszenz-basierender Verfahren zur Erkennung der zeitlichen und räumlichen Dynamik von Blatt- und Pflanzenreaktionen auf ökonomisch relevante Stressfaktoren zu ermitteln und somit eine Grundlage für den Einsatz dieser Techniken im Präzisionspflanzenbau zu schaffen. Die frühe Phase des Infektionsverlaufes von Braunrost (*Puccinia triticina*) und Echtem Mehltau (*Blumeria graminis*) wurde mittels bildgebender Puls-Amplituden-Modulierter (PAM) Fluoreszenz an Weizenblättern (*Triticum aestivum* L.) visualisiert und untersucht. Gleichzeitig wurde die Notwendigkeit der Vorverdunkelung des Pflanzenmaterials für eine zuverlässige Stresserkennung ermittelt. Der Ansatz der 'multipoint' scannenden Laser-Induzierten Fluoreszenz (LIF) wurde unter Lichtbedingungen zur Erkennung und Unterscheidung biotischer (Braunrost und Echter Mehltau) und abiotischer (Stickstoffmangel) Stressfaktoren auf Blatt- und Bestandesebene an Weizen getestet. Zur Vermeidung von Fehlinterpretationen von Fluoreszenzsignalen im Präzisionspflanzenbau wurde der Einfluss erhöhter UV-B Strahlung auf LIF- und PAM-Parameter an Apfelsämlingen (*Malus domestica* Borkh.) eingehend untersucht. Eine weitere Fragestellung dieser Arbeit war es, das Potenzial von LIF- und Remissions-Techniken zur Erkennung Seneszenz-induzierter Heterogenitäten im Chlorophyllgehalt der Apfelschale (cvs 'Jonagold' und 'Golden Delicious') und innerer Fruchtqualitätsmerkmale unter 'shelf life' Bedingungen zu bestimmen.

1. Die bildgebende PAM Fluoreszenz ermöglichte eine prä-symptomale Pathogenerkennung und Visualisierung von räumlichen Unterschieden während des Infektionsverlaufes von *Blumeria graminis* und *Puccinia triticina* auf der Ebene einzelner Weizenblätter. Beide Pilze verursachten zu Beginn der Infektion einen Anstieg der Grundfluoreszenz (Fo) und eine Verringerung der photochemischen Effizienz (Fv/Fo, Fv/Fm). Unter allen erhobenen Fluoreszenzparametern zeigte Fv/Fo die stärkste Reaktion auf vorgenannte pilzliche Erreger. Fluoreszenzaufnahmen ohne Vorverdunklung erschwerten eine gesicherte Erkennung des Pathogenbefalls.

2. Die 'multipoint' scannende LIF Technik ermöglichte eine Visualisierung räumlicher Unterschiede der Fluoreszenzsignale auf Blatt- und Bestandesebene. Die Kreuzvalidierung der Messwerte ergab, dass anhand dieses Verfahrens eine eindeutige Unterscheidung zwischen Pathogeninfektionen und N-Mangel nicht gewährleistet werden kann. Allerdings führte die zusätzlich zu den Mittelwerten vorgenommene Berücksichtigung der Standardabweichung bei F690 und F730 sowohl auf Blatt- als auch auf Bestandesebene zu einer signifikanten Verbesserung der Identifikationsgenauigkeit von N-Mangel und Braunrost.

3. Kurzzeitiger UV-B Stress beeinflusste weder den Chlorophyllgehalt noch die rote/nahe-infrarote Lichtreflexion von Apfelblättern, konnte jedoch sehr gut mit PAM- und LIF-Techniken erfasst werden. Signifikant reduzierte Fluoreszenzintensitäten und F686/F740 Fluoreszenzverhältnisse sowie eine hohe räumliche Heterogenität der photosynthetischen Effizienz nach einem UV-B Stress sind bei einem Einsatz dieser Techniken im Präzisionspflanzenbau unbedingt zu berücksichtigen. Auf die Störung in der photosynthetischen Funktionalität folgte ein kontinuierlicher Regenerationsprozess, der sich in einer Rückstellung der Fluoreszenzparameter niederschlug. Die Regenerationsrate war dabei abhängig von der UV-B Dosis.

4. Veränderungen in der Grundfarbe von Äpfeln wurden erfolgreich mittels LIF- und Remissions- Techniken ermittelt, wobei unter den erhobenen Parametern der Normalised-Differenced-Vegetation-Index (NDVI) und die Fluoreszenzemission bei 730 nm die stärkste Korrelation mit dem Chlorophyllgehalt in der Apfelschale lieferten. Der scannende 'multipoint' Fluoreszenzmodus der LIF Technik ermöglichte eine detaillierte Erfassung von Heterogenitäten in der Fruchtfarbe. Die Korrelation von Remissions- und Fluoreszenzparametern mit internen Frucht- und Reifemerkmalen konnte unter Berücksichtigung von Unterschieden im Pigmentgehalt und der Fruchtfleischeigenschaften von Sonnen- und Schattenseiten signifikant verbessert werden.

Table of Contents

List of abbreviations

Abs	absorption
AL	actinic light
AOI	area of interest
ATP	adenosine triphosphate
BP	band pass
C_a	chlorophyll a
C_b	chlorophyll b
CCD	charge-coupled device
cm	centimetre
CO_2	carbon dioxide
cv.	cultivar
dai	day after inoculation
DMSO	dimethyl sulfoxide
Fe^{2+}	ferrous (II)
FF	fruit firmness
Fig.	figure
Fm	maximum fluorescence
Fo	ground fluorescence
F690	fluorescence emission at 690 nanometres
F730	fluorescence emission at 730 nanometres
Fv	variable fluorescence
Fv/Fm	maximal photochemical efficiency
Fv/Fo	maximal photochemical efficiency over Fo
FWHM	full width at half maximum
g	gram
GPS	global positioning system
°C	grade Celsius
ha	hectare
HSD	honestly significant difference
kHz	kilo hertz
kJ	kilo joule
l	litre
LIF	laser-induced fluorescence
LP	long pass
M	mol
m	metre
mg	milligram
min	minutes
ML	measuring light
ml	millilitre
mm	millimetre
Mn	manganese
ms	milliseconds

µg	microgram
µl	microlitre
µmol	micromole
N	nitrogen *or* newton
NAI	normalised anthocyanin index
NaOH	sodium hydroxide
NDVI	normalised-differenced-vegetation index
NIR	near-infra-red
Nm	nanometre
nmol	nanomole
P	probability of error
PAM	pulse-amplitude-modulated
PAR	photosynthetic active radiation
%	per cent
Φ_{II}	photochemical efficiency of photosystem II
PS I	photosystem I
PS II	photosystem II
PQ	plastoquinone
Q_A	primary quinone acceptor
Q_B	secondary quinone acceptor
R	remission
r	Pearson`s correlation coefficient
R^2	coefficient of determination
rel. units	relative units
rh.	relative humidity
s	second
S. tritici	S*eptoria tritici*
SB	starch breakdown
SD	standard deviation
SE	standard error
SI	Streif index
SP	saturation pulse
SS	soluble solids
t	temperature
TA	titratable acid
Tab.	table
Tyr	tyrosine
Uv	ultraviolet
UV-B_{BE}	biological effective uv-b dose
V	volume
VIS	visible
W	Watt

A Introduction

1 Overview

Agricultural crops can be affected by a lot of biotic (e.g. fungi, insects, nematodes, weed) and abiotic (e.g. UV-B light, nutrient deficiency, drought) stresses during growth, being responsible for important economic yield losses. The common reaction of farmers after detecting stress symptoms in crop canopies is to apply inputs, such as fertilisers, pesticides and fungicides uniformly over the fields despite of great heterogeneities in soil type, weed distribution, crop density, nitrogen availability and disease pressure (West et al., 2003). However, such management practises deploit production means and exert a negative effect on the environment.

The consideration of this in-field variability is the main idea of 'Precision Agriculture'. The concept is based on a site-specific application of agrochemicals and fertilisers at an appropriate dose and only when and where needed, resulting in significant product as well as economical savings. Since many years farmers try to consider heterogeneities within their fields; with the development of new technologies, such as high-sensitive sensors, global positioning system (GPS), variable rate spraying and a fast data processing, an effective site-specific and automatic field management became possible (West et al., 2003).

Tractor-mounted online-systems enabling the detection of the target (e.g. weeds, chlorophyll, diseases) at high spatial and temporal resolution, processing the data and triggering an action (e.g. spraying, hoeing, and fertilisation) in one operation are preferred to suit this purpose. However, this requires sensors delivering reliable and precise information about the kind and degree of stress and allowing differentiation of multiple stresses which often occur simultaneously under field conditions. The integration of decision support systems and information collected by the farmer may enhance the accuracy of such a management technique (Fig. 1; West et al., 2003). In the last few years, great advances have been made particularly in the field of site-specific herbicide application (Sökefeld et al., 2007) and nitrogen fertilisation (Schächtl et al., 2005; Limbrunner and Maidl, 2007), whereas first commercial systems are available now.

However, only a few reports can be found on specific sensors for plant disease detection in the field (Bodria et al., 2002), despite of the fact that these crop disorders usually occur very patchy and could be managed site-specifically. Since pesticides are one of the most cost intensive components in crop production and are major contributors to groundwater and food contamination, the pressure to reduce their

application steadily increases. Unfortunately, until now the only practicable attempt for a site-specific fungicide application is based on the determination of the wettable leaf area (pendulum sensor) and the adaptation of the application rate (Dammer et al., 2001).

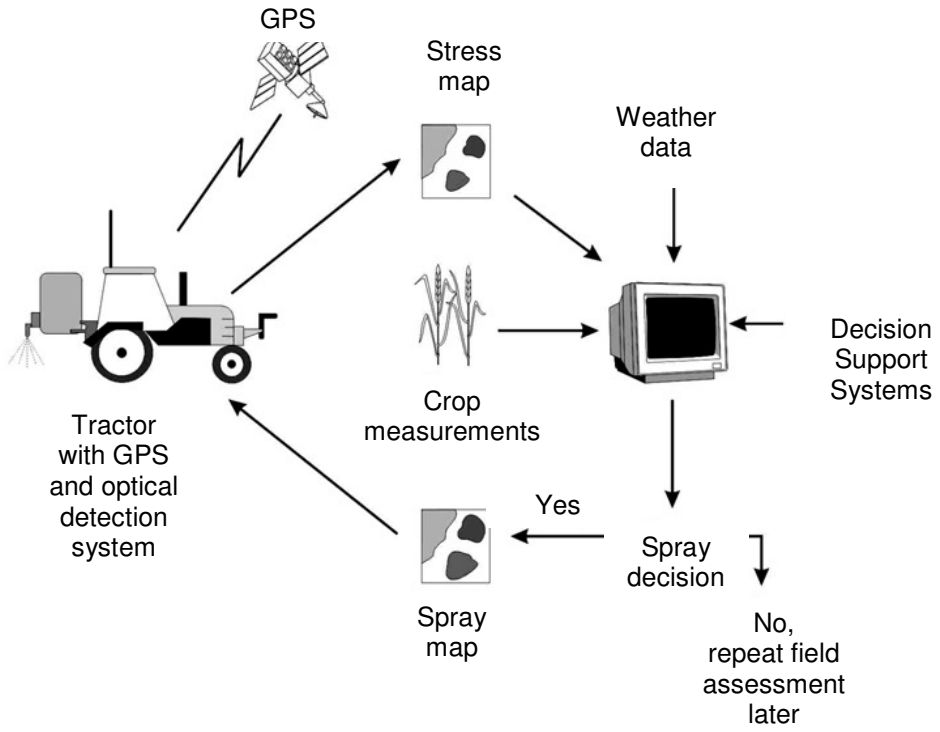

Fig. 1: Possible information flow for a site-specific crop management (modified after West et al., 2003)

Indeed, reflectance based systems, which rely on making measurements simultaneously in one or more wavebands, have shown a high potential for disease detection in the field; a disadvantage of this approach is the relatively late recognition of infection potential (Lorenzen and Jensen, 1989; Nicolas, 2004; Franke et al., 2005). Since the first plant responses to different types of pathogen stress are changes in leaf photosynthetic rate or electron transport chain (Lichtenthaler and Rinderle, 1988), chlorophyll fluorescence technique has a higher potential to recognise pre-symptomal fungal infections (Scholes and Rolfe, 1996; Bassanezi et al., 2002; Bodria et al., 2002; Tartachnyk et al., 2006). However, fluorescence is an unspecific reaction to various stress factors and discrimination between different kinds of stress may be difficult to accomplish. Nevertheless, more detailed information on temporal and spatial changes in leaf response to stress factors may help to overcome this problem.

Thus, in this thesis, different fluorescence techniques providing a fast data acquisition and a high spatial resolution were applied on wheat (*Triticum aestivum* L.) and apple (*Malus domestica* Borkh.) in order to visualise spatial differences in fluorescence signals upon stress events. The influence of important economic pathogens (*Blumeria graminis*, *Puccinia triticina*), N-deficiency and UV-B light as representatives for biotic and abiotic stress factors on host plant photosynthesis was investigated in detail.

2 Chlorophyll fluorescence

Chlorophyll fluorescence is a very useful tool to study the impact of stresses on plants at an early stage, when no symptoms are visible. This non-invasive technique delivers fast and extensive information about the potential and current efficiency of photosynthesis, the integrity of the photosynthetic apparatus, the relative functionality of different physiological protective mechanisms and the rate of photosynthetic electron transfer (for reviews see e.g. Maxwell and Johnson, 2000; Baker and Rosenqvist, 2004). In this introduction only a very short overview about fluorescence can be given, due to the very complex underlying theory.

Antenna molecules (e.g. chlorophylls and carotenoids) of photosynthetic apparatus are the primary initiators of energy transduction in the process of photosynthesis, while absorbing light and transforming it into photochemical energy. Under normal conditions the main part of captured photons (> 80%) is used in photosynthetic light reaction and the associated electron transport to build-up ATP and NADPH. These substances are essential for further CO_2 assimilation in the Calvin cycle (Lichtenthaler et al., 2005). However, during the process of energy transduction a small part of the absorbed light energy is dissipated as heat and red fluorescence light (1-2%, Maxwell and Johnson, 2000). The latter is of longer wavelength than the excitation energy and mainly emitted (> 90%) from photosystem II (PS II) (Gitelson et al., 1998). Since the three processes 1) photochemistry, 2) heat, and 3) fluorescence are in competition with each other, fluorescence is a very good indicator of all stresses affecting the pathway of photosynthetic energy conversation (Maxwell and Johnson, 2000).

In general, information about plant status can be obtained from temporal and spectral chlorophyll fluorescence measurements.

Kautsky and Hirsch (1931) reported already in the 30s of the previous century about the phenomenon of fluorescence after transferring a leaf from the dark into the light. Nearly 50 years later the first Pulse-Amplitude-Modulated (PAM) chlorophyll fluorometers were developed, which allowed an exact estimation of fluorescence and

the underlying processes also in the presence of background illumination (Quick and Horton, 1984). A typical PAM measurement curve is shown in Fig.2.

After dark adaptation of plant material for 15-20 minutes which opens all PS II reaction centres, different light sources are applied (Lichtenthaler et al., 2005).

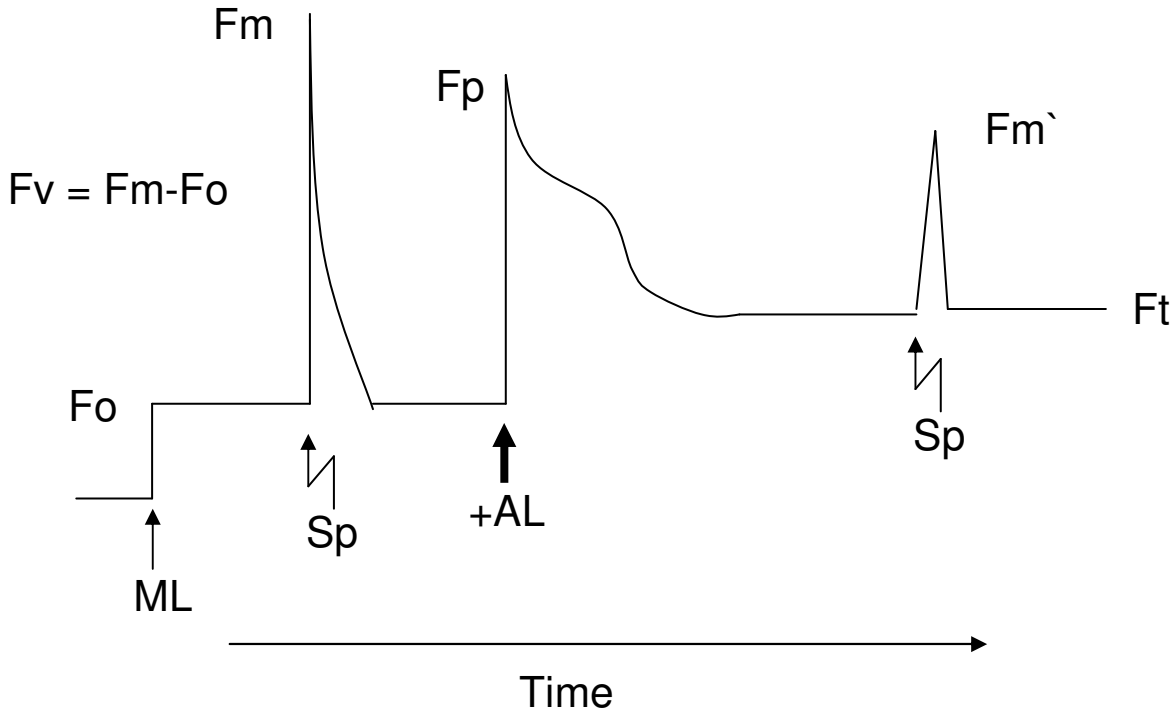

Fig. 2: Typical measurements of chlorophyll fluorescence by the PAM method. ML = weak modulated measuring light; SP = saturation light pulse; AL = continuous actinic light (modified from van Kooten and Snel, 1990)

First, a very weak measuring light (ML) is given to obtain ground fluorescence (Fo), originating exclusively from the light-harvesting complexes of PS II. A following saturation pulse (SP) induces a fast (100-200 ms) fluorescence rise from the ground state to a maximum value (Fm), whereas in this increase also the reaction centres of PS II are involved (Govindjee, 2004; Lichtenthaler et al., 2005). In this condition the first stable electron acceptor (Q_A) of PS II is fully reduced. The change in fluorescence emission between the two defined states is termed as variable fluorescence (Fv). From the measured parameters the maximal photochemical efficiency of PS II can now be calculated as Fv/Fm, which has been established as a widely used parameter in fluorescence research (Krause and Weis, 1991). Healthy leaves usually display Fv/Fm values in the range of 0.82±0.004, independent of plant species, whereas under stress conditions this parameter tends to decrease (Krause and Weis, 1991).

More detailed information about photosynthetic performance of leaves can be obtained by further determination of the different photochemical and non-photochemical quenching processes. Therefore, plants are illuminated by an actinic light (AL) source, which induces a fast (300-800 ms) and transient rise in fluorescence yield to a maximum level (Fp), which is lower than the Fm obtained after a saturation flash (Lichtenthaler et al., 2005). Within 1s, different quenching mechanisms are initiated, and the cooperation between the two photosystems is reactivated (Lichtenthaler et al., 2005). These processes result in a decrease of fluorescence yield (over a period of a few minutes) to a low steady state (Ft) (Maxwell and Johnson, 2000).

Besides photochemical quenching, which is related to the proportion of excitation energy trapped by open reaction centres, various ways of non-photochemical quenching (NPQ), not related to the Q_A re-oxidation, are involved in this decrease (Maxwell and Johnson, 2000). The application of additional saturation pulses in parallel to actinic illumination gives a measure of maximal fluorescence in the light (Fm´), which allows further discrimination of the different quenching processes.

However, determination of fluorescence quenching parameters takes about 15-20 minutes, being not applicable for 'Precision Farming'. Parameters of fast fluorescence kinetics (Fo, Fm), in contrast, may have a higher potential for this purpose because signal excitement and detection can be accomplished in split seconds. Recently developed PAM-imaging systems allow detection of whole leaf reactions to plant stress in spatial and temporal resolution (Chaerle and van der Straeten, 2000), providing a very interesting tool for visualisation of e.g. a patchy fungal infection.

At room temperature the chlorophyll fluorescence emission spectrum is characterised by two maxima in the red (685-690nm) and in the near-infra-red (730-740nm) region whereas for both the main source of fluorescence is the PS II (Buschmann, 2007). Only in the near-infra-red range, photosystem I (PS I) seems to contribute up to 50% to the ground fluorescence (Fo) and about 10% to the maximal fluorescence (Fm) (Pfündel, 1998). Indeed, the above described PAM technique delivers very useful information about the photosynthetic performance of leaves and plants in terms of different stress factors, but they do not provide reliable information about chlorophyll content (Buschmann, 2007).

Recently developed 'multipoint' scanning Laser-Induced Fluorescence (LIF) technique has shown to be a highly valuable tool to fill this lack of information (Limbrunner and Maidl, 2007). Thereby, a red laser beam is applied to plant tissue and fluorescence signals in the red (690 nm) and near-infra-red (730 nm) region of the emission spectrum are recorded separately (Fig. 3). Since green leaves display an

absorption maximum in the red wavelength range, the red fluorescence light (~ 685-690 nm) can be partially re-absorbed by chlorophyll in plant tissue (Rinderle and Lichtenthaler, 1988). In parallel, the near-infra-red fluorescence at ~ 730 nm passes the leaf nearly unabsorbed; this is independent of chlorophyll concentration.
Thus, the calculation of the red/near-infra-red fluorescence ratio (F690/F730) gives very detailed information about leaf and plant chlorophyll content (Fig. 3, Buschmann, 2007). Furthermore, this parameter can be used as an indicator of plant nitrogen supply (Limbrunner and Maidl, 2007), because this nutrient plays a major role in chlorophyll synthesis (Peltonen et al., 1995). Due to the 'multipoint' scanning mode of this technique a high spatial resolution during measurement can be obtained.

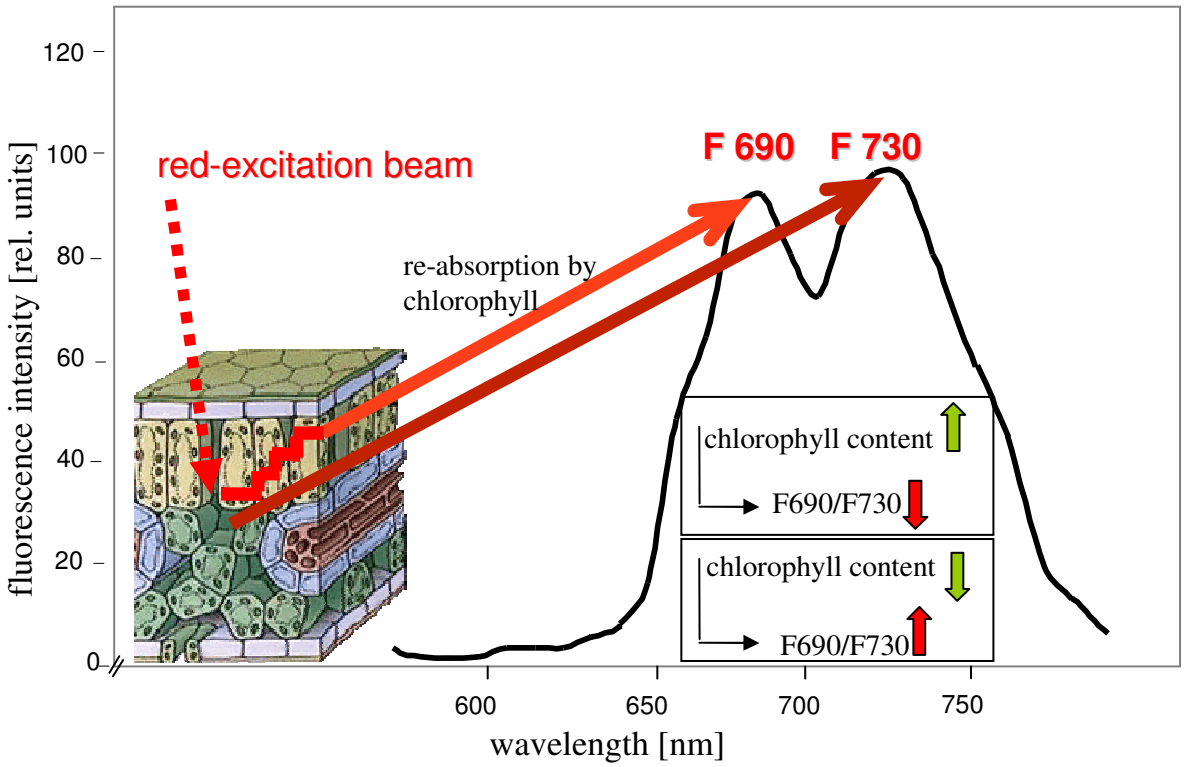

Fig. 3: Emission of LIF with a scheme showing the re-absorption effect of red fluorescence light (F690) by chlorophyll pigments on F690/F730 ratio.

3 Stress factors

3.1 Nitrogen (N)

Nitrogen has an outstanding importance among all nutrients, because it is the most crucial factor for crop yields. It is a main component of e.g. cell walls, enzymes, proteins, proteids, chlorophyll and phytohormones and therefore belongs to the basic elements of plant life (Amberger, 1996). Crops growing under reduced N supply are

characterised first by a decreased photosynthesis rate (Harper, 1994) and later by chlorotic, yellow-green leaves, due to a degradation of chlorophyll in plant tissue. In cereals N-deficiency causes a reduction in many yield parameters such as e.g. leaf blade, tillering, shoot formation, growth, ears, grain weight and proteins (Shangguan et al., 2000; Lawlor et al., 2001).

Whereas a sufficient N supply is important for high yields, an excessive use of this fertiliser may result in densely packed and high grown crops, being susceptible to diseases and wind. Over-fertilisation increases the amount of 1) nitrate (NO_3^-) in the soil and ground water due to the high mobility of this element and 2) trace gases such as NO_x, N_2O and N_2, which contribute significantly to world global warming and acid rain (Amberger, 1996). In the last few years the amount of applied N fertiliser has continuously increased, and it is expected to be about 50% higher in the year 2050 (Tilman et al., 2002), whereas only 30 to 50% of the applied N is used by the agricultural crop directly (Raun and Johnson, 1999). Thus, a site-specific N application reduces significantly the amount of applied fertiliser, improving the economic and ecological situation.

3.2 Plant pathogens

Powdery mildew (*Blumeria graminis*) and leaf rust (*Puccinia triticina*) are two of the most important foliar pathogens in cereal crops worldwide. Due to a deflection of carbohydrate transport, both fungi cause a decrease in photosynthetic activity in infected leaves by reducing green leaf area (Shtienberg, 1992; Scholes and Rolfe, 1996; Percival and Fraser, 2002; Robert et al., 2005). However, the exact site of infection-induced inhibition of photosynthetic apparatus is uncertain, but photoinhibition of PS II or impairment of the photosynthetic electron transport, affecting both the acceptor and donor side of PS II, has been suggested (Magyarosy et al., 1976; Magyarosy and Malkin, 1978; Percival and Fraser, 2002).

In order to develop a fluorescence-based detection and identification system and to provide an effective pest-management, a detailed understanding of pathogens life-cycle is necessary.

3.2.1 Powdery mildew

Wheat powdery mildew belongs to the Ascomycotina and is caused by the fungus *Blumeria* (syn. *Erysiphe*) *graminis* f. sp. *tritici*. Like all obligate biotrophic pathogens it requires living plant tissue for its life cycle. The wind dispersed spores can actually

infect all green parts of the host plant, whereas they are most prevalent on the adaxial leaf sides (Yang and Ellingboe, 1972). Under optimal environmental conditions (Tab. 1) already 0.5-2.0 h after inoculation a primary germ tube develops from the mildew conidia. This produces a short penetration peg that enters the host surface where it causes first local cell responses (Carver et al., 1996). A second germ tube emerges 3.0-3.5 h later, which induces the development of an appressorial lobe (Carver et al., 1996), enabling the fungi to penetrate the host cuticle and cell wall directly. After succeeded penetration (12-15 h after inoculation) first haustoria appear in the infected cells. These feeding structures export nutrients to the surface where main hyphal growth takes place (Carver et al., 1996).

During the next days further haustoria emerge for a sufficient feeding of the new colonies. Within a week conidiophores produce a new generation of conidia, completing the asexual life cycle of the fungi (Carver et al., 1996).

Tab. 1: Environmental parameters for the optimal development of powdery mildew structures in wheat*.

	temperature (°C)		relative humidity (%)
	optimum	threshold	
conidia germination	5 – 20	0 – 30	no
infection	20 – 25	0 – 30	> 95%
pustule growth	15 – 20	4 – 31	no
sporulation	15 – 20	– 30	> 95%
total development	15 – 20		

* Adapted from Kluge et al., 1999.

First visual symptoms can be usually observed 3 to 5 days after inoculation (Kluge et al., 1999) as typical whitish mycelium patches of irregular size and shape at the infected leaf surface. At the late stages of pathogen development often the whole leaf is covered by these mycelium structures.

At the end of the vegetation period sexual fruiting bodies (cleistothecia) with ascospores inside occur at the senescent wheat leaves, which are the primary inoculum for the new winter wheat seed. During the winter the fungus survives in form of mycelium at the abaxial leaf sheaths or as conidia (Börner, 1997; Kluge et al., 1999).

3.2.2 Leaf rust

Wheat leaf rust (*Puccinia triticina*) belongs to the Basidiomycotina and is also a biotrophic pathogen. After germination of the urediospores at the leaf surface a germ tube enters the plant tissue through the stomata openings and develops a complex system of infection structures within the leaf composed of appressoria, substomatal vesicles, primary infection hyphae and haustorial mother cells (Zhang and Dickinson, 2001). Thereafter the fungus penetrates the mesophyll cells, forms haustoria and takes up nutrients from the plant cells for the fungal feeding (Zhang and Dickinson, 2001). Within 7-14 days after infection uredia with urediaspores mature, rupture the epidermis and build the typical reddish-brownish pustules at the leaf surface. Each wind dispersed spore can now initiate a new infection. The incubation period is about 6-8 days depending strongly on the environmental conditions (Tab. 2, Kluge et al., 1999).

Tab. 2: Environmental parameters for the optimal development of leaf rust structures in wheat*.

	temperature (°C)		relative humidity (%)
	optimum	threshold	
urediospores germ.	15 – 21	2 – 32	
infection	15 – 18	4 – 25	100% for > 4h
mycelium growth	20 – 26	2 – 35	
sporulation			
total development	15 – 25		

* Adapted from Kluge et al., 1999.

At the end of vegetation period teliospores appear at the abaxial leaf sides indicating the beginning of the sexual life cycle of *Puccinia triticina*. In spring these teliospores produce basidia and basidiospores which are reliant on the alternate host *Thalictrum flavum* (*Ranunculaceae*).

After recombination of genetic information, a new spore type, the aecidiospores can infect the wheat host plants again. Although the alternate host is thought to provide only a little direct inoculum at the early vegetation period, it may play a major role in the evaluation of new races (Samborski, 1985). The prime sources of inoculum each

year could be referred to the mycelium surviving on volunteer wheat or winter wheat and/or wind-dispersed spores (Börner, 1997).

3.3 UV-B

In the last few years a continuous reduction of the stratospheric ozone layer (Stolarski et al., 1992) and enhanced UV-B radiation (Herman et al., 1996) reaching the earth surface has been reported. Generally, ultraviolet radiation is divided into three spectral ranges; the UV-A (320-400 nm), UV-B (280-320 nm) and UV-C (200-280 nm), whereas the UV-B seemed to be most affected by a depletion of the ozone layer (Krupa et al., 1998; Tevini, 2004). Reviewing the recent literature elevated UV-B levels have shown a lot of negative impacts on plant organs (Tab. 3).

Tab. 3: Effects of enhanced UV-B on plant characteristics*.

plant characteristic	effect
photosynthesis	reduced at low light intensities
leaf conductance	reduced at low light intensities
water use efficiency	reduced in most species
leaf area	reduced in many species
specific leaf weight	increased in many species
reproductive development	reduced
flowering	inhibited or stimulated
dry matter and yield	reduced in many species

* Table based on: Runeckles and Krupa, 1994; Gao et al., 2004; Koti et al., 2004.

At cellular level, damages can occur directly e.g. on proteins, photosynthetic pigments, quinones and unsaturated fatty acids by absorption of high energy UV-B or indirectly by reactive oxygen species, appearing during their destruction (Tevini, 2004).
Multiple sites of UV-B inhibition in photosynthesis have been detected. However chloroplasts and PSII seem to be the most vulnerable targets (Bornman, 1989; Vass, 1997), enabling chlorophyll fluorescence as a highly sensitive tool for its detection.

4 Further applications of non-invasive sensor technology

Non-invasive sensor technologies are not only of interest in cereal crops. Modern quality management and safety practices in e.g. apple fruit marketing require strict

documentation and traceability of fruit data in whole supply chains from the production to the consumer site (Kramer, 2005). Moreover, growers may be only successful on the national and international food markets if they can offer constant high quality products. However, in this aspect there are still enormous problems with inconsistencies. Indeed, fruit sorting lines provide a classification in size, weight and blush colour, a determination of internal quality parameters of each fruit is not possible with the present procedures.

Currently, mainly destructive methods estimating fruit firmness, starch breakdown, content of soluble solids and titratable acids in fruit flesh (Streif, 1996) are applied to receive information about the fruit status. However, these methods are labour and time consuming and since different fruit are characterised by a high variability, the accuracy is limited.

Thus, non-destructive sensing technologies for a fast prediction of fruit maturity, quality and storability are highly appreciated, whereas chlorophyll fluorescence seems to have a high potential to close this lack of information in a fast and non-destructive way (Song et al., 1997; Noh and Lu, 2005).

5 Objective of this study

Recent studies on chlorophyll fluorescence have shown that this technique delivers early and fast information on plant/fruit health status, stress effects and quality parameters (for reviews see e.g. De Ell et al., 1999; Maxwell and Johnson, 2000; Baker and Rosenqvist, 2004). However, since chlorophyll fluorescence is an unspecific reaction to various stress factors, discrimination between different kinds of stress may be difficult to accomplish. More detailed information on the course of temporal and spatial changes in leaf response to different stress factors could help to overcome this problem and may enhance the potential of this technique for implementation in ‘Precision Farming’.

Furthermore, the majority of fluorescence studies on stress detection is based on parameters recorded e.g. in fluorescence quenching analyses or after previous dark-adaptation (Scholes and Rolfe, 1996; Bassanezi et al., 2002; Schmitz et al., 2006). Both prolong time for measurement being impracticable for ‘Precision Farming’. In this study 1) Pulse-Amplitude-Modulated (PAM) fluorescence imaging and 2) Laser-Induced-Fluorescence (LIF) ‘multipoint’ technique were applied on wheat (*Triticum aestivum* L.) and apple (*Malus domestica* Borkh.) in order to visualise temporal and spatial differences in fluorescence signals upon stress events. Thereby, the focus was on fluorescence parameters, which can be acquired in split seconds, being a very

important premise for further field application. The influence of important economic pathogens (*Blumeria graminis*; *Puccinia triticina*), N-deficiency and UV-B light as representative biotic and abiotic stress factors on host plant photosynthesis was investigated in detail. Additionally the capability of LIF and light-remission technique for detection of senescence-induced changes in apple (cvs 'Jonagold' and 'Golden Delicious') peel chlorophyll content and internal fruit quality characteristics under shelf life conditions was studied.

The questions to be answered in this study are:

1. Does PAM-fluorescence imaging with and without pre-darkening enable pre-symptomal pathogen detection and visualisation of spatial differences during progression of *Blumeria graminis* and *Puccinia triticina* infections in wheat at the individual leaf level?
2. Do LIF measurements in high frequency 'multipoint' scanning mode enable detection and discrimination of pathogen infections (*Puccinia triticina*, *Blumeria graminis*) and N-deficiency at wheat leaf and canopy level?
3. Do LIF and PAM techniques enable early detection of low UV-B stress on apple seedlings as well as visualisation of recovery processes?
4. Do LIF and remission technique enable a reliable detection of senescence based fruit quality changes considering the differences in apple peel pigment content and main flesh parameters on the sunlit and shaded sides?

6 References

Amberger, A. 1996. Pflanzenernährung, Vol. 4 (Ulmer, Stuttgart, Germany).

Baker, N.R. and Rosenqvist, E. 2004. Applications of chlorophyll fluorescence can improve production strategies: an examination of future possibilities. Journal of Experimental Botany **55**, 1607-1621.

Bassanezi, R.B., Amorim, L., Bergamin Filho, F. and Berger, R.D. 2002. Gas exchange and emission of chlorophyll fluorescence during the monocycle of rust, angular leaf spot and anthracnose on bean leaves as a function of their trophic characteristics. Journal of Phytopathology **150**, 37-47.

Bodria, L., Fiala, M., Naldi, E. and Oberti, R. 2002. Chlorophyll fluorescence sensing for early detection of crop's diseases symptoms. In: Proceedings 2002 International ASAE Conference and XV CIGR World Congress / ASAE-CIGR, 2002, Paper No. 021114, p. 1-15.

Börner, H. 1997. Pflanzenkrankheiten und Pflanzenschutz (Ulmer, Stuttgart, Germany).

Bornman, J.F. 1989. Target sites of UV-B radiation in photosynthesis of higher plants. Journal of Photochemistry and Photobiology B-Biology **4**, 145-158.

Buschmann, C. 2007. Variability and application of the chlorophyll fluorescence emission ratio red/far-red of leaves. Photosynthesis Research **92**, 261-271.

Carver, T.L.W., Ingerson, S.M. and Thomas, B.J. 1996. Influences of host surface features on development of *Erysiphe graminis* and *Erysiphe pisi*. In: Plant Cuticles - An Integrated Functional Approach, edited by G. Kerstiens (BIOS Scientific Publishers, Oxford, UK), p. 255-266.

Chaerle, L. and van der Straeten, D. 2000. Imaging techniques and the early detection of plant stress. Trends in Plant Science **5**, 495-501.

Dammer, K.-H., Reh, A., Wartenberg, G., Ehlert, D., Hammen, V., Dohmen, B. and Wagner, U. 2001. Recording of present plant parameters by pendulum sensor, remote sensing and ground measurements as fundamentals for site-specific fungicide application in winter wheat. In: Precision Agriculture Vol. 2: Proceedings of 3rd European Conference on Precision Agriculture, edited by G. Grenier and S. Blackmore (Montepellier, France), p. 647-652.

De Ell, J.R., van Kooten, O., Prange, R.K. and Mur, D.P. 1999. Applications of chlorophyll fluorescence techniques in postharvest physiology. In: Horticultural Reviews, Vol. 23, edited by J. Janick (John Wiley and Sons Inc.), p. 69-107.

Franke, J., Menz, G., Oerke, E-C. and Rascher, U. 2005. Comparison of multi- and hyperspectral imaging data of leaf rust infected wheat plants. In: Remote Sensing for Agriculture, Ecosystems, and Hydrology VII: Proceedings of the SPIE, edited by M. Owe and G. D'Urso, 5978(50), p. 1-11.

Gao, W., Zheng, Y., Slusser, J.R., Heisler, G.M., Grant, R.H., Xu, J. and He, D. 2004. Effects of supplementary ultraviolet-b irradiance on maize yield and qualities: a field experiment. Journal of Photochemistry and Photobiology B-Biology **80**, 127-131.

Gitelson, A.A., Buschmann, C. and Lichtenthaler, H.K. 1998. Leaf chlorophyll fluorescence corrected for re-absorption by means of absorption and reflectance measurements. Journal of Plant Physiology **152**, 283-296.

Govindjee, 2004. Chlorophyll *a* fluorescence: a bit of basics and history. In: Chlorophyll fluorescence: a signature of photosynthesis, edited by G.C. Papageorgiou and Govindjee (Springer, Dordrecht, NL), p.1-42.

Harper, J.E. 1994. Nitrogen metabolism. In: Physiology and determination of crop yield, edited by K.J. Boote, J.M. Bennett, T.R. Sinclair and G.M. Paulsen (Madison: ASA/CSSA/SSSA), p. 285-302.

Herman, J.R., Bhartia, P.K., Ziemke, J., Ahmad, Z. and Larko, D. 1996. UV-B increases (1979-1992) from decreases in total ozone. Geophysical Research Letters **23**, 2117-2120.

Kautsky, H. and Hirsch, A. 1931. Neue Versuche zur Kohlensäureassimilation. Naturwissenschaften **19**, 964.

Kluge, E., Enzian, S. and Gutsche, V. 1999. Befallsatlas. Atlas der potentiellen Befallsgefährdung durch wichtige Schadorganismen im Ackerbau Deutschlands (Saphir Verlag, Ribbesbüttel, Germany).

Koti, S., Reddy, K.R., Kakani, V.G., Zhao D. and Reddy, V.R. 2004. Soybean (Glycine max) pollen germination characteristics, flower and pollen morphology in response to enhanced ultraviolet-B radiation. Annals of Botany **94**, 855-864.

Kramer, E. 2005. Risk management in the supply chain for fresh fruit and vegetables. In: Improving the safety of fresh fruit and vegetables, edited by W. Jongen (Abington Cambridge: Woodhead Publishing Ltd), p. 179-228.

Krause, G.H. and Weis, E. 1991. Chlorophyll fluorescence and photosynthesis: the basics. Annual Review of Plant Physiology and Plant Molecular Biology **42**, 313-349.

Krupa, S.V., Kickert, R.N. and Jäger, H.-J. 1998. Elevated (UV)-B radiation and crops. In: Elevated (UV)-B radiation and agriculture, edited by S.V. Krupa, R.N. Kickert and H.J. Jäger (Springer, Berlin, Germany), p. 105-132.

Lawlor, D.W., Lemaire, G. and Gastal, F. 2001. Nitrogen, plant growth and crop yield. In: Plant Nitrogen, edited by P.J. Lea and J.-F. Morot-Gaudry (Springer, Berlin, Germany), p. 343-367.

Lichtenthaler, H.K. and Rinderle, U. 1988. The role of chlorophyll-fluorescence in the detection of stress conditions in plants. CRC Critical Reviews in Analytical Chemistry **19**, 29-85.

Lichtenthaler, H.K., Buschmann, C. and Knapp, M. 2005. How to correctly determine the different chlorophyll fluorescence parameters and the chlorophyll fluorescence decrease ratio R_{Fd} of leaves with the PAM fluorometer. Photosynthetica **43**, 379-393.

Limbrunner, B. and Maidl, F.-X. 2007. Non-contact measurement of the actual nitrogen status of winter wheat canopies by laser-induced chlorophyll fluorescence. In: Precision Agriculture'07: Proceedings of 6th European Conference on Precision Agriculture, edited by J.V. Stafford (Wageningen Academic Publishers, The Netherlands), p. 173-179.

Lorenzen, B. and Jensen, A. 1989. Changes in leaf spectral properties induced in barley by cereal powdery mildew. Remote Sensing of Environment **27**, 201-209.

Magyarosy, A.C., Schutmann, P. and Buschmann, B.B. 1976. Effects of powdery mildew infection on photosynthesis by leaves and chloroplasts of sugar beet. Plant Physiology **57**, 486-489.

Magyarosy, A.C. and Malkin, R. 1978. Effects of powdery mildew infection of sugar beet on the content of electron carriers in chloroplasts. Physiological and Molecular Plant Pathology **13**, 183-188.

Maxwell, K. and Johnson, G.N. 2000. Chlorophyll fluorescence - a practical guide. Journal of Experimental Botany **51**, 659-668.

Nicolas, H. 2004. Using remote sensing to determine of the date of a fungicide application on winter wheat. Crop Protection **23**, 853-863.

Noh, H.K. and Lu, R. 2005. Hyperspectral reflectance and fluorescence for assessing apple quality. ASAE Paper No. 053069.

Peltonen, J. Virtanen, A., Haggren, E. 1995. Using a chlorophyll meter to optimize nitrogen fertiliser application for intensively-managed small-grain cereals. Journal of Agronomy and Crop Science **174**, 309-318.

Percival, G.C. and Fraser, G.A. 2002. The influence of powdery mildew infection on photosynthesis, chlorophyll fluorescence, leaf chlorophyll and carotenoid content of three woody plant species. Arboricultural Journal **26**, 333-346.

Pfündel, E. 1998. Estimating the contribution of photosystem I to total leaf chlorophyll fluorescence. Photosynthesis Research **56**, 185-195.

Quick, W.P. and Horton, P. 1984. Studies on the induction of chlorophyll fluorescence in barley protoplasts. I. Factors affecting the observation of oscillations in the yield of chlorophyll fluorescence and the rate of oxygen evolution. Proceedings of the Royal Society of London B **220**, 361-370.

Raun, W.R. and Johnson, G.V. 1999. Improving nitrogen use efficiency for cereal production. Agronomy Journal **91**, 357-363.

Rinderle, U. and Lichtenthaler, H.K. 1988. The chlorophyll fluorescence ratio F690/F735 as a possible stress indicator. In: Applications of chlorophyll fluorescence, edited by H.K. Lichtenthaler (Dordrecht: Kluwer Academic Publishers), p. 189-196.

Robert, C., Bancal, M.-O., Ney, B. and Lannou, C. 2004. Wheat leaf photosynthesis loss due to leaf rust, with respect to lesion development and leaf nitrogen status. New Phytologist **165**, 227-241.

Runeckles, V.C. and Krupa, S.V. 1994. The impact of UV-B radiation and ozone on terrestrial vegetation. Environmental Pollution **83**, 191-213.

Samborski, D.J. 1985. Wheat leaf rust. In: The cereal rusts (Vol.2), edited by A.P. Roelfs and W.R. Bushnell (Academic Press; New York, London, Orlando), p. 39-59.

Schächtl, J., Huber, G., Maidl, F.-X. and Sticksel, E. 2005. Laser-induced chlorophyll fluorescence measurements for detecting the nitrogen status of wheat (*Triticum aestivum* L.) canopies. Precision Agriculture **6**, 143-156.

Schmitz, A., Tartachnyk, I., Kiewnick, S., Sikora, R. and Kühbauch, W. 2006. Detection of *Heterodera schachtii* infestation in sugar beet by means of laser-induced and pulse amplitude modulated chlorophyll fluorescence. Nematology **8**, 273-286.

Scholes, J.D. and Rolfe, S.A. 1996. Photosynthesis in localised regions of oat leaves infected with crown rust (*Puccinia coronata*): quantitative imaging of chlorophyll fluorescence. Planta **199**, 573-582.

Shangguan, Z., Shao, M. and Dyckmanns, J. 2000. Effects of nitrogen nutrition and water deficit on net photosynthetic rate and chlorophyll fluorescence in winter wheat. Journal of Plant Physiology **156**, 46-51.

Shtienberg, D. 1992. Effects of foliar diseases on gas exchange processes: a comparative study. Phytopathology **82**, 760-765.

Song, J., Deng, W., Beaudry, R.M. and Armstrong, P.R. 1997. Changes in chlorophyll fluorescence of apple fruit during maturation, ripening and senescence. HortScience **32**, 891-896

Sökefeld, M., Gerhards, R., Oebel, H. and Therburg, R.-D. 2007. Image acquisition for weed detection and identification by digital image analysis. In: Precision Agriculture'07: Proceedings of 6th European Conference on Precision Agriculture, edited by J.V. Stafford (Wageningen Academic Publishers, The Netherlands), p. 523-528.

Stolarski, R., Bojokov, R., Bishop, L., Zerefos, C., Straehlin, J. and Zawodny, J. 1992. Measured trends in stratospheric ozone. Science **256**, 343-349.

Streif, J. 1996. Optimum harvest date for different apple cultivars in the 'Bodensee' area. In: The Postharvest Treatment of Fruit and Vegetables: Determination and Prediction of Optimum Harvest date of Apple and Pears, ECSC-EC-EAEC, 1996 (Brussels), edited by A. de Jager, D. Johnson and E. Hohn, p. 15-20.

Tartachnyk, I., Rademacher, I. and Kühbauch, W. 2006. Distinguishing nitrogen deficiency and fungal infection of winter wheat by laser-induced fluorescence. Precision Agriculture **7**, 281-293.

Tevini, M. 2004. Plant responses to ultraviolet radiation stress. In: Chlorophyll fluorescence: a signature of photosynthesis, edited by G.C. Papageorgiou and Govindjee (Springer, Dordrecht, NL), p.605-621.

Tilman, D., Cassman, K.G., Matson, P.A., Naylor, R. and Polasky, S. 2002. Agricultural sustainability and intensive production practises. Nature **418**, 668-670.

Van Kooten, O. and Snel, J.F.H. 1990. The use of chlorophyll nomenclature in plant stress physiology. Photosynthetic Research **25**, 147-150.

Vass, I. 1997. Adverse effects of UV-B light on the structure and function of the photosynthetic apparatus. In: Handbook of photosynthesis, edited by M. Pessarakli (Marcel Dekker Inc., New York, the Netherlands), p. 931-949.

West, J.S., Bravo, C., Oberti, R., Lemaire, D., Moshou, D. and McCartney, H.A. 2003. The potential of optical canopy measurement for targeted control of field crop diseases. Annual Review of Phytopathology **41**, 593-614.

Yang, S.L. and Ellingboe, A.H. 1972. Cuticle layers as a determining factor for the formation of mature appressoria of *Erysiphe graminis* on wheat and barley. Phytopathology **62**, 708-714.

Zhang, L. and Dickinson, M. 2001. Fluorescence from rust fungi: a simple and effective method to monitor the dynamics of fungal growth *in planta*. Physiological and Molecular Plant Pathology **59**, 137-141.

B Temporal and spatial changes of chlorophyll fluorescence as basis for early and precise detection of leaf rust and powdery mildew infections in wheat leaves

1 Introduction

In modern agriculture, there is an increasing pressure to reduce the application of fertilisers and plant protection means to minimise costs of production and impact on environment. In large heterogeneous field plots, chemicals have to be applied site specifically, only where they are needed. In recent years, the technique for evaluation of plant nitrogen status and site specific application of nitrogen fertilisers has been developed. However, only few reports are available on specific sensors for early plant pathogen detection in the field, despite the fact that these crop disorders usually occur very patchy and could be also managed site specifically. Previous studies have shown that fungal infections such as leaf rust and powdery mildew can be detected in crop canopies by reflectance measurement (Lorenzen and Jensen, 1989; Franke et al., 2005). Moreover, Nicolas (2004) observed a high correlation between the severity of *S. tritici* infection and Normalised-Differenced-Vegetation-Index (NDVI) in winter wheat. However, a disadvantage of this approach is the relative late recognition of infection.

The first plant responses to different types of pathogen infection are changes in leaf photosynthesis rate, which can be easily estimated by chlorophyll fluorescence. This technique delivers fast and extensive information on the potential and current efficiency of photosynthesis and the integrity of photosynthetic apparatus even at very early stages of stress conditions (for reviews see e.g. Baker and Rosenqvist, 2004; Govindjee, 2004). A couple of studies have been conducted to investigate the influence of pathogens on the host leaf photosynthesis and fluorescence (Scholes and Farrar, 1986; Moll et al., 1995; Scholes and Rolfe, 1996; Bassanezi et al., 2002), but results vary markedly. This may be explained by the fact that plant response to fungal infection depends on both, e.g. plant and pathogen development stage as well as on the environmental conditions during progression of infection. Besides, pathogen infections proceed heterogeneously on the leaf surface resulting in heterogeneous patterns of fluorescence in tissues directly invaded by the fungus; and those areas which are not invaded, could be modified by its impact (Scholes and Rolfe, 1996; Tartachnyk et al., 2006).

In this context, information on the course of temporal and spatial changes in leaf response to different kinds of infection is needed as basis for development of remote sensing techniques for detecting pathogen infections in the field.

The objective of the present study therefore was to assess and compare leaf spatial and temporal fluorescence responses to economically important pathogens such as leaf rust (*Puccinia triticina*) and powdery mildew (*Blumeria graminis*) in wheat (*Triticum aestivum* L.) over a period of two weeks after inoculation. In our work, we focused on parameters of fast fluorescence kinetics Fo and Fm, because signal excitement and detection have to be carried out in practise in split seconds. In physiological studies, a pre-darkening period of 10-20 minutes is usually needed for an accurate evaluation of these parameters. Since such pre-darkening may be problematic and even insufficient (Bodria et al., 2002) under field conditions, an additional question addressed in this work was, whether both fluorescence measurements with and without previous dark adaptation will enable detection of pathogen infection with comparable efficiency.

2 Material and Methods

2.1 Plant material

Winter wheat seeds (*Triticum aestivum* L. cv. Kanzler) were sown in 150 cm^3 pots with a substrate containing 50% commercial potting mixture and 50% sand. The plants were grown in a growth chamber with a photoperiod of 14/10 h (day/night), a temperature of 20/18 ± 2 °C, a relative humidity of 60/70 ± 15% and a light intensity of 100 µmol m^{-2} s^{-1}. Plants were fertilised twice a week with a modified Hoagland nutrient solution with a nitrogen concentration of 224 mg l^{-1}. Water was supplied from the bottom without wetting the leaves. For the experiments, uniformly developed plants at the 4-leaf stage were selected. Control plants were treated with a fungicide (Fortress, Dow AgroScience, USA) to prevent uncontrolled infections. For initiation of leaf rust, leaves were sprayed with a suspension of *Puccinia triticina* spores in a Tween 20 solution. Thereafter, plants were placed under a plastic cover for 24 h to maintain high humidity. For mildew inoculation, a ventilator was used to assure spreading of fresh mildew spores (*Blumeria graminis*) on the leaf surface.

2.2 Fluorescence and remission measurements

The PAM-imaging chlorophyll fluorometer (Walz, Effeltrich, Germany) was used for the detection of chlorophyll fluorescence as well as Red and NIR remission characteristics in wheat leaves. At the beginning of experiment, control and infected

leaves were fixed with a clip in the fluorescence system to prevent shifting of leaves during measurement. All fluorescence and remission images were captured daily with the mounted CCD camera (640 x 480 pixels) between 09.00 and 09.30 a.m. under constant environmental conditions on the same areas of fixed leaves. The CCD camera was protected from stray excitation light by long-pass filter (Schott, RG 645; Mainz, Germany) and from long-wavelength ambient light by a short-pass filter (Balzer, Calflex-X, λ<780 nm; Bingen, Gemany).

Ground fluorescence (Fo) was recorded after illumination of the sample with blue light (470 nm) at 0.5 µmol m^{-2} s^{-1} PAR. Maximum fluorescence (Fm) was measured after applying a blue light saturation pulse of 2400 µmol m^{-2} s^{-1} PAR for 0.6 s. The Fo and Fm fluorescence images were taken with and without dark-adaptation for 20 min. Following fluorescence recordings, the red (Red, 650 nm) and near-infrared (NIR, 780 nm) remission images were taken. After completing the measurements, the CCD camera was dismantled to provide full irradiation of the fixed leaves.

2.3 Data processing

The collected fluorescence (Fo and Fm) and remission (Red and NIR) images were processed at the end of experiment with IDL routine (Version 6.0.1. 2003, Research Systems Inc., Boulder, USA) to calculate - pixel by pixel - variable fluorescence (Fv) as Fm-Fo, the ratio of the variable fluorescence to Fo (Fv/Fo) and maximum photochemical efficiency (Fv/Fm); Normalised-Differenced-Vegetation-Index (NDVI) was calculated as: NDVI=(NIR-Red)/(NIR+Red). In order to assess the influence of infection on spatial development of fluorescence and remission parameters, 10 points were marked on control leaves and 3 types of areas of interest (AOI, 10 repetitions, 21x21 pixels each) were chosen on the images of infected leaves at the end of experiment on the 13th day after inoculation (dai): 1) areas of pustules, 2) areas around the pustules and 3) apparently healthy areas of infected leaves. Thereafter, fluorescence and remission parameters for the same marked points were recalculated for all sampling dates using the software implemented co-ordinate plane. This allowed estimation of the course of fluorescence and remission characteristics during pathogen development for exactly the same leaf spots.

2.4 Statistics

Chlorophyll fluorescence and remission data in the figures (2-4) represent mean values with standard deviations from 10 replicated points per leaf. The experimental data

were subjected to ANOVA with the SPSS statistical package (SPSS Inc., Chicago, USA). The 95% probability level was accepted to indicate significant differences. Means were compared by the Tukey HSD multiple range test after data were checked for normal distribution and variance homogeneity. The experiment was repeated twice, with comparable results.

3 Results

3.1 Development of pathogen infestation

The rust inoculated leaves did not display visual symptoms of infection for six days after inoculation. At 7th dai, first heterogeneously distributed chlorotic spots became apparent on the upper leaf surface (Fig.1). Within 24 h, these spots enlarged and became more conspicuous, and at 9th dai, small red-brown pustules appeared in the centre of these spots. At this stage, about 2% of the investigated leaf surface displayed symptoms of infection. During the next days, chlorotic spots with pustules expanded and, at the end of the experiment (13th dai), almost 10% of the leaf surface was covered by rust pustules.

In mildew infected leaves, visual symptoms first appeared at 9th dai; i.e. two days later than in rust infected leaves (Fig. 1). At this time, 0.8% of detected leaf surface revealed small patches of whitish mycelium, which increased in size during the following days. Chlorotic lesions, as found in rust infected leaves, were not observed during development of mildew infection. As compared to rust, mildew inoculated leaves displayed a lower number of pustules, but area of single pustules was much larger throughout the experiment. At 13th dai, 11% of the leaf surface was covered with whitish mycelium.

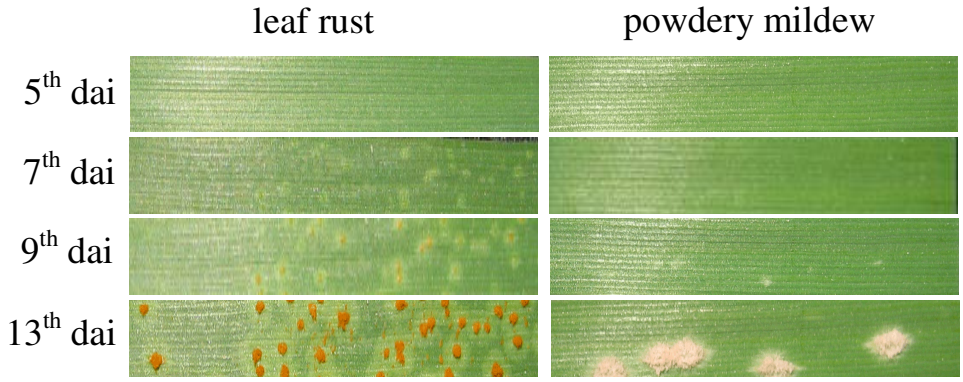

Fig. 1: Leaves inoculated with leaf rust (left) and powdery mildew (right) on 5th, 7th, 9th, and 13th day after inoculation.

3.2 NDVI index

In all AOI NDVI of rust and mildew inoculated leaves did not change before visual symptoms became evident (Fig. 2). With development of chlorotic patches in rust infected leaves at 7th dai, NDVI slightly decreased (- 2%) from 0.711 to 0.697 units in the pustule areas. This reduction became significant (- 18%) with the appearance of the first red-brown pustules, and at the 13th dai NDVI was 0.366 and about 50% lower than the control at this day. The enlargement of chlorotic areas around pustules caused also a significant reduction of NDVI at 13th dai (- 7%), whereas values in the apparently healthy tissue decreased only slightly at the end of the experiment.
Mildew infected leaves reduced NDVI in the areas of pustules from 0.750 to 0.623 units by 17% with occurrence of first whitish mycelia on the leaf surface. At the end of experiment, NDVI was 0.348 and about 52% lower in these areas. No changes in NDVI were observed in the other AOI of mildew infected leaves during the experimental period.

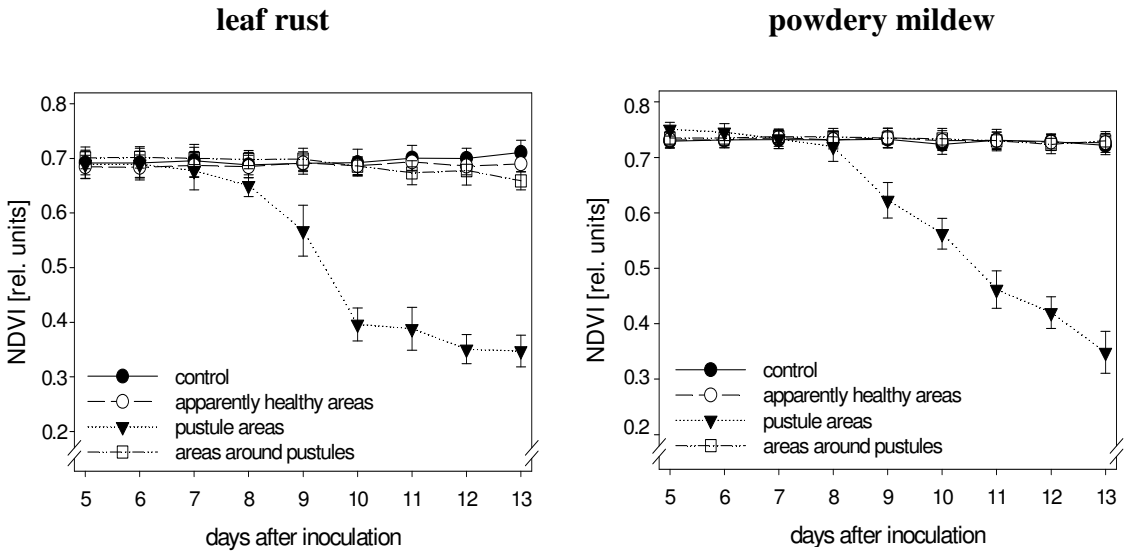

Fig. 2: NDVI in the different areas of interest in winter wheat leaves infected with leaf rust (left) and powdery mildew (right). Vertical bars indicate $\pm$ standard deviations (n=10).

3.3 Fluorescence imaging after previous dark-adaptation

Fluorescence imaging allowed earlier detection of pathogen infection as compared to NDVI. Ground fluorescence (Fo) in the areas of pustules of rust inoculated leaves slightly increased at 6th dai (+ 6%), whereas first visual symptoms (chlorotic patches) became evident at 7th dai.

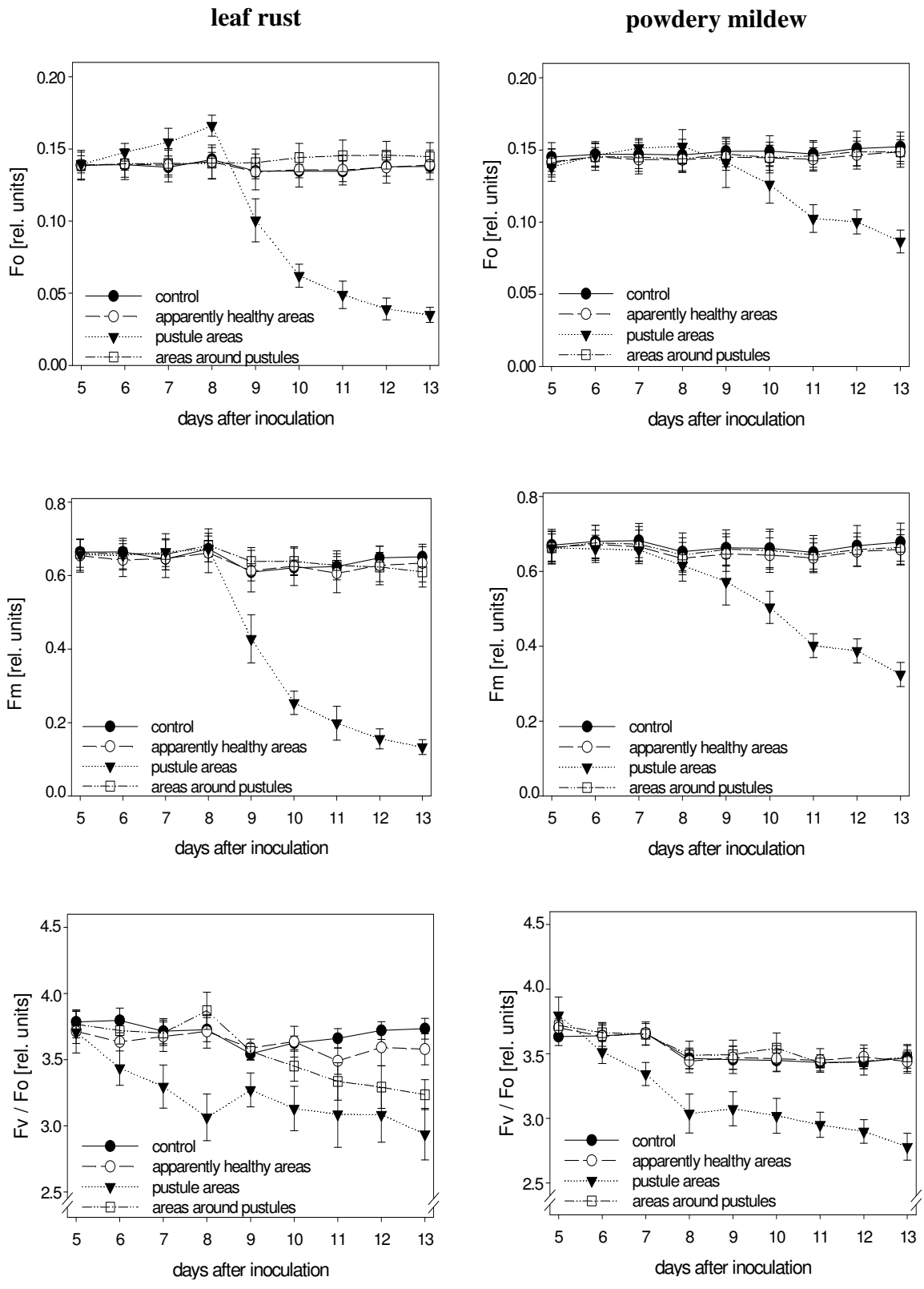

Fig. 3: Fo (top), Fm (middle) and Fv/Fo (bottom) values of leaf rust (left) or powdery mildew (right) infected winter wheat leaves in different areas of interest. Measurements were provided after 20 minutes dark adaptation. Vertical bars indicate ± standard deviations (n=10).

At the 8th dai, Fo displayed 0.166 units, representing 19% higher values as compared to control (Fig. 3). Mildew inoculated leaves displayed a slightly increased Fo in the areas of pustules, e.g. 0.151 (+ 3%) and 0.153 (+ 4%) units, respectively, one or two days before visual symptoms became evident, even though appearance of mycelium was not preceded by chlorotic patches (Fig. 3). However, this increase was less pronounced as compared to rust infected leaves. For both types of infection, no significant changes in maximum fluorescence (Fm) were observed during these early stages of pathogen development.

The formation of rust and mildew pustules was accompanied by a strong decrease of both Fo and Fm (Fig. 3). This reduction became more pronounced with pustule growth. At the 13th dai, Fo and Fm values in the areas of pustules decreased to 25% (0.035 units) and 20% (0.133 units) of uninfected control for rust and to 57% (0.087 units) and 48% (0.325 units) for mildew inoculated leaves, respectively.

Both kinds of infection displayed a lower impact on Fo and Fm values in the areas around the pustules and in the apparently healthy areas. Only in the chlorotic areas around rust pustules Fo was tendentiously higher from 9th to 13th dai (Fig. 3).

As early as 2-3 days before emergence of powdery mildew mycelium and reddish rust pustules, parameters of photochemical efficiency were significantly decreased. For rust, at the 6th dai Fv/Fm or Fv/Fo were reduced by 2 or 10% and for powdery mildew at the 7th dai by 2 or 9%, respectively. At the end of experiment, both pathogen treatments displayed by 6-7% lower Fv/Fm and by 20-21% lower Fv/Fo values. In contrast to Fo and Fm parameters, both Fv/Fm and Fv/Fo showed significant lower values in the areas around rust pustules at the 10th dai. This reduction became mostly pronounced (3-14%) in comparison to control at the last day of experiment. Both parameters were also slightly reduced in the period from 11th to 13th dai in the apparently healthy areas of leaf rust treatment. For powdery mildew, no changes of these parameters could be detected around fungal colonies (Fig. 3).

3.4 Fluorescence imaging without previous dark-adaptation

The measurements without dark adaptation showed the same tendency as those with 20 minutes pre-darkening in terms of temporal and spatial responses to pathogen infections (Fig. 4). However, leaves without previous dark adaptation displayed slightly higher Fo and lower Fm values (Fig. 4). Besides, all the fluorescence images taken without dark adaptation, including uninfected control, appeared more heterogeneous as compared to those taken after 20 minutes of dark adaptation (Fig. 4).

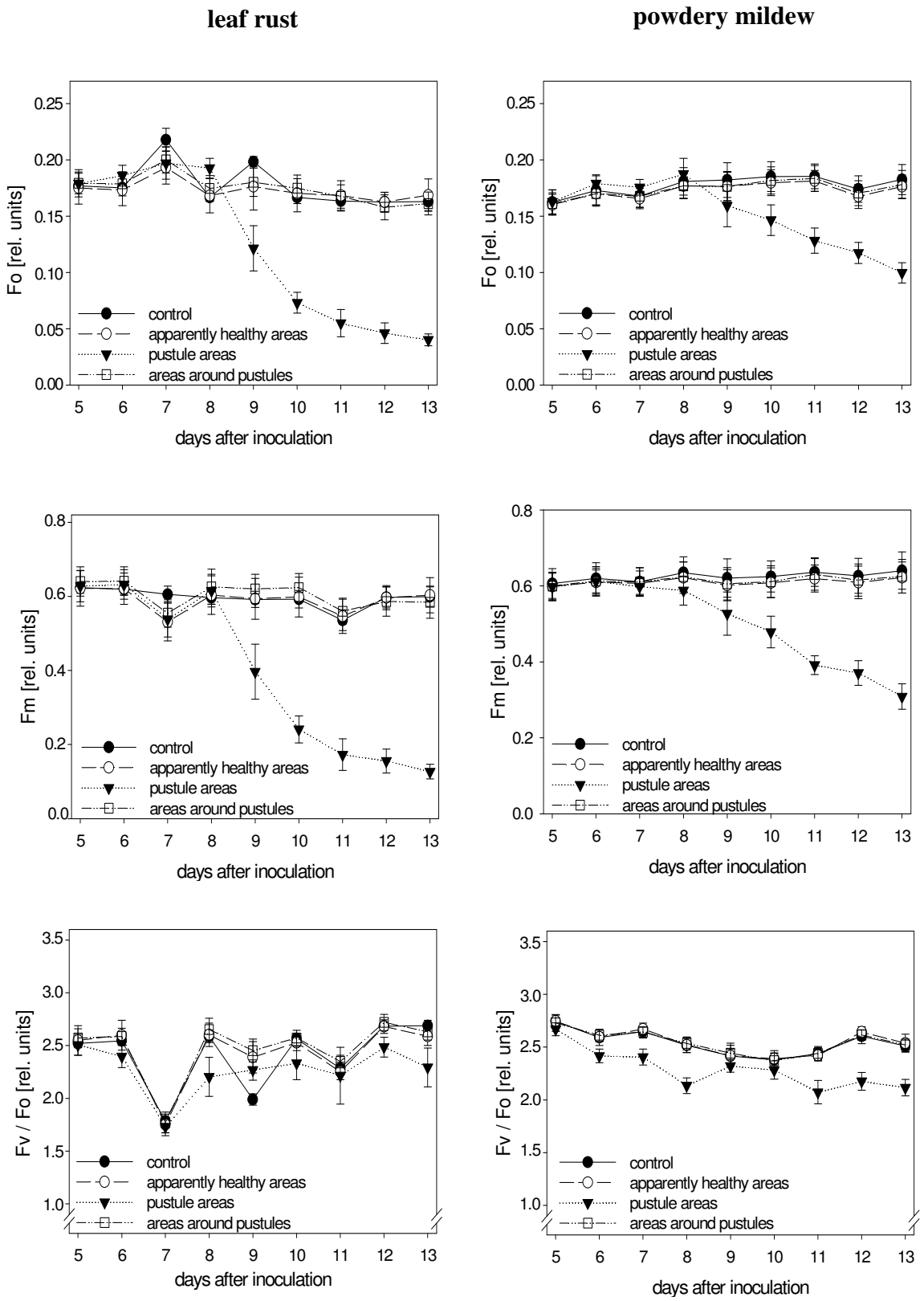

Fig. 4: Fo (top), Fm (middle) and Fv/Fo (bottom) values of leaf rust (left) or powdery mildew (right) infected winter wheat leaves in different areas of interest. Measurements were provided without dark adaptation. Vertical bars indicate ± standard deviations (n=10).

4 Discussion

NDVI did not allow a pre-symptomal detection of both pathogen infections in our experiment (Fig. 2), which is in agreement with previous findings of Franke et al. (2005) for leaf rust detection by means of reflection technique.

Healthy green leaves are usually characterised by a low red reflectance due to the strong absorption in this region by chlorophyll molecules and by a high reflection of NIR caused by multiple scattering at the air-cell interfaces in the internal leaf tissues (West et al., 2003). The observed decrease of NDVI during development of both pathogens in our experiment was due to the increase of Red remission at constant NIR values. In the rust infected leaves, first chlorophyll breakdown in the chlorotic patches and later brownish pustules caused higher Red light remission in these leaf regions. In the mildew infected leaves, stronger Red remission was observed within the pustule areas due to the shielding of green tissues by whitish fungal mycelium. This is in agreement with the results of Lorenzen and Jensen (1989), who reported distinct changes in the visible wavelength bands and slight or no response in the NIR range for wheat leaves infected with powdery mildew.

Fluorescence imaging after dark-adaptation allowed a pre-symptomal detection of both pathogen infections in wheat leaves (Fig. 3), confirming the high potential of this technique for an early and efficient detection of plant responses to pathogen infections (Bodria et al., 2002; Chaerle et al., 2004). For both pathogen treatments, initial infection was accompanied by increased ground fluorescence Fo in the areas of infection, which was most pronounced at 9^{th} dai within the chlorotic patches of leaf rust. Significantly enhanced Fo values within the chlorotic patches of rust infected leaves could be referred to chlorophyll breakdown in the area of infection, lowering re-absorption of red fluorescence light (Gitelson et al., 1998). At the same time, maximal fluorescence Fm displayed unchanged values. This may indicate stronger disturbances in light-harvesting complexes than in reaction centres of PSII (Govindjee, 2004; Lichtenthaler and Babani, 2004) at the initial stages of infestation.

With the appearance of first reddish pustules or whitish mycelium, both ground and maximum fluorescence decreased. At the end of experiment Fo and Fm were reduced to 25% and 20% of uninfected control for rust and to 57% and 48% for mildew inoculated leaves, respectively. However, removal of rust pustules from the leaf surface at the end of experiment led to a partial restoring of Fo and Fm values to 75% and 63% of control leaves, respectively. In the case of mildew infected leaves, removal of mycelium restored Fo and Fm to 91% and 77% of control values, respectively. This means that the observed strong reduction in both parameters resulted mainly from

shielding of plant tissues from the excitation light through fungal structures and, to lesser extent, from the internal disturbances in leaf photosynthetic apparatus or chlorophyll breakdown in the areas of pustules.

Fv/Fm and Fv/Fo, in contrast, remained unchanged after the fungal pustules were removed. Thus, the absolute values of Fo and Fm parameter appeared to be dependent on the optical properties of overlaying fungal structures, whereas fluorescence ratios were independent, representing reliable indices of photosynthetic performance.

The early significant detection of both kinds of infection, 3 and 2 days before the emergence of first reddish rust and whitish mildew pustules, was provided by means of Fv/Fo and Fv/Fm ratios. Similar results were reported by Scholes and Rolfe (1996), who found a slightly reduced photochemical efficiency [Φ_{II} = (Fm´ - Ft)/Fm´] in the pustule area at the early stage (5 dai) of crown rust infection. Bassanezi et al. (2002) reported only small changes in Fv/Fm in rust infected bean leaves with up to 100% infestation severity. This was probably due to the fluorescence recordings averaging from a large leaf area (38.5 mm²) with and without lesions.

In our experiment, Fv/Fo appeared to be the most affected parameter during the development of infections among all evaluated fluorescence characteristics (Fig. 2). This is in agreement with Babani and Lichtenthaler (1996) and Lichtenthaler et al. (2005) who reported higher amplitude of this ratio as compared to Fv/Fm, also in response to other kinds of stress. While a similar tendency in the fluorescence pattern was observed in the areas of pustules for mildew and rust infected leaves, areas around the pustules and apparently healthy regions differed in their response to these pathogens. Mildew infection influenced fluorescence characteristics neither in the direct vicinity of mycelium nor in the apparently healthy leaf regions. Rust infected plants, in contrast, displayed significantly reduced photochemical efficiency in the chlorotic areas around the pustules, mainly due to enhanced ground fluorescence. The same tendency, but less pronounced, was found in the apparently healthy regions of rust infected leaves at the last days of experiment. The observed discrepancy in photochemical efficiency of investigated leaf areas for both types of infection clearly reflects differences in their development. Whereas the main fungal growth of mildew with building-up whitish mycelia occurs at the leaf surface (Carver et al., 1996), leaf rust develops a complex system of infection structures within the leaf tissue (Zhang and Dickinson, 2001) leading to stronger damage in photosynthetic apparatus and chlorophyll breakdown. Thus, fluorescence imaging under laboratory conditions enabled early, pre-symptomatic detection of mildew and rust infections and visualisation of spatial differences during their development. Our findings on leaf rust

fluorescence patterns are in agreement with Scholes and Rolfe (1996), who observed at sporulation stage, a reduced Φ_{II} throughout the infected leaf with the strongest reduction in regions invaded by the fungal pustules. However, in another study of Scholes and Farrar (1986), barley leaves infected with brown rust displayed inhibited photosynthesis preferentially in regions between fungal pustules, whereas within infected regions photosynthesis was similar or even higher as compared to uninfected leaves. Thus, the spatial response of leaf photosynthesis to infection with biotrophic fungi may vary depending upon the pathogen and host involved. Differences in the spatial fluorescence patterns of leaf rust and powdery mildew infected leaves observed in our study indicate a significant potential for discrimination of these pathogens by means of PAM-Imaging.

An additional objective of our study was to compare fluorescence images taken with and without previous dark adaptation to clarify if they enable the detection of pathogen infection with comparable success. Both kinds of measurements showed the same tendency in terms of temporal and spatial responses to infection process. However, leaves without previous dark adaptation displayed slightly higher Fo and lower Fm values (Fig. 4). Besides, all the fluorescence images taken without dark adaptation, including uninfected control, appeared more heterogeneous as compared to those taken after 20 minutes of dark adaptation. For this reason, differentiation between pathogen infected and uninfected leaves with fluorescence imaging without pre-darkening of plant tissue appeared less accurate, even in laboratory experiments under constant light and temperature conditions. These results support the findings of Bodria et al. (2002), who showed that a reliable detection of brown rust in wheat plants by multi-spectral fluorescence imaging in field was only possible during night time. Day time measurements after long exposure to direct sun and diffusive light did not provide sufficient information in spite of short pre-darkening of plants. Besides, further technical challenges, e.g. leaf exposure and distance to sensor still have to be tackled for applying fluorescence imaging in practise.

5 References

Babani, F. and Lichtenthaler, H.K. 1996. Light-induced and age-dependent development of chloroplasts in etiolated barley leaves as visualized by determination of photosynthetic pigments, CO_2 assimilation rates and different kinds of chlorophyll fluorescence ratios. Journal of Plant Physiology **148**, 555-566.

Baker, N.R. and Rosenqvist, E. 2004. Applications of chlorophyll fluorescence can improve production strategies: an examination of future possibilities. Journal of Experimental Botany **55**, 1607-1621.

Bassanezi, R.B., Amorim, L., Bergamin Filho, F. and Berger, R.D. 2002. Gas exchange and emission of chlorophyll fluorescence during the monocycle of rust, angular leaf spot and anthracnose on bean leaves as a function of their trophic characteristics. Journal of Phytopathology **150**, 37-47.

Bodria, L., Fiala, M., Naldi, E. and Oberti, R. 2002.Chlorophyll fluorescence sensing for early detection of crop's diseases symptoms. In: Proceedings 2002 International ASAE Conference and XV CIGR World Congress / ASAE-CIGR. - ASAE-CIGR, 2002, Paper No. 021114, p. 1-15.

Carver, T.L.W., Ingerson, S.M. and Thomas, B.J. 1996. Influences of host surface features on development of *Erysiphe graminis* and *Erysiphe pisi*. In: Plant Cuticles - An Integrated Functional Approach, edited by G. Kerstiens (BIOS Scientific Publishers, Oxford, UK), p. 255-266.

Chaerle, L., Hagenbeek, D., De Bruyne, R., Valcke, R. and Van Der Straeten, D. 2004. Thermal and chlorophyll-fluorescence imaging distinguish plant-pathogen interactions at an early stage. Plant Cell Physiology **45** (7), 887-896.

Gitelson, A.A., Buschmann, C. and Lichtenthaler, H.K. 1998. Leaf chlorophyll fluorescence corrected for re-absorption by means of absorption and reflectance measurements. Journal of Plant Physiology **152**, 283-296.

Govindjee, 2004. Chlorophyll *a* fluorescence: a bit of basics and history. In: Chlorophyll fluorescence: a signature of photosynthesis, edited by G.C. Papageorgiou and Govindjee (Springer, Dordrecht, NL), p.1-42.

Franke, J., Menz, G., Oerke, E-C. and Rascher, U. 2005. Comparison of multi- and hyperspectral imaging data of leaf rust infected wheat plants. In: Remote Sensing for Agriculture, Ecosystems, and Hydrology VII: Proceedings of the SPIE, edited by M. Owe and G. D'Urso, **5978**(50), p. 1-11.

Lichtenthaler, H.K. and Babani, F. 2004. Light adaptation and senescence of the photosynthetic apparatus. Changes in pigment composition, chlorophyll fluorescence parameters and photosynthetic activity. In: Chlorophyll fluorescence: a signature of photosynthesis, edited by G.C. Papageorgiou and Govindjee (Springer, Dordrecht, NL), p.713-736.

Lichtenthaler, H.K., Buschmann, C. and Knapp, M. 2005. How to correctly determine the different chlorophyll fluorescence parameters and the chlorophyll fluorescence decrease ratio R_{Fd} of leaves with the PAM fluorometer. Photosynthetica **43**, 379-393.

Lorenzen, B. and Jensen, A. 1989. Changes in leaf spectral properties induced in barley by cereal powdery mildew. Remote Sensing of Environment **27**, 201-209.

Moll, S., Serrano, P. and Boyle, C. 1995. *In vivo* chlorophyll fluorescence in rust-infected bean plants. Angewandte Botanik **69**, 163-168.

Nicolas, H. 2004. Using remote sensing to determine of the date of a fungicide application on winter wheat. Crop Protection **23**, 853-863.

Scholes, J.D. and Farrar, J.F. 1986. Increased rates of photosynthesis in localised regions of a barley leaf infected with brown rust. New Phytologist **104**, 601-612.

Scholes, J.D. and Rolfe, S.A. 1996. Photosynthesis in localised regions of oat leaves infected with crown rust (*Puccinia coronata*): quantitative imaging of chlorophyll fluorescence. Planta **199**, 573-582.

Tartachnyk, I., Rademacher, I. and Kühbauch, W. 2006. Distinguishing nitrogen deficiency and fungal infection of winter wheat by laser-induced fluorescence. Precision Agriculture **7**, 281-293.

West, J.S., Bravo, C., Oberti, R., Lemaire, D., Moshou, D. and McCartney, H.A. 2003. The potential of optical canopy measurement for targeted control of field crop diseases. Annual Review of Phytopathology **41**, 593-614.

Zhang, L. and Dickinson, M. 2001. Fluorescence from rust fungi: a simple and effective method to monitor the dynamics of fungal growth *in planta*. Physiological and Molecular Plant Pathology **59**, 137-141.

C Detection and differentiation of nitrogen-deficiency, *Blumeria graminis* and *Puccinia triticina* infections at wheat leaf and canopy level by laser-induced chlorophyll fluorescence

1 Introduction

Reflectance or Laser-Induced Fluorescence (LIF) techniques enable fast and non-invasive estimation of plant nitrogen (N) status for site-specific crop fertilisation (Schächtl et al., 2005; Bélanger et al., 2006; Noh et al., 2006; Zillmann et al., 2006; Limbrunner and Maidl, 2007). With LIF, detection of plant N-deficiency is based on the close relationship established between leaf chlorophyll content and red/near-infra-red chlorophyll fluorescence ratio F690/F730 (for review see Buschmann, 2007). Pathogen infestations, occurring very patchy, could also be managed site specifically. However, only few studies are available on sensor-based pathogen detection under field conditions (Bodria et al., 2002; Nicolas, 2004) and on discrimination between biotic stress and nutrient deficiencies (Tartachnyk et al., 2006).

LIF measurements on winter wheat leaves under laboratory conditions showed that both N-deficiency and prolonged pathogen infection induced chlorophyll breakdown as well as increase of F690/F730 ratio (Lichtenthaler and Miehe, 1997; Tartachnyk et al., 2006). At the same time, fluorescence imaging studies at leaf level have shown that fungal infections result in spatially heterogeneous patterns of chlorophyll fluorescence and chlorophyll breakdown (Scholes and Rolfe, 1996; Kuckenberg et al., 2007). For dark adapted leaves, discrimination of these stress types was possible by estimating spatial heterogeneity of combined fluorescence and reflection indices (Tartachnyk et al., 2006).

A recently developed LIF system allows assessment of chlorophyll heterogeneities in crop canopies by ‘multipoint’ scanning technique (Limbrunner and Maidl, 2007). The objective of the present study was to test, whether high frequency ‘multipoint’ scanning fluorescence measurements may also enable detection of pathogen infections, such as leaf rust (*Puccinia triticina*) and powdery mildew (*Blumeria graminis*) in wheat (*Triticum aestivum* L.). We further hypothesised that estimation of spatial variability of chlorophyll fluorescence parameters will allow differentiation between N-deficiency and pathogen infection at both leaf and canopy level. In order to estimate the possible sources of canopy heterogeneities, recordings from adaxial and abaxial leaf sides have been compared.

2 Material and Methods

2.1 Plant material

Winter wheat seeds (*Triticum aestivum* L. cv. Kanzler) were sown in two rows in plant containers (37 x 15 cm) with a substrate consisting of 50% clay and 50% sand. Plants raised in growth chamber with photoperiod of 14/10 h (day/night), a light intensity of 100/0 µmol m^{-2} s^{-1}, a temperature of 20/18±2 °C and a relative humidity of 60/70±5%. Water was supplied from the bottom without wetting the leaves. Control and rust-infected plants were fertilised with nitrogen (60 kg N/ha) as supplied by ammonium nitrate. Plants in the treatment with N-deficiency remained unfertilised.

2.2 Pathogen infection

Mildew and rust infections were induced at the 3-4 leaf stage when plant height was approximately 20 cm. For initiation of leaf rust infection, plants were sprayed with a suspension of *Puccinia triticina* spores in a Tween 20 solution and placed under a plastic cover for 24 h to maintain high humidity. Mildew inoculation was conducted by dispersing freshly collected *Blumeria graminis* spores on the top of the trial plants. In order to prevent uncontrolled infections, plants of control and N-deficiency groups were treated with a fungicide (Fortress®, Dow AgroScience, USA).

2.3 Laser-induced chlorophyll fluorescence

LIF measurements were done with a hand-held fluorometer of MiniVegN (Fritzmeier GmbH & Co KG, Großhelfendorf, Germany). Chlorophyll fluorescence was induced with a red (662 nm) light emitting laser diode with full width at half maximum of 3 nm, pulse energy of 200 mW and laser pulse frequency of 500 Hz. The fluorescence signals were detected with two photomultipliers at 692±2 nm (F690) and 730±2 nm (F730) at a sensor viewing area of about 0.5 mm^2 for each measuring point. The fluorescence ratio was calculated as F690/F730. Fluorescence measurements were started two days after inoculation with pathogens and conducted at a 1-2 day interval in the growth chamber. Fluorescence was recorded in the light at leaf and canopy levels. During leaf measurements, sensor was moved from the middle to the top of leaf lamina with close contact to the leaf surface. Recordings were taken on upper (adaxial) and lower (abaxial) leaf sides. Canopy fluorescence was recorded in plant rows (35 cm in length, 30 plants each), by manually moving the sensor with constant velocity at 2/3

of plant height. For both leaf and canopy measurements, mean values and standard deviations were calculated from 4 s fluorescence readings.

2.4 Leaf chlorophyll content

The leaf chlorophyll content was assessed with Minolta SPAD 502 chlorophyll meter (Konica Minolta, Langenhagen, Germany). The instrument quantifies leaf chlorophyll content by measuring red (~ 650 nm) and infra-red (~ 940 nm) light transmission. The SPAD values were estimated on adaxial leaf sides immediately after fluorescence recordings. As reference, chlorophyll content was determined destructively in leaf sections of 1.5 cm^2 with dimethyl sulfoxide (DMSO) according to Blanke (1992). The absorbance of extracts was evaluated at 665 nm (A_{665}) and 647 nm (A_{647}) with a UV-VIS spectrophotometer (Perkin-Elmer, Lambda 5, Massachusetts, USA). Chlorophyll a (C_a) and b (C_b) concentrations were calculated according to the following equations: $C_a = 12.7 \times A_{665} - 2.79 \times A_{647}$, $C_b = 20.7 \times A_{647} - 4.64 \times A_{665}$ (Moran, 1982; Blanke, 1992). A linear function (y=1.05x-0.73) between chlorophyll content and SPAD values was established for plants differing in N supply (Fig. 1) and used for calculation of leaf chlorophyll content on basis of SPAD measurements.

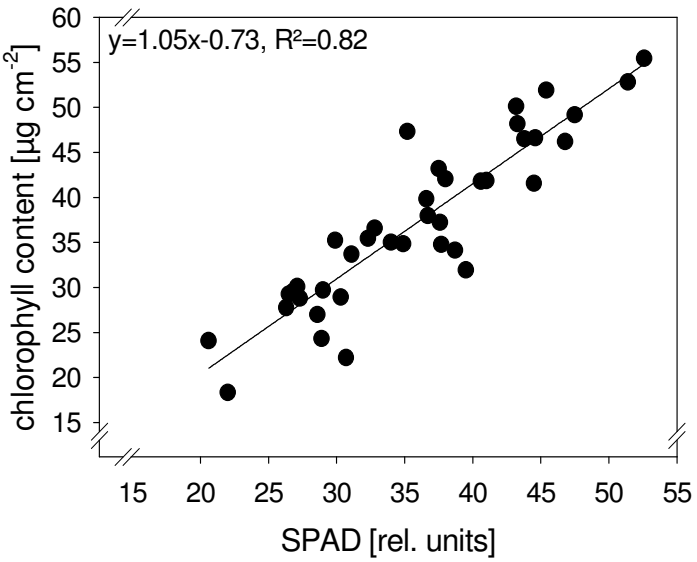

Fig. 1: Correlation between SPAD values and chlorophyll content of winter wheat leaves as affected by different levels of nitrogen supply (n=40).

2.5 Statistics

Experimental data were analysed with the SPSS 12.0 software for Windows (SPSS Inc., Chicago, USA). After testing for normal distribution and variance homogeneity, data were subjected to analysis of variance (ANOVA). The 95 % probability level was taken to indicate significant differences. Means were compared by Tukey HSD multiple range test. Values presented in the figures 3-4 were averaged from the recordings taken on upper and lower leaf sides. Data in figures represent means calculated from replicate measurements.

Leave-one-out-cross-validation analysis was performed with recordings taken at the last three sampling dates (7, 8, 10 dai, days after inoculation) to examine whether treatments of control, N-deficiency, leaf rust and powdery mildew could be differentiated by means of estimated fluorescence parameters. Analysis was conducted with 1) mean values of F690 and F730 and 2) mean and standard deviation (SD) values of F690 and F730.

3 Results

3.1 Development of N-deficiency and pathogen infection symptoms

As early as at the first sampling date, winter wheat plants with N-deficiency displayed less green leaves due to the lower chlorophyll content. These symptoms became more pronounced during the following days (Fig. 2). At the end of experiment, N-deficient plants showed reduced growth and green-yellow coloured leaves with distinct chlorosis on the leaf tips.

First visual symptoms of leaf rust infection became apparent at the 6^{th} dai as heterogeneously distributed chlorotic spots on upper and lower leaf sides (Fig. 2). Within 24 h, these spots enlarged, and small red-brown pustules appeared in their centres. At the end of the experiment (10^{th} dai), 5-10% of the leaf surface was covered by rust pustules.

Plants inoculated with powdery mildew showed first visual symptoms in form of small whitish mycelium patches at the 8^{th} dai, e.g. two days later than those with rust infection (Fig. 2). During the next two days, the number of these patches increased and strong pronounced chlorosis became visible underneath the pustules. At the last sampling date, approximately 15% of leaf surface was covered by mildew mycelium.

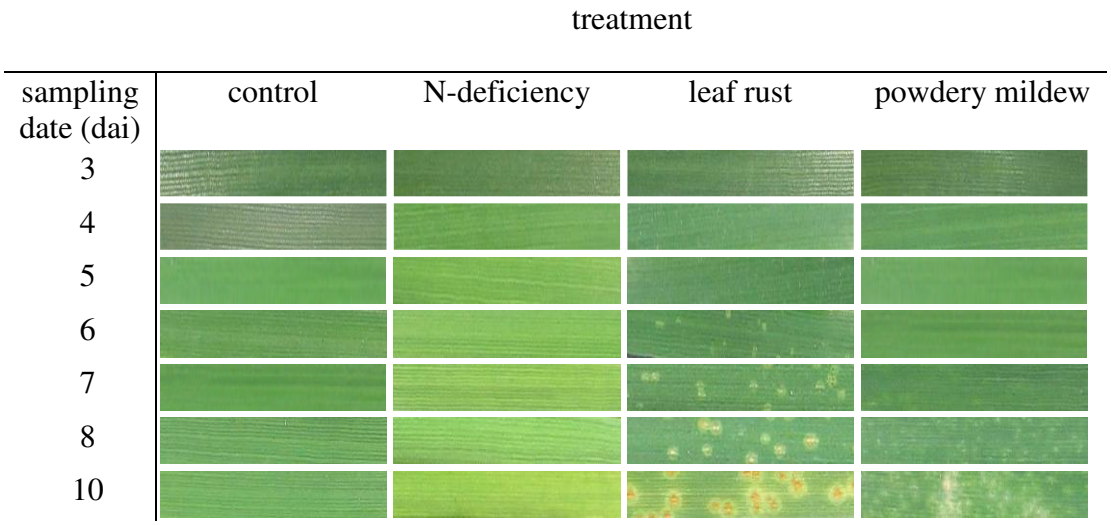

Fig. 2: Development of N-deficiency, leaf rust and powdery mildew symptoms on adaxial leaf sides of winter wheat during the experimental period.

3.2 Fluorescence measurements at leaf level

Chlorophyll content in the plants with N-deficiency was decreased by 17% in comparison to control at the first sampling date. As a consequence, F690/F730 ratio was by 10% higher than in control (Fig. 3A) due to an increased fluorescence emission at 690 nm. During the following days, N-deficiency treatment showed a continuous loss in leaf chlorophyll accompanied by an increase in F690/F730 values. At the last day of experiment, N-deficient leaves showed by 37% lower chlorophyll content and by 20% increased F690/F730 index as compared to control. Correlation analysis of control and N-deficiency treatment data revealed a strong linear relationship (R^2=0.81) between chlorophyll content and F690/F730 ratio (Fig. 4A). However, when including data of the pathogen treatments in the correlation analysis, only a very low (R^2=0.16) relationship was found (Fig. 4B).

In contrast to N-deficiency, leaves with pathogen infection did not differ significantly from control either in chlorophyll content or in F690/F730 ratio at the beginning of experiment. Wheat seedlings inoculated with leaf rust displayed a slightly higher fluorescence ratio one day after the appearance of first reddish pustules (8^{th} dai). Within the next two days, rust pustules with surrounding chlorosis enlarged and F690/F730 increased to 1.18 units (Fig. 3A).

The development of mildew infection was not accompanied by significant changes in mean values of F690/F730 ratio during 8 days after inoculation. However, at the end

of experiment, at 10th dai, a distinct increase of F690/F730 ratio to 1.67 units (Fig. 3A) was observed in this treatment.

Throughout the experiment, control and N-deficient treatments did not differ in the standard deviation of F690/F730 recordings taken at the leaf level. From the 8th dai, a higher heterogeneity of fluorescence ratio was detected in seedlings inoculated with leaf rust (Fig. 3B). The increased standard deviation of fluorescence recordings taken on leaves with powdery mildew infection was found only at the 10th dai. At this sampling date, heterogeneity of F690/F730 ratio was 7-8 fold higher for leaf rust and 14-15 fold higher for powdery mildew in comparison to N-deficiency and control treatments (Fig. 3B).

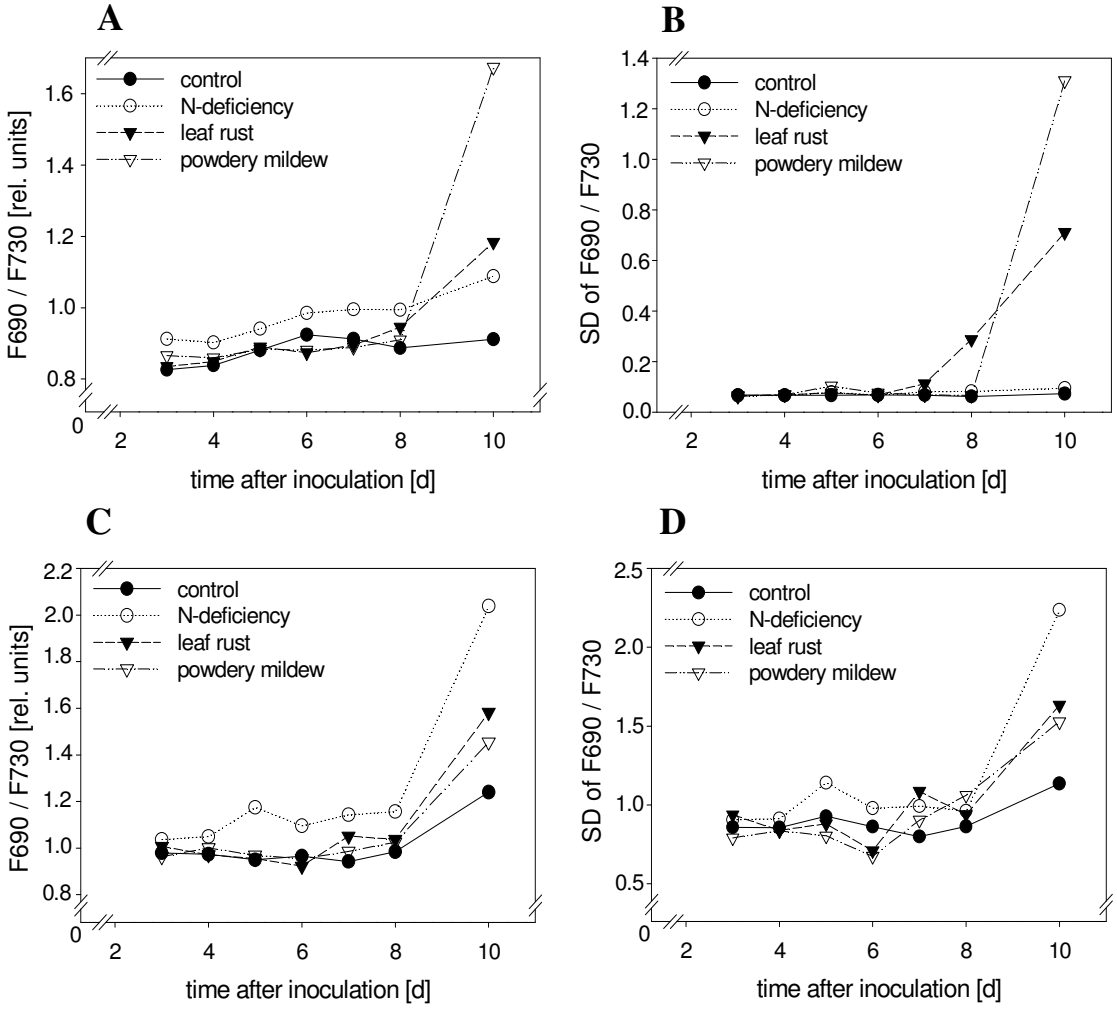

Fig. 3: Mean values (A, C) and standard deviation (B, D) of F690/F730 fluorescence ratio of winter wheat leaves as affected by N-deficiency, leaf rust and powdery mildew infections. Readings were taken at leaf (A, B) and canopy (C, D) level. Data presented for the measurements at leaf level were averaged from values of adaxial and abaxial leaf sides (n=6).

Comparison of fluorescence parameters on the upper and lower leaf sides revealed some differences in fluorescence parameters. In all treatments, except for those with leaf rust and mildew infections at the 8th and 10th dai (Fig. 5), respectively, by 1-7% lower F690/F730 values were detected on the abaxial in comparison to adaxial leaf sides. At 8th dai, leaf sides of rust infected seedlings did not show major differences in chlorophyll fluorescence ratio, whereas leaves with mildew pustules (Fig. 5) displayed by 19% lower F690/F730 values at the end of experiment (10 dai).

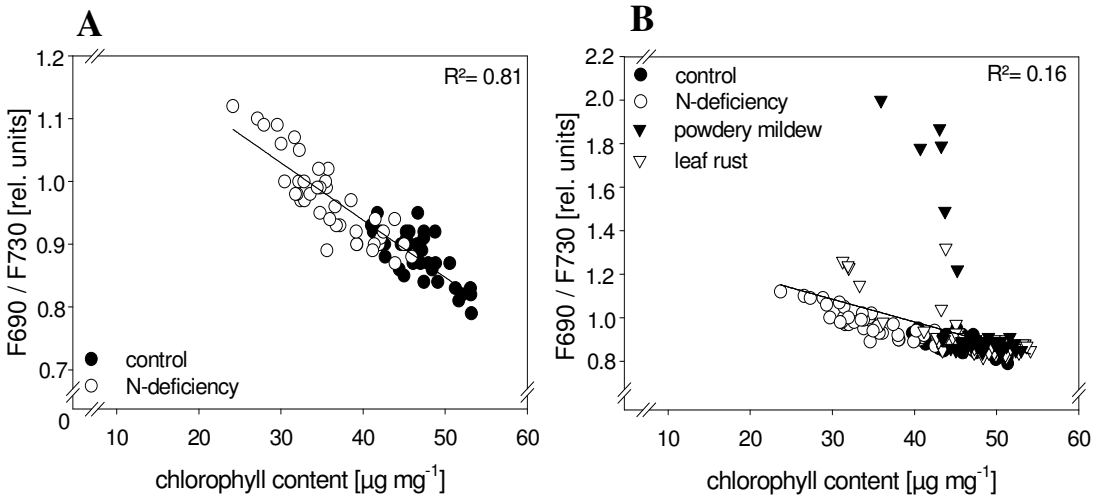

Fig. 4: Relation between chlorophyll content and F690/F730 ratio, calculated for the treatments of A) control and N-deficiency (n=84), B) control, N-deficiency, leaf rust and powdery mildew (n=168). Data presented are averaged from adaxial and abaxial leaf sides.

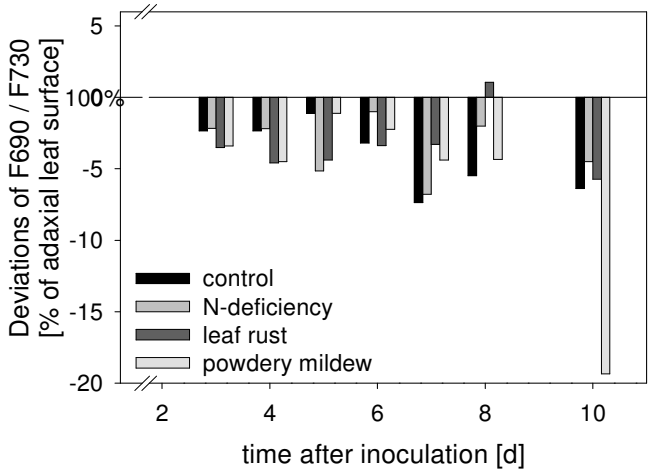

Fig. 5: Comparison between F690/F730 ratio of N-deficiency, powdery mildew and leaf rust infections on adaxial and abaxial sides of winter wheat leaves during the experimental period, as related to adaxial (=100%) leaf surface (n=6).

3.3 Fluorescence measurements at canopy level

Mean values of F690/F730 in the treatment with N-deficiency displayed at canopy level a similar tendency as those found at leaf level. At the beginning of experiment, N-deficient plants showed a chlorophyll fluorescence ratio of 1.04 units which was 6% higher in comparison to control (Fig. 3C). During the experimental period, a continuous increase of this index was observed, and at the end of experiment, a value of 2.04 was reached. In leaf rust and powdery mildew treatments, F690/F730 increased significantly by 16% and 27%, respectively, as compared to control, only at the last sampling date. However, this was by 23% or 51% lower than ratio of N-deficient plants at this date (Fig. 3C).

Heterogeneity of F690/F730 ratio was more pronounced at canopy than at leaf level, indicated by e.g. 3-12-fold higher variation coefficients for all sampling dates (data not shown). As for heterogeneity of fluorescence signals at the canopy level, plants with N-deficiency displayed higher values of standard deviation at 5^{th}, 6^{th} and 10^{th} sampling date as compared to other treatments. At the last day of experiment, a strong, but less pronounced increase in standard deviation in the pathogen infected variants was detected (Fig. 3D), as compared to N-deficient wheat plants.

3.4 Cross-validation analysis

In order to evaluate the potential of LIF parameters for discrimination between control, N-deficiency, leaf rust and powdery mildew treated wheat leaves or plants, leave-one-out-cross-validation was performed. Analysis was made for the data obtained at the last three sampling dates (7^{th}, 8^{th}, 10^{th} dai), when visual symptoms of pathogen infections became evident. The results showed that percentage of misclassified N-deficiency samples increased with progression of leaf rust infection at both tested levels if only mean values of F690 and F730 were taken for analysis (Tab. 1). At the last sampling date, 70% or 33%, of N-deficient samples were misclassified as leaf rust at leaf or canopy level, respectively.

At leaf level, analysis based only on mean values of both fluorescence maxima resulted in 83%, 67% and 30% of correct N-deficiency classification at 7^{th}, 8^{th} and 10^{th} dai, respectively. However, classification rates could be improved to 83%, 92% and 90%, when the heterogeneity at F690 and F730 was additionally included as discrimination criterion. The same, but more pronounced tendency could also be observed for canopy level.

Tab. 1: Classification matrix of "leave-one-out-cross-validation" analysis as assigned for control, N-deficiency, leaf rust and powdery mildew treatments. Analysis was performed on basis of 1) mean values (Mean) of F690 and F730 and 2) mean values + standard deviation (SD) of F690 and F730. Values in **bold** indicate the percentage of correctly identified cases (n=6).

	Percent classified into treatment							
	control	N-deficient	leaf rust	powdery mildew	control	N-deficient	leaf rust	powdery mildew
	(F690 and F730) Mean				**(F690 and F730) Mean + SD**			
Measurements at 'leaf level'								
				7 dai				
control	**30**	10	40	20	**20**	10	40	30
N-deficient	0	**83**	0	17	0	**83**	0	17
leaf rust	17	0	**25**	58	8	8	**50**	33
powdery mildew	17	0	25	**58**	50	0	8	**42**
				8 dai				
control	**50**	0	8	42	**58**	8	0	33
N-deficient	0	**67**	33	0	0	**92**	0	8
leaf rust	50	33	**0**	17	0	0	**58**	42
powdery mildew	17	0	50	**33**	50	0	17	**33**
				10 dai				
control	**100**	0	0	0	**92**	8	0	0
N-deficient	0	**30**	70	0	10	**90**	0	0
leaf rust	17	42	**25**	17	17	0	**75**	8
powdery mildew	0	0	17	**83**	0	17	0	**83**
Measurements at 'canopy level'								
				7 dai				
control	**0**	67	0	33	**0**	0	0	100
N-deficient	17	**0**	33	50	17	**83**	0	0
leaf rust	17	33	**17**	33	17	17	**50**	17
powdery mildew	50	17	0	**33**	50	0	33	**17**
				8 dai				
control	**17**	33	33	17	**50**	0	33	17
N-deficient	20	**40**	20	20	0	**100**	0	0
leaf rust	33	0	**33**	33	0	0	**67**	33
powdery mildew	0	25	25	**50**	25	25	25	**25**
				10 dai				
control	**75**	0	25	0	**75**	0	25	0
N-deficient	33	**33**	33	0	0	**83**	0	17
leaf rust	0	33	**17**	50	33	0	**50**	17
powdery mildew	17	17	17	**50**	17	17	33	**33**

Cross-validation conducted with mean values and standard deviation caused an increase in classification results for N-deficient plants by 83%, 60% and 50% to 83%, 100% and 83% at the 7th, 8th and 10th dai, respectively. The percentage of correctly classified cases for plants treated with leaf rust also increased from 0-25% to 50-75% at leaf level and from 17-33% to 50-67% at canopy level for the last three sampling dates. However, the low identification accuracy of plants infected with powdery mildew was not improved by considering spatial heterogeneity of chlorophyll fluorescence intensities.

4 Discussion

In the literature, the relation between chlorophyll content and F690/F730 ratio is well described (Agati et al., 1993; Buschman 2007). Recent investigations indicate a great potential of LIF for detection of N-deficiency in crop fields (Bredemeier and Schmidhalter, 2003; Schächtl et al., 2005; Limbrunner and Maidl, 2007). However, the possible influence of a pathogen infection on chlorophyll content and F690/F730 ratio was neglected in these studies.

Our results clearly show that a close correlation between fluorescence ratio and chlorophyll content as detected by SPAD measurements (Fig. 4A) may be missing in case samples with leaf rust and powdery mildew pustules are included in the correlation analysis (Fig. 4B). This may be due to the shielding effect of the fungal structures on the leaf surface (Kuckenberg et al., 2007) reducing absorption (Tartachnyk et al., 2006) and penetration depth of the light applied for fluorescence or transmission measurements and affecting in this way corresponding records. Also the alterations in the internal leaf anatomy with progression of fungal development may contribute to the variation in chlorophyll fluorescence ratio and SPAD values.

In our work, we compared effects of N-deficiency and leaf rust or mildew infections on the fluorescence recordings taken in ‘multipoint’ scanning mode with high measuring frequency at leaf and canopy level. We supposed that considering the variability of the fluorescence signals estimated by standard deviation for ‘multipoint’ fluorescence recording may improve identification accuracy of these plant stresses.

Fluorescence recordings taken on canopy displayed by 1.1-1.3 fold higher mean values and by 3-12 fold higher variation coefficients of F690/F730 as compared to those taken at leaf level in all tested treatments. This can be explained by the fact, that with canopy measurements, plant tissues with low chlorophyll content, such as leaf veins and stems, also contribute to the averaged fluorescence values. A possible source of higher variation at the canopy level might be the difference between the values of

fluorescence ratio on the upper and lower leaf sides as established in our experiment. In most treatments we observed slightly (by 1-7%) lower F690/F730 values on abaxial than on adaxial leaf sides (Fig. 5). This extends previous findings in which noticeable differences in chlorophyll fluorescence ratio on the opposite leaf sides have been described for leaves with bifacial structure (Tartachnyk and Rademacher, 2003; Lichtenthaler et al., 2005; Buschman 2007). Higher F690/F730 ratio found on the adaxial sides of winter wheat leaves indicates the high sensitivity of the employed LIF system, since it allowed detecting the lower chloroplast density on the adaxial as compared to the abaxial side. This is most certainly related to the larger portion of sclerenchyma, vascular bundle and bulliform cells on the adaxial leaf side of graminaceae (Takahashi et al., 1994; Kirby, 2002).

With fluorescence signals at the canopy level, plants with N-deficiency displayed higher values of standard deviation at 3 sampling dates as compared to other treatments. This reflects a vertical gradient in chlorophyll content due to strong nutrient re-mobilisation, which is typical for plants grown under reduced N supply (Dreccer et al., 2000). At the last sampling date, strong chlorosis on the leaf tips of N-deficient plants, could also contribute to the enhanced heterogeneity at the canopy level.

Our results on higher variability of fluorescence signals in the canopy with nitrogen deficiency are consistent with the study of Bélanger et al. (2006) on potato plants, in which the impact of measurement angles on the potential of LIF for nutrient deficiency detection was evaluated. Different values of F690/F740 ratio were observed in this work by taking fluorescence measurements at an angle of 0°, 45°or 90°. It has been concluded that N-deficiency was more easily detected when the fluorometer was targeted at older leaves (angle of 45), which were earlier affected by the nitrogen shortage.

With respect to identification of plant stress, the results of cross-validation analysis conducted with mean F690 and F730 values showed that percentage of miss-classified plants with N-deficiency increased with progression of pathogen infections at both leaf and canopy levels (Tab. 1). Beside this, samples with pathogen (rust and mildew) infections were miss-classified to some extend as N-deficiency at both levels at the last three sampling dates. In addition, samples with leaf rust were more often miss-recognised as N-deficiency than those with powdery mildew. This is probably due to the stronger chlorophyll breakdown in leaves during progression of rust infection. This is consistent with our previous results on discrimination between abiotic and biotic plant stresses (Tartachnyk et al., 2006) and shows that with F690, F730 measurements

at canopy level, patches with advanced pathogen infection with high probability may be miss-interpreted as N-deficiency.

Combination of F690 and F730 mean values with their standard deviations significantly improved the accuracy of discrimination between N-deficiency and pathogen (leaf rust and powdery mildew) infection treatments. This was documented also at the last day of experiment despite of increased standard deviation of chlorophyll fluorescence ratio in the treatment with N-deficiency. Thus, the results of our experiment do confirm our hypothesis and clearly indicate that estimation of spatial variability of chlorophyll fluorescence parameters improve identification accuracy of N-deficiency and pathogen infection at both leaf and canopy level. However, reliable differentiation under field conditions may be difficult to accomplish due to variability of symptoms induced by these stresses.

The discrimination rating between rust and mildew infection was insufficient on the base of employed parameters. At the same time, for the treatment with powdery mildew, the lowest percentage of correct classification was found, especially at stages with initial visual symptoms. Here, a high percentage of samples was miss-classified as control, N-deficiency and leaf rust at both leaf and canopy level. These results indicate that early recognition of mildew infection can not be accomplished by means of the employed chlorophyll fluorescence technique. For early detection of this pathogen, a combination of chlorophyll fluorescence with UV-induced blue and green fluorescence (Lüdecker et al. 1996) or/and reflection parameters (Tartachnyk et al. 2006) would be more promising. Further studies are still needed to develop the LIF technique for early detection and discrimination of biotic and abiotic stresses.

5 References

Agati, G., Fusi, F., Mazzinghi, P., and Lipucci Di Paola, M. 1993. A simple approach to the evaluation of the reabsorption of chlorophyll fluorescence spectra in intact leaves. Journal of Photochemistry and Photobiology B-Biology **17**, 163-171.

Bélanger, M.-C., Viau, A. A., Samson, G. and Chamberland, M. 2006. Near-field fluorescence measurements for nutrient deficiencies detection on potatoes (*Solanum tuberosum* L.): Effects of the angle of view. International Journal of Remote Sensing **27** (19), 4181-4198.

Blanke, M. M. 1992. Determination of chlorophyll using DMSO. Wein-Wissenschaft **47**, 32-35.

Bodria, L., Fiala, M., Naldi, E. and Oberti, R. 2002.Chlorophyll fluorescence sensing for early detection of crop's diseases symptoms. In: Proceedings 2002 International ASAE Conference and XV CIGR World Congress / ASAE-CIGR. - ASAE-CIGR, 2002, Paper No. 021114, p. 1-15.

Bredemeier, C. and Schmidhalter, U. 2003. Non-contacting chlorophyll fluorescence sensing for site-specific nitrogen fertilization in wheat and maize. In: Precision Agriculture'03: Proceedings of 4th European Conference on Precision Agriculture, edited by J.V. Stafford and A. Werner (Wageningen Academic Publishers, The Netherlands), p. 103-108.

Buschmann, C. 2007. Variability and application of the chlorophyll fluorescence emission ratio red/far-red of leaves. Photosynthesis Research **92**, 261-271.

Dreccer, M. F., Van Oijen, M., Schapendonk, A. H. C. M., Pot, C. S. and Rabbinge, R. 2000. Dynamics of vertical leaf nitrogen distribution in a vegetative wheat canopy. Impact on canopy photosynthesis. Annals of Botany **86**, 821-831.

Kirby, E. J .M. 2002. Botany of the wheat plant. In: Bread Wheat, Improvement and Production, edited by B.C. Curtis, S. Rajaram and H. Gomez Macpherson, FAO Plant Production Series No. 30, Rome 2002.

Kuckenberg, J., Tartachnyk, I., Schmitz-Eiberger, M. and Noga, G. 2007. Early detection of leaf rust and powdery mildew infections on wheat leaves by PAM fluorescence imaging. In: Precision Agriculture'07: Proceedings of 6th European Conference on Precision Agriculture, edited by J.V. Stafford (Wageningen Academic Publishers, The Netherlands), p. 515-521.

Lichtenthaler, H. K. and Miehe, J. A. 1997. Fluorescence imaging as a diagnostic tool for plant stress. Trends in Plant Science **2** (8), 316-320.

Lichtenthaler, H. K., Buschmann, C. and Knapp, M. 2005. How to correctly determine the different chlorophyll fluorescence parameters and the chlorophyll fluorescence decrease ratio R_{Fd} of leaves with the PAM fluorometer. Photosynthetica **43** (3), 379-393.

Limbrunner, B. and Maidl, F.-X. 2007. Non-contact measurement of the actual nitrogen status of winter wheat canopies by laser-induced chlorophyll fluorescence. In: Precision Agriculture'07: Proceedings of 6th European Conference on Precision Agriculture, edited by J.V. Stafford (Wageningen Academic Publishers, The Netherlands), p. 173-179.

Lüdecker, W., Dahn, H. G. and Guenther, K. P. 1996. Detection of fungal infection of plants by laser-induced fluorescence: an attempt to use remote sensing. Journal of Plant Physiology **148** (5), 579-585.

Moran, R. 1982. Formulae for determination of chlorophyllous pigments extracted with N,N-Dimethylformamide. Plant Physiology **69**, 1376-1381.

Nicolas, H. 2004. Using remote sensing to determine of the date of a fungicide application on winter wheat. Crop Protection **23**, 853-863.

Noh, H., Zhang, Q., Shin, B., Han, S. and Feng, L. 2006. Neural network model of maize crop nitrogen stress assessment for a multi-spectral imaging sensor. Biosystems Engeneering **94** (4), 477-485.

Schächtl, J., Huber, G., Maidl, F.-X. and Sticksel, E. 2005. Laser-induced chlorophyll fluorescence measurements for detecting the nitrogen status of wheat (*Triticum aestivum* L.) canopies. Precision Agriculture **6**, 143-156.

Scholes, J.D. and Rolfe, S. A. 1996. Photosynthesis in localised regions of oat leaves infected with crown rust (*Puccinia coronata*): quantitative imaging of chlorophyll fluorescence. Planta,**199**, 573-582.

Takahashi, K., Mineuchi, K., Nakamura, T., Koizumi, M. and Kano, H. 1994. A system for imaging transverse distribution of scattered light and chlorophyll fluorescence in intact rice leaves. Plant, Cell & Environment **17** (1), 105-110.

Tartachnyk, I. and Rademacher, I. 2003. Estimation of nitrogen deficiency of sugar beet and wheat using parameters of laser induced and pulse amplitude modulated chlorophyll fluorescence. Journal of Applied Botany **77**, 61-67.

Tartachnyk, I., Rademacher, I. and Kühbauch, W. 2006. Distinguishing nitrogen deficiency and fungal infection of winter wheat by laser-induced fluorescence. Precision Agriculture **7**, 281-293.

Zillmann, E., Graef, S., Link, J., Batchelor, W. D. and Claupein, W. 2006. Assessment of cereal nitrogen requirements derived by optical on-the-go sensors on heterogeneous soils. Agronomy Journal **98**, 682-690.

D UV-B induced damage and recovery processes in apple leaves as assessed by LIF and PAM fluorescence techniques

1 Introduction

The stratospheric ozone depletion of at average 1.8% per decade in Europe (Stolarski et al., 1992) and consequent increases in UV-B radiation (Herman et al., 1996) in the last years stimulate investigations on assessing UV-B radiation effects on plants (Kakani et al., 2003). Enhanced UV-B radiation usually has negative impacts on photosynthetic activity (Zhao et al., 2004), growth (Gao et al., 2004) and reproductive development (Musil, 1994; Koti et al., 2004) of plants, resulting in significant reductions in crop quality and yield (Runeckles and Krupa, 1994).

At the cellular level, the major sites of UV-B impairment are chloroplasts, and PS II seems to be the most vulnerable component of thylakoid membranes (Bornman, 1989; Vass, 1997). Within electron transport chain, UV-B induced damages in Mn clusters of water-splitting enzyme complex (Renger et al., 1989; Post et al., 1996; Vass et al., 1996), Tyr-Z and Tyr-D electron donors (Vass et al., 1996), primary (Q_A) and secondary (Q_B), quinone acceptors of PSII, Q_AFe^{2+} complex and in plastoquinone (P_Q) pool have been established (Melis et al., 1992; Jansen et al., 1996; Vass et al., 1996). Besides electron transport components, also D1 and D2 protein subunits of PS II reaction centres may degrade due to UV-B radiation (Trebst and Depka, 1990; Melis et al., 1992; Friso et al., 1993; Friso et al., 1994). A protective mechanism of plants to enhanced UV-B irradiation is a rapid biosynthesis of UV-screening phenolic compounds such as flavonoids (Fedina et al., 2006) and hydroxycinnamic acid derivates in epidermal cells; also a rapid turnover and a replacement of damaged chloroplast proteins during UV-B stress have been reported (Burchard et al., 2000; Gao et al., 2004).

Since high UV-B flux affects components of photosynthetic apparatus, chlorophyll fluorescence may be a well suited method for monitoring UV-B stress. This technique delivers fast and extensive information about the potential and current efficiency of photosynthesis, the integrity of the photosynthetic apparatus, the relative functionality of different physiological protective mechanisms and the rate of photosynthetic electron transfer (for reviews see e.g. Maxwell and Johnson, 2000; Baker and Rosenqvist, 2004).

With PAM method, fluorescence is measured at different stages of electron transport chain by applying different light sources. Recently developed Puls-Amplitude-Modulated (PAM) imaging systems allow detecting whole leaf reactions to plant stress

in spatial and temporal resolution (Chaerle and van der Straeten, 2000). In most studies with PAM fluorescence techniques on different plant species, an increased ground fluorescence Fo and a decreased maximum fluorescence Fm was observed in response to UV-B stress (Sharma et al., 1998; Vass et al., 1999; Heraud and Beardall, 2000; Gilbert et al., 2004).

Less and very controversial information is available on detection of UV-B stress by means of Laser-induced-fluorescence (LIF). Recently, this method was developed as a technique of 'Precision farming' for determination of nitrogen requirement of plants and site-specific fertilisation under field conditions (Cecchi et al., 1994; Sticksel et al., 2001). The principle behind this approach is a negative correlation established between leaf chlorophyll concentration and red/near-infra-red chlorophyll fluorescence ratio F690/F735 (Rinderle and Lichtenthaler, 1988).

Precise information on the effect of enhanced UV-B irradiation on the LIF and PAM parameters is necessary for the interpretation of remote sensing data as basis for management decisions in precision agriculture. Further studies on UV-B stress are still needed to quantify the effects of UV-B radiation on crops in order to establish dose-response relationships (Kakani et al., 2003). In order to facilitate the development of dynamic simulation models for use in UV-B and other environmental impact assessments, information on course and rate of photosynthetic recovery from UV-B stress is also required.

Due to lack of such studies, the objective of this work was to evaluate the potential of LIF and PAM fluorescence techniques for early detection and quantification of UV-B induced damages in apple leaves. Of particular interest in this work was to assess dose-response relationships and time course of photosynthetic recovery from short term UV-B stress. We hypothesise that a) the impact of low UV-B radiation on apple leaves can be detected by LIF and PAM techniques with comparable success, even if no macroscopic damage is apparent; and b) that UV-B affected plants are able to recover from UV-B stress, dependent on the dose of UV-B radiation and the degree of damage.

2 Materials and Methods

2.1 Plant material

Apple (*Malus domestica* Borkh.) seeds were subjected to stratification for 21 days at 4 °C. After germination, seedlings were planted in pots (V=150 cm^3) with a substrate containing 50% commercial potting mixture and 50% sand and then transferred to

growth chamber. The apple seedlings were grown with a photoperiod of 14/10 h (day/night) at a temperature of 20/18±2 °C, a relative humidity of 60/70±15% and a light intensity of 100 µmol m^{-2} s^{-1}. The plants were fertilised with a Hoagland nutrient solution twice a week and supplied with water from the bottom, without wetting the leaves. For the experiments, uniformly developed apple seedlings at the stage of 5-6 fully expanded leaves were selected.

2.2 UV-B irradiation

UV-B stress was induced in an irradiation chamber with ten narrow-band (λ =311 nm) fluorescent lamps (Philips, TL 100 W/01) and ambient PAR intensity of about 100 µmol m^{-2} s^{-1}. The intensity of UV-B radiation was measured with a RM-21 spectroradiometer (Gröbel UV-Electronics, Ettlingen, Germany). In the experiment for assessment of dose-response relationships, plants were irradiated with UV-B fluxes of 10, 13, 18 or 26 W m^{-2} for 180 minutes. These resulted in a total biological effective UV-B (UV-B_{BE}) dose of 5.4, 7.0, 9.7, and 14.0 kJ m^{-2}, respectively, as weighted by Caldwell's generalised plant action spectrum (Caldwell, 1971).
Time course of photosynthetic recovery of the apple leaves was evaluated after exposure of seedlings to 20 W m^{-2} of UV-B light for 240 min and 360 min or 14.4 and 21.6 kJ m^{-2} biological effective UV-B doses, respectively. After UV-B treatments, plants were placed in the growth chamber with 100 µmol $m^{-2}s^{-1}$ PAR.

2.3 Chlorophyll a fluorescence

All fluorescence measurements were done at the adaxial side of the largest fully developed leaf after dark adaptation of plants for 20 minutes. The first fluorescence readings were conducted 2 hours after UV-B irradiation.

2.3.1 Laser-induced-fluorescence (LIF)

A blue light emitting diode with a maximum wavelength of 408 nm was applied for the excitation of fluorescence. The fluorescence spectra were recorded with a spectroradiometer Fieldspec™ VNIR (Analytical Spectral Devices ASD Inc., Boulder, USA) using an integration time of 1 s. The fiber-optic detector of this spectrometer had a conical view subtending a full angle of about 25 degrees. During the fluorescence measurements, the distance between detector and object level was set to 1 cm, providing a viewing surface area of about 0.2 cm^2. From the recorded spectra, the intensities of chlorophyll fluorescence at 686 nm (F686) and 740 nm (F740), the

F686/F740 ratio and the integral of fluorescence spectrum between 650 nm and 900 nm were estimated.

2.3.2 PAM-Imaging

The Imaging-PAM chlorophyll fluorometer (Walz, Effeltrich, Germany) was used to investigate the patterns of chlorophyll fluorescence and Red/NIR-light remission of UV-B irradiated apple leaves in temporal as well as in spatial resolution. Leaf images of ground fluorescence (Fo) were recorded by the mounted CCD camera (640 x 480 pixel) after illumination of the sample with blue light (470 nm) of 0.5 µmol m^{-2} s^{-1} PAR. The CCD camera was protected from stray excitation light by long-pass filter (RG 645, Schott, Mainz, Germany) and from long-wavelength ambient light by a short-pass filter (Calflex-X λ<780 nm, Balzer, Bingen, Gemany). Images of maximum fluorescence (Fm) were taken after a blue light saturation pulse of 2400 µmol m^{-2} s^{-1} PAR for 0.6 seconds at a stage when all reaction centres of PSII are closed, i.e. primary quencher Qa are completely reduced. The variable fluorescence (Fv) was estimated as Fm-Fo, the ratio of the variable fluorescence to Fo as (Fv/Fo) and the maximum photochemical efficiency (Fv/Fm) as (Fm-Fo)/Fm. In addition to fluorescence images, the remissions (reflected and scattered) of red (650 nm, Red) and near-infra-red (780 nm, NIR) light were estimated from which the PAR-Absorption (ABS) as 1-Red/NIR and the Normalised-Differenced-Vegetation-Index (NDVI) as (NIR-Red)/(NIR+Red) of investigated leaves were calculated.

2.3.3 PAM-2000

The portable chlorophyll fluorometer PAM-2000 (Walz, Effeltrich, Germany) was taken for assessing the photosynthetic recovery processes after UV-B treatment. Leaves were illuminated with red (with a peak of 650 nm) modulated light of 0.1 µmol m^{-2} s^{-1} PAR for the estimation of ground fluorescence (Fo). This was followed by a white saturation pulse of 1800 µmol m^{-2} s^{-1} PAR for 0.6 seconds in order to assess maximum fluorescence (Fm).

2.4 Chlorophyll content of leaves

For the assessment of chlorophyll content, leaf sections of 2.0 cm^2 in size were taken and stored in plastic bottles at –20 °C. The concentration of chlorophyll was determined according to Blanke (1992) after extraction with DMSO. The absorbance of extracts was evaluated at 665 nm (A_{665}) and 647 nm (A_{647}) with a UV-VIS

spectrophotometer (Perkin-Elmer, Lambda 5). The concentrations of chlorophyll a (C_a) and b (C_b) were calculated with the following equations:
$C_a = (12.7*A_{665} – 2.79*A_{647})$ and $C_b = (20.7*A_{647} – 4.64*A_{665})$.

2.5 Statistics

The experimental data were subjected to ANOVA with the SPSS 11.0 statistical package for windows (SPSS Inc., Chicago, USA). The 95 % probability level was accepted to indicate significant differences. Means were compared by Tukey HSD multiple range test after data were evaluated for normal distribution and variance homogeneity. Fluorescence, remission and chlorophyll content data presented were calculated from replicate measurements.

3 Results

3.1 Effect of different UV-B doses on remission and fluorescence characteristics of apple leaves

After irradiation with UV-B fluxes of 10, 13, 18 or 26 W m^{-2} for 180 minutes, apple leaves did not display any visible symptoms of damage. Neither leaf chlorophyll content nor chlorophyll a/b ratio or red and near-infra-red remission were affected by these doses (data not shown). In all treatments, apple leaves exhibited a chlorophyll content of 25 ± 3 µg cm^{-2} and ABS and NDVI values of 0.91 ± 0.01 and 0.84 ± 0.02, respectively.
As expected, both LIF and PAM fluorescence methods appeared to be well suited for an early detection of UV-B stress in apple seedlings.
Exposure of apple seedlings to UV-B radiation in the range of 10-26 W m^{-2} for 180 minutes reduced the intensity of chlorophyll fluorescence, estimated by the integral of fluorescence spectrum, by 17-30% (Fig. 1). Thereby, the decline of 25-41% to 4817-3764 units in the intensity of red fluorescence (F686) was more pronounced than that of 19-34% to 6287-5160 units in near-infra-red (F740). This resulted in a significant (6-12%) reduction of F686/F740 ratio to 0.76-0.72 units in all UV-B treatments except for the level of 18 W m^{-2} (Fig. 1).
A weak linear dose-effect relationship was found for the applied UV-B doses and the evaluated LIF parameters with determination coefficients (R^2) of 0.12 for the F686/F740 ratio, 0.30 for the integral of the spectrum, 0.34 for F686 and 0.38 for F740. Thus, among LIF parameters, F686 and F740 showed the strongest correlation with the applied UV-B doses. These parameters also enabled discrimination between

control plants, those treated with 10-18 W m^{-2} and 26 W m^{-2} of UV-B light. However, no significant difference among LIF parameters was found between the plants irradiated with 10, 13 or 18 W m^{2}.

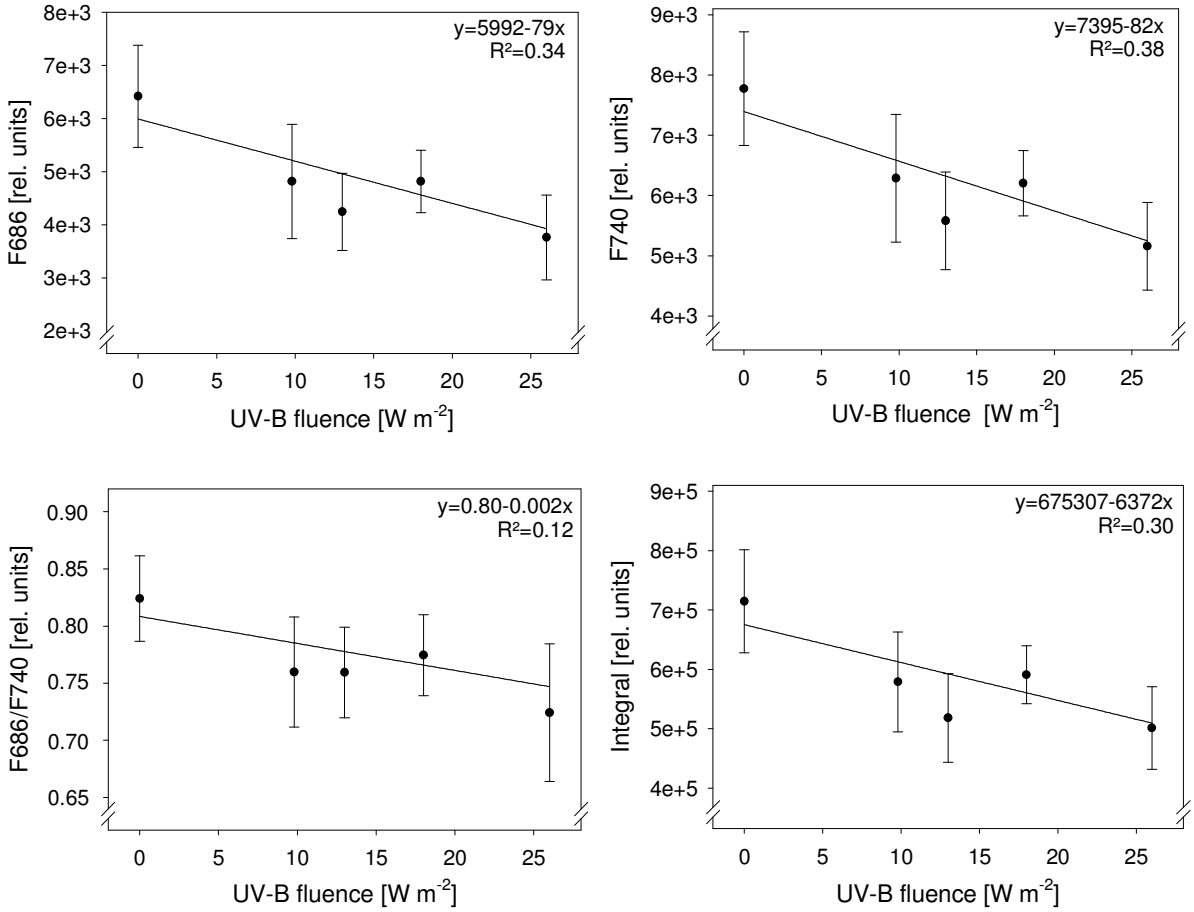

Fig. 1: Effect of different UV-B doses on LIF parameters of apple leaves. Leaves were irradiated for 180 minutes with UV-B fluencies of 10, 13, 18 or 26 W m^{-2}. Fluorescence measurements were done 2 hours after UV-B treatment. Vertical bars indicate ± standard deviation (n=15).

Measurements with PAM-Imaging showed slight increases of Fo and significant decreases of Fm, Fv, Fv/Fm and Fv/Fo in all UV-B treatments (Fig. 2). Two hours after exposure of plants to UV-B irradiation, ground fluorescence displayed 6-10% higher values than untreated plants. Other PAM fluorescence parameters were affected more strongly and showed significant reductions of 8-35% for Fm, 12-47% for Fv, 4-20% for Fv/Fm and 18-52% for Fv/Fo as compared to control (Fm=0.651; Fv=0.517; Fv/Fm=0.793; Fv/Fo=3.873 units). Thus, the most noticeable changes were observed for Fv/Fo ratio. A linear dose-effect relationship between PAM parameters and UV-B doses was found with higher determination coefficients compared to LIF

parameters of 0.44 for Fm, 0.50 for Fv, 0.48 for Fv/Fm and 0.58 for Fv/Fo. Similarly to the results obtained with LIF, significant differences in Fm related parameters were observed between control plants, those treated with 10-18 W m^{-2} or 26 W m^{-2} of UV-B light, respectively.

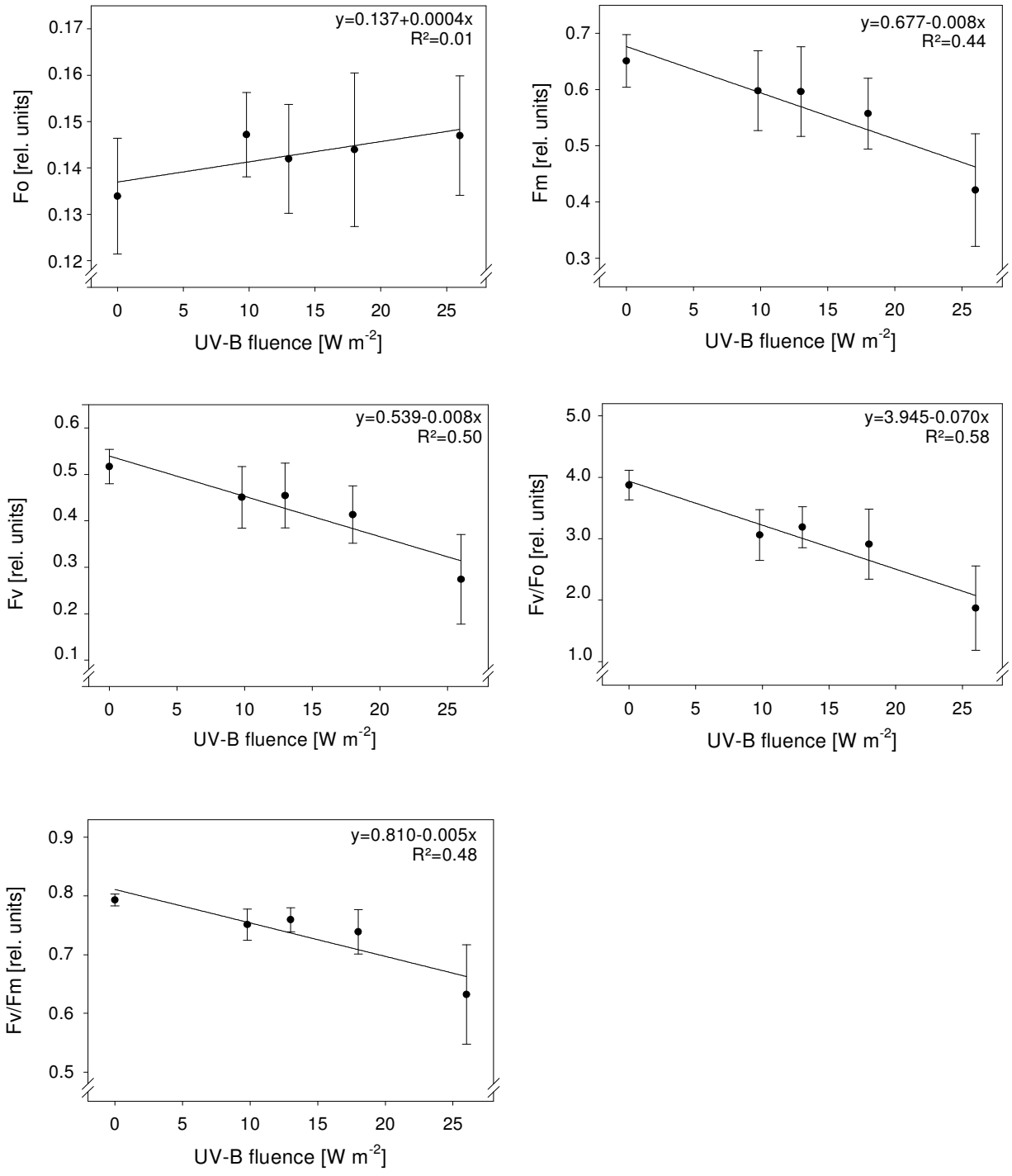

Fig. 2: Effect of different UV-B doses on PAM fluorescence parameters of apple leaves. Leaves were irradiated for 180 minutes with UV-B fluencies of 10, 13, 18 or 26 Wm^{-2}. Fluorescence readings were taken 2 hours after UV-B treatment. Vertical bars indicate ± standard deviation (n=15).

UV-B irradiation resulted in higher heterogeneity of PAM fluorescence parameters on the surface of apple leaves, evaluated on the basis of fluorescence imaging. Images of photochemical efficiency displayed more intense reduction along the leaf veins than in intercostal regions (Fig. 3), reflecting more pronounced changes in Fm as compared to Fo values in these areas.

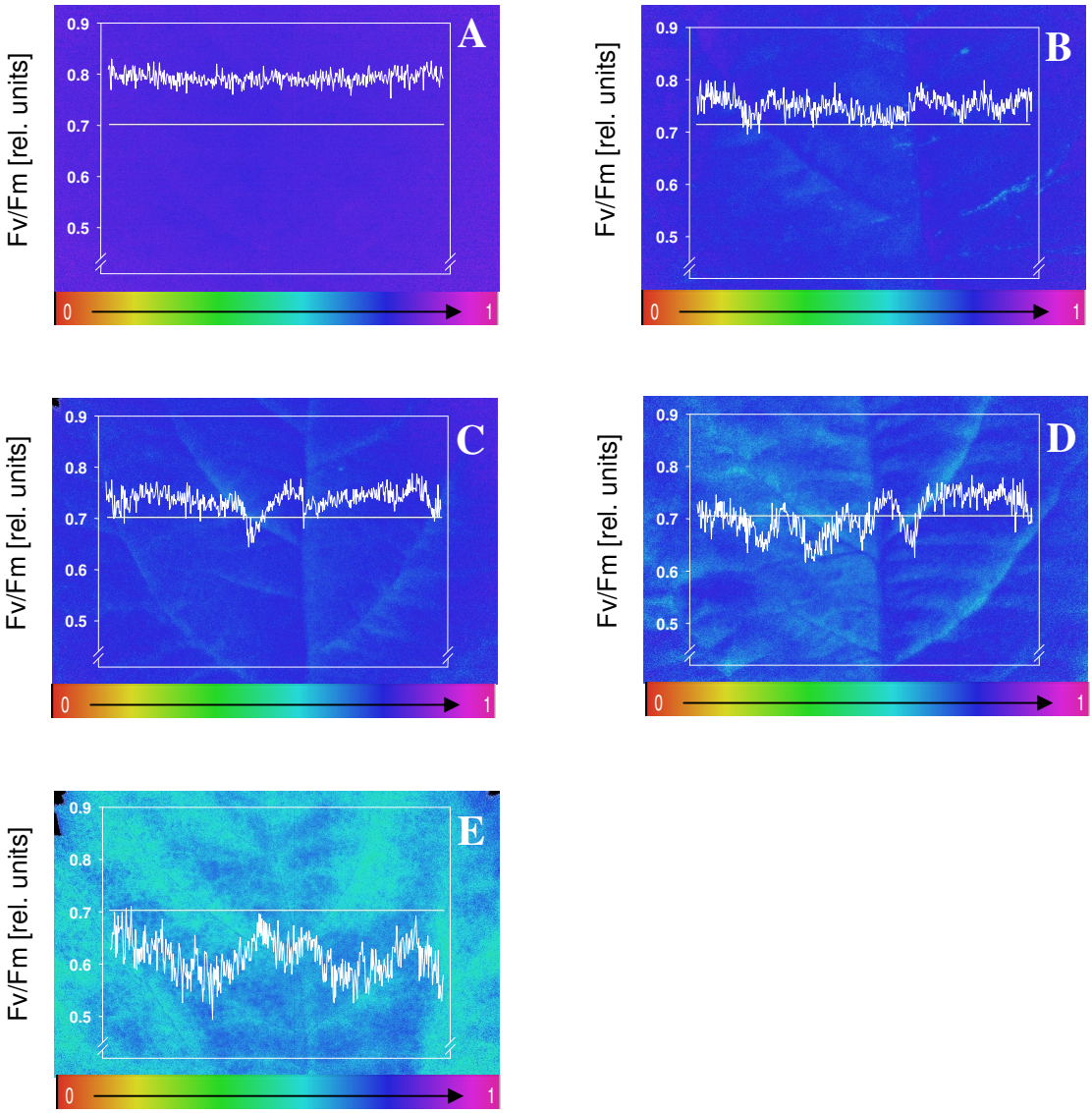

Fig. 3: Fv/Fm images of apple leaves irradiated for 180 minutes with UV-B fluencies of 0 (A), 10 (B), 13 (C), 18 (D) or 26 W m^{-2} (E). The Fv/Fm values are displayed for each pixel in the leaf profile (white horizontal line). Fluorescence measurements were made 2 hours after UV-B treatment.

3.2 Recovery of apple leaves after UV-B stress

The temporal response of photosynthetic recovery of apple leaves was studied after irradiation with 20 W m^{-2} of UV-B light for 240 or 360 minutes (Fig. 4).

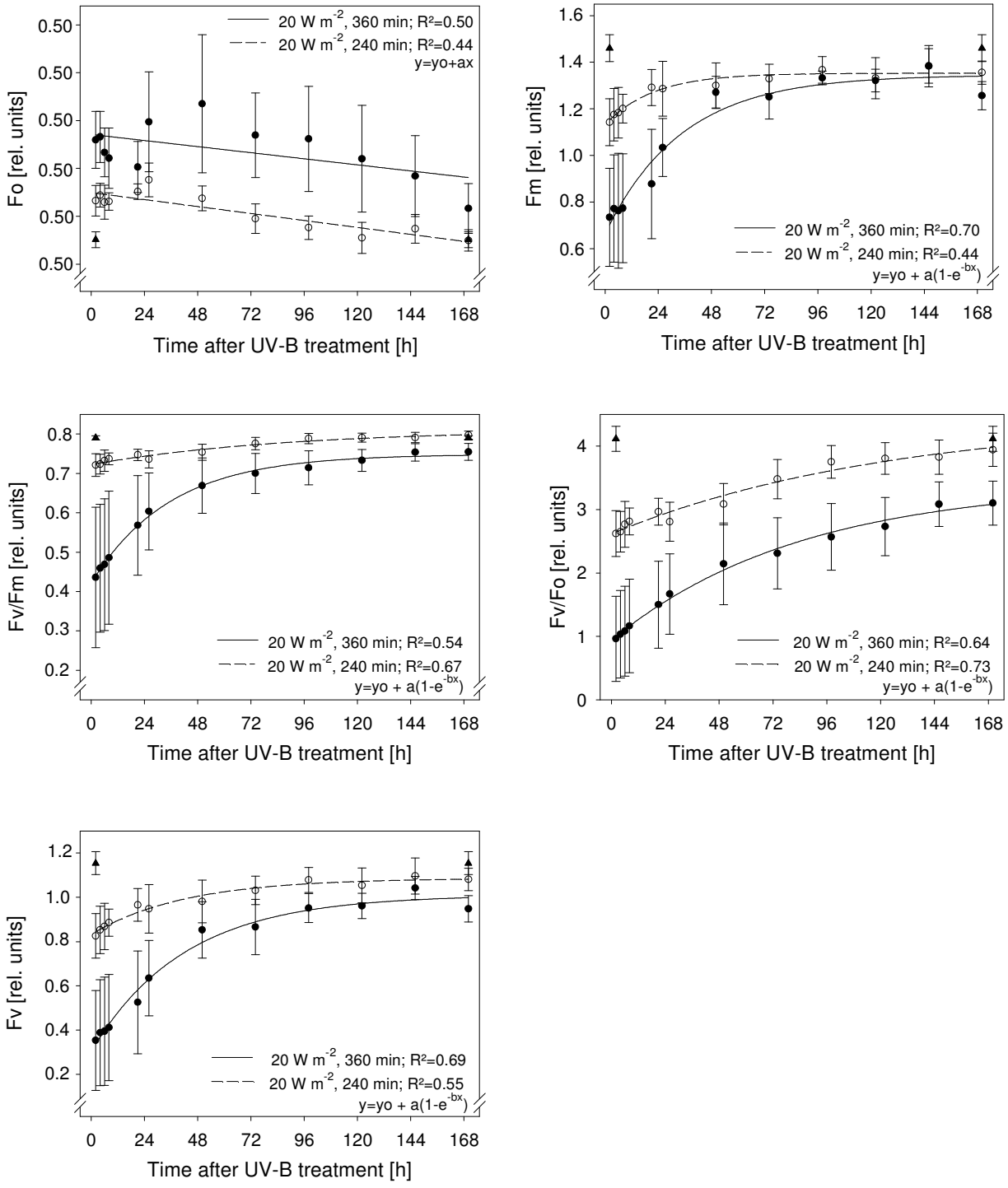

Fig. 4: Parameters of pulse amplitude modulated chlorophyll fluorescence of apple leaves before (triangle symbol) and after (circle) exposure to UV-B light. Leaves were irradiated for 240 (open symbols) or 360 minutes (closed symbols) with UV-B fluence of 20 Wm^{-2}. Vertical bars indicate ± standard deviation (n=8).

Two hours after these treatments, apple leaves exhibited 14% or 24% higher Fo and 19% or 50% lower Fm values than control plants (Fo=0.276 or 0.306; Fm=1.409 or 1.460 units). These changes resulted in a decrease of Fv, Fv/Fo, and Fv/Fm, respectively, by 27%, 36% and 10% after 240 and by 69% 74% and 45% after 360 minutes of UV-B irradiation.

The disturbance in photosynthetic functionality was followed by a continuous recovery process as indicated by restoring PAM fluorescence parameters (Fig. 4). The increase of Fm related parameters was most pronounced during the first two days after exposure to UV-B light for 240 and 360 minutes with a rate of 3.2×10^{-3} and 1.1×10^{-2} units per hour for Fm, 3.2×10^{-3} and 1.0×10^{-2} for Fv, 9.8×10^{-3} and 2.4×10^{-2} for Fv/Fo, 6.7×10^{-4} and 4.8×10^{-3} for Fv/Fm, respectively.

In contrast to this, ground fluorescence (Fo) did not display a rectilinear recovery response during the first two days after UV-B treatment. The recovery curves of Fm, Fv, Fv/Fo and Fv/Fm during a week after UV-B exposure showed a good fitting with exponential rise to maximum function, such as: $y = y_o + a(1 - e^{-bx})$. Within 7 days after UV-B stress, apple leaves irradiated for 240 or 360 minutes still displayed lower values of Fm (by 4% or 14%), of Fv (by 5% or 18%) of Fv/Fo (by 4% or 18%) and of Fv/Fm (by 5% or 1%) compared to control (Fig. 4), indicating partial recovery from UV-B stress. The spatial heterogeneity of all PAM fluorescence parameters, as affected by UV-B stress, also decreased in the course of recovery processes (Fig. 5). However, 7 days after exposure to UV-B irradiation, apple leaves still displayed higher variability of leaf fluorescence parameters in comparison to control plants.

4 Discussion

The exposure of apple seedlings to UV-B radiation of 10-26 W m^{-2} for 180 minutes affected neither leaf chlorophyll content nor chlorophyll a/b ratio or ABS and NDVI. Damages induced by UV-B irradiation were not visually evident 2 hours after irradiation; however, they could be successfully detected both by PAM and LIF fluorescence techniques. With both fluorescence techniques, significant differences were found between control plants and those treated with 10-18 W m^{-2} or 26 W m^{-2} of UV-B light. However, neither PAM nor LIF allowed discrimination between plants irradiated with 10 W m^{-2}, 13 W m^{-2} or 18 W m^{-2} of UV-B light (Figs. 1, 2).

In our study apple leaves showed a decreased LIF after UV-B treatment. Similar results were obtained for peanut leaves in experiments conducted by Mineuchi et al. (2001), in which intensities of red and near-infra-red fluorescence, induced by Ar laser (351-364 nm), decreased when increasing UV-B dose from 50 kJ m^{-2} to 150 kJ m^{-2}.

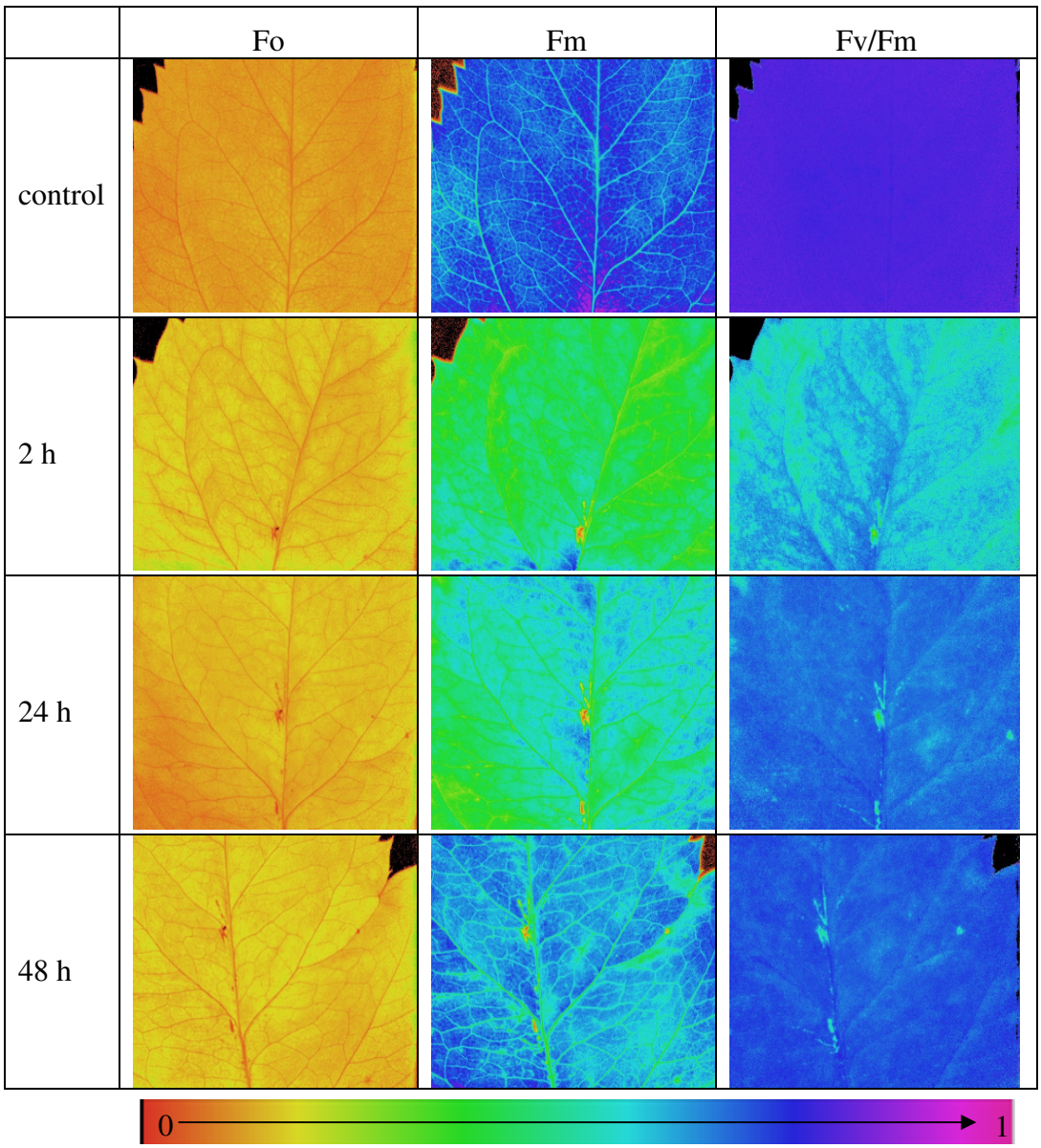

Fig. 5: PAM fluorescence images of apple leaves 2, 24 and 48 h after UV-B irradiation with 20 W m^{-2} for 240 minutes compared to control.

Since a strong reduction in the intensity of emitted fluorescence is common for photoinhibition (Lawlor, 2001), such a response of leaves may indicate a photoinhibitory effect of UV-B light or damages in the photosynthetic membranes similar to those induced by photoinhibition. However, a decrease in LIF intensity is not always observed in response to UV-B stress. In the study of Middleton et al. (1996), UV-B treatment at 340 nm reduced intensity of leaf chlorophyll fluorescence in an UV-B sensitive cucumber cultivar, but did not affect chlorophyll fluorescence intensity in leaves of an insensitive cultivar. Krizek et al. (2001) reported significantly decreased chlorophyll fluorescence in cucumber leaves if LIF was excited by the wavelength of 380 nm, no effect by excitation with 280 nm and increased intensity

with broad-band (300-400 nm) excitation source centred at 360 nm. Subhash et al. (1995) found an increase in the intensity of chlorophyll fluorescence of *Salvia splendens* L. leaves by fluorescence excitement with 337 nm and no significant changes by excitement with 458 nm. Such discrepancy in the results may be explained by distinct differences in absorption and penetration depth of excitation light of different wavelengths in leaf profiles. Another possible reason might be a different magnitude of damage caused by UV light (from photoinhibition to chlorophyll breakdown) due to previous growing conditions and/or leaf age. In addition, a long-term exposure to UV-B irradiation as well as a prolonged period between UV-B treatment and fluorescence measurements may also facilitate recovery processes in leaves, accompanied by reconstitution of chlorophyll fluorescence.

In our study, apple seedlings were grown at low light intensity, and this could enhance photoinhibition effects and fluorescence quenching due to UV-B irradiation. Different extent in decrease of red and near-infra-red fluorescence resulted in a significant reduction of F686/F740 ratio in the UV-B treatments. The decrease in red/near-infra-red ratio has been already described for the shade-adapted leaves exposed to PAR with intensity higher than 1000 µmol $m^{-2}s^{-1}$ (Agati et al., 1995). In the experiments of Subhash et al. (1995), prolonged UV-B irradiation in combination with PAR, only slightly affected F685/F730 ratio in mature and young leaves of *Salvia splendens* L. In the study on cucumber plants of Middleton et al. (1996), the reduction of leaf chlorophyll content in response to UV-B stress was accompanied by an increase of red/near-infra-red ratio. No UV-B effects were detected on this ratio in cucumber leaves with slightly decreased chlorophyll a content in the experiments of Krizek et al. (2001) by LIF excitation with 380 nm.

The negative correlation between leaf chlorophyll content and F686/740 ratio can be used for determination of the nitrogen status of plants (Tartachnyk and Rademacher, 2003) and site-specific fertilisation under field conditions (Cecchi et al., 1994; Sticksel et al., 2001). However, results of our and previous investigations (Agati et al., 1995) indicate that this ratio may be significantly affected by UV-B or PAR radiation of high intensity also when no changes in leaf chlorophyll content occur. This has to be taken in account for management decisions in remote sensing technologies in order to avoid misinterpretation of plant nutritional status when referring to F686/F740 ratio.

In respect to PAM fluorescence, apple leaves displayed a strong and significant reduction in maximum fluorescence and an increase in ground fluorescence after UV-B treatment. A similar tendency was reported by Larkum and Wood (1993) for sea grasses and phytoplankton and Gilbert et al. (2004) for barley and tomato leaves. In

these studies, among PAM parameters variable fluorescence Fv displayed strongest changes in comparison to control due to concomitant increase in Fo and decrease in Fm values and was therefore postulated as the most sensitive parameter for monitoring UV-B stress. Derived from the fluorescence signals of PS II antenna complexes Fo and reaction centres Fm, variable fluorescence Fv reflects the balance of energy between these units and is related to the efficiency with which this energy is used by the photochemical processes (Lawlor, 2001). In present work, admittedly, normalised Fv/Fo ratio showed most noticeable changes in response to UV-B stress and the strongest correlation with applied doses (Fig. 2) demonstrating better suitability than Fv for an early detection of this stress and better evaluation of dose-effect responses of plants. Similar to the results of Gilbert et al. (2004), who did not find any differences in Fv values of barley leaves irradiated with lower UV-B intensities, e.g. 1.9 and 3.8 W m^{-2}, a discrimination of UV-B doses in the range of 10-18 W m^{-2} was not possible when referring to Fv/Fo ratio in our experiment. However, fluorescence images of apple leaves visualised an enhanced heterogeneity of estimated parameters with increasing UV-B doses. Images of photochemical efficiency displayed more intense reduction alongside the leaf veins (Fig. 3) indicating higher susceptibility of these leaf areas to oxidative UV-B stress. The higher variability of chlorophyll fluorescence within the leaf after UV-B exposure was also reported by Krizek et al. (2001) suggesting heterogeneous states in the photosynthetic apparatus due to localized differences in chlorophyll concentration and photosynthetic rate. Two-photon fluorescence imaging of intact chloroplasts also showed more random spatial distribution of fluorescence compared with untreated samples (Lukins et al., 2005).

Of particular interest in this study was to examine the time course of recovery process in apple leaves after UV-B treatment. Our results indicate that disturbance in photosynthetic functionality was followed by a continuous recovery process as indicated by increased maximum fluorescence. This increase was mostly pronounced during the first two days after termination of UV-B stress. The rate of photosynthetic recovery, estimated by Fv/Fm, appeared faster in the treatment with longer exposure to UV-B (Fig. 4). This result is consistent with the Kok (1956) model, which assumes a dynamic interaction between damage and repair with repair being proportional to the pool size of inactivated targets. Heraud and Beardall (2000), taking into account lincomycin sensitivity of fluorescence parameters in *Dunaliella tertiolecta,* assumed that rate of recovery or repair is dependent on chloroplast-encoded protein synthesis. The fast rate of repair processes during the first hours after UV-B exposure has to be considered for a reliable assessment of damages induced by UV-B. However, also

irreversible destructions in PS II may occur. For example, primary barley leaves in the study of Gilbert et al. (2004) displayed continuing inhibition of PS II after exposure to 1.9 W m^{-2} for 4 hours. Chow et al. (1992) reported no recovery of Fv/Fm within 3 days after UV irradiation in pea plants.

In our study, the recovery curves of Fm, Fv, Fv/Fm and Fv/Fo parameters throughout 7 days after UV-B treatment were well fitted with an exponential rise to maximum function. Such kinetics of recovery processes resembled those found in the study of Heraud and Beardall (2000) for *Dunaliella tertiolecta* cells exposed to UV-B radiation of 4.9 W m^{-2} for 30 minutes. As in our experiment, the relaxation kinetic of Fv/Fm was well described by an equation $y = y_o + a(1 - e^{-bx})$. Fv/Fm values in the experiment of Heraud and Beardall (2000) returned to a control level within 270 min after UV-B irradiance. Complete recovery of Fv/Fm values was also observed on cucumber plants within 24 hours after ceasing UV-B treatment with 1.17 W m^{-2} for 8 hours (Hunt et al., 1996). In our study, fluorescence parameter values of apple leaves did not completely restore to the level of control plants during 7 days after irradiation indicating only partial recovery from applied UV-B treatments. So far, the magnitude of repair processes after UV-B stress seems to be dependent on UV-B doses, plant species and physiological state of leaves and may range from irreversible damages, partial and complete recovery.

5 References

Agati, G., Mazzinghi, P., Fusi, F. and Ambrosini, I. 1995. The F685/F730 chlorophyll fluorescence ratio as a tool in plant physiology: response to physiological and environmental factors. Journal of Plant Physiology **145**, 228-238.

Baker, N.R. and Rosenqvist, E. 2004. Review article: Applications of chlorophyll fluorescence can improve production strategies: an examination of future possibilities. Journal of Experimental Botany **55**, 1607-1621.

Blanke, M.M. 1992. Determination of chlorophyll using DMSO. Wein-Wissenschaft **47**, 32-35.

Bornman, J.F. 1989. Target sites of UV-B radiation in photosynthesis of higher plants. Journal of Photochemistry and Photobiology B-Biology **4**, 145-158.

Burchard, P., Bilger, W. and Weissenbock, G. 2000. Contribution of hydroxycinnamates and flavonoids to epidermal shielding of UV-A and UV-B radiation in developing rye primary leaves as assessed by ultraviolet-induced chlorophyll fluorescence measurements. Plant Cell and Environment **23**, 1373-1380.

Caldwell, M.M. 1971. Solar ultraviolet radiation and the growth and development of higher plants. In: Photophysiology, Vol. 6, edited by A.C. Giese (Academic Press, New York, USA), pp. 131–177.

Chaerle, L. and Van der Straeten, D. 2000. Imaging techniques and the early detection of plant stress. Trends in Plant Science **5**, 495-501.

Cecchi, G., Mazzinghi, P., Pantani, L.R., Valentini, R., Tirelli, D. and Angelis, P.D. 1994. Remote sensing of chlorophyll a fluorescence of vegetation canopies: near and far field measurement techniques. Remote Sensing of Environment **47**, 18-28.

Chow, W.S., Strid, E. and Anderson, J.M. 1992. Short-term treatment of pea plants with supplementary ultraviolet-B radiation: recovery time-courses of some photosynthetic functions and components. In: Research in photosynthesis, edited by N. Murata (Kluwer Academic Publishers, Dordrecht, The Netherlands), p. 361-213.

Fedina, I., Georgieva, K., Veltchkova, M. and Grigorova, I. 2005. Effect of pretreatment of barley seedlings with different salts on the level of UV-B induced and UV-B absorbing compounds. Environmental and Experimental Botany **56**, 225-230.

Friso, G., Spetea, C., Giacometti, G.M., Vass, I. and Barbato, R. 1993. Degradation of photosystem-II reaction-center D1-protein induced by UV-B radiation in isolated thylakoids – identification and characterization of C-terminal an N-terminal breakdown products. BBA-Bioenergetics **1184**, 78-84.

Friso, G., Barbato, R., Giacometti, G.M. and Barber, J. 1994. Degradation of D2 protein due to UV-B irradiation of the reaction-center of photosystem-II. FEBS Letters **339**, 217-221.

Gao, W., Zheng, Y., Slusser, J.R., Heisler, G.M., Grant, R.H., Xu, J. and He, D. 2004. Effects of supplementary ultraviolet-b irradiance on maize yield and qualities: a field experiment. Journal of Photochemistry and Photobiology B-Biology **80**, 127-131.

Gilbert, M., Skotnica, J., Weingart, I. and Wilhelm, C. 2004. Effects of UV irradiation on barley and tomato leaves: thermoluminescence as a method to screen the impact of UV radiation on crop plants. Functional Plant Biology **31**, 825-845.

Heraud, P. and Beardall, J. 2000. Changes in chlorophyll fluorescence during exposure of *Dunaliella tertiolecta* to UV radiation indicate a dynamic interaction between damage and repair processes. Photosynthesis Research **63**, 123-134.

Herman, J.R., Bhartia, P.K., Ziemke, J., Ahmad, Z. and Larko, D. 1996. UV-B increases (1979-1992) from decreases in total ozone. Geophysical Research Letters **23**, 2117-2120.

Hunt, J.E., Kelliher, F.M. and MC Neil, D.L. 1996. Response in chlorophyll a fluorescence of six New Zealand tree species to a step-wise increase in ultraviolet-B irradiance. New Zealand Journal of Botany **34**, 401-410.

Jansen, M.A.K., Greenberg, B.M., Edelman, M., Mattoo, A.K. and Gaba, V. 1996. Accelerated degradation of the D2 protein in photosystem II under ultraviolet radiation. Photochemistry and Photobiology **63**, 814-817.

Kakani, V.G., Reddy, K.R., Zhao, D. and Sailaja, K. 2003. Field crop responses to ultraviolet-B radiation: a review. Agriculture and Forest Meteorology **120**, 191-218.

Kok, B. 1956. On the inhibition of photosynthesis by intense light. Biochimica et Biophysica Acta **21**, 234-244.

Koti, S., Reddy, K.R., Kakani, V.G., Zhao D. and Reddy, V.R. 2004. Soybean (Glycine max) pollen germination characteristics, flower and pollen morphology in response to enhanced ultraviolet-B radiation. Annals of Botany **94**, 855-864.

Krizek, D.T., Middleton, E.M., Sandhu, R.K. and Kim, M.S. 2001. Evaluating UV-B effects and EDU protection in cucumber leaves using fluorescence images and fluorescence emission spectra. Journal of Plant Physiology **158**, 41-53.

Larkum, A.W.D. and Wood, W.F. 1993. The effect of UV-B radiation on photosynthesis and respiration of phytoplankton, benthic macroalgae and seagrasses. Photosynthesis Research **36**, 17-23.

Lawlor, D.W. 2001. Photosynthesis (Springer, New York, USA).

Lukins, P.B., Rehman, S., Stevens, G.B. and George, D. 2005. Time-resolved spectroscopic fluorescence imaging, transient absorption and vibrational spectroscopy of intact and photo-inhibited photosynthetic tissue. Luminescence **20**, 143-151.

Maxwell, K. and Johnson, G.N. 2000. Chlorophyll fluorescence - a practical guide. Journal of Experimental Botany **51**, 659-668

Melis, A., Nemson, J.A. and Harrison, M.A. 1992. Damage to functional components and partial degradation of photosystem II reaction center proteins upon chloroplast exposure to ultraviolet-B radiation. Biochimica et Biophysica Acta **100**, 312-320.

Middleton, E.M., Chapelle, E.W., Cannon, T.A., Ademse, P. and Britz, S.J. 1996. Initial assessment of physiological response to UV-B irradiation using fluorescence measurements. Journal of Plant Physiology **148**, 69-77.

Mineuchi, K., Takahashi, K. and Tatsumoto, H. 2001. Effects of UV-B radiation on laser-induced fluorescence spectra in crop leaves. Environmental Technology **22**, 151-155.

Musil, C.F. 1994. Ultraviolet-B irradiation of seeds affects photochemical and reproductive performance of the arid-environment ephemeral *dimorphotheca pluvialis*. Environmental and Experimental Botany **34**, 371-378.

Post, A., Lukins, P.B., Walker, P.J. and Larkum, A.W.D. 1996. The effects of ultraviolet irradiation on P680(+) reduction in PSII core complexes measured for individual S-states and during repetitive cycling of the oxygen-evolving complex. Photosynthesis Research **49**, 21-27.

Renger, G., Völker, M., Eckert, H.J., Fromme, P., Hohm-Veit, S. and Gräber, P. 1989. On the mechanism of photosystem II deterioration by UV-B irradiation. Photochemistry and Photobiology **49**, 97-105.

Rinderle, U. and Lichtenthaler, H.K. 1988. The chlorophyll fluorescence ratio F690/F735 as a possible stress indicator. In: Applications of chlorophyll fluorescence, edited by H.K. Lichtenthaler (Dordrecht: Kluwer Academic Publishers), p. 189-196.

Runeckles, V.C. and Krupa, S.V. 1994. The impact of UV-B radiation and ozone on terrestrial vegetation. Environmental Pollution **83**, 191-213.

Sharma, P.K., Anand, P., Sankhalkar, S. and Shetye, R. 1998. Photochemical and biochemical changes in wheat seedlings exposed to supplementary ultraviolet-B radiation. Plant Science **132**, 21-30.

Sticksel, E., Maidl, F.-X., Schächtl, J., Huber, G. and Schulz, J. 2001. Laser-induced Chlorophyll fluorescence – a tool for online detecting nitrogen status in crop stands. In: Precision Agriculture´01: Proceedings of the 3rd European Conference on Precision Agriculture, edited by G. Grenier and S. Blackmore (Montepellier, France), p. 959-964.

Stolarski, R., Bojokov, R., Bishop, L., Zerefos, C., Straehlin, J. and Zawodny, J. 1992. Measured trends in stratospheric ozone. Science **256**, 343-349.

Subhash, N., Mazzinghi, P., Agati, G., Fusi, F. and Lercari, B. 1995. Analysis of laser-induced fluorescence line shape of intact leaves: Application to UV stress detection. Photochemistry and Photobiology **62**, 711-718.

Tartachnyk, I. and Rademacher, I. 2003. Estimation of nitrogen deficiency of sugar beet and wheat using parameters of laser induced and pulse amplitude modulated chlorophyll fluorescence. Journal of Applied Botany **77**, 61-67.

Trebst, A. and Depka, B. 1990. Degradation of the D-1 protein subunit of photosystem II in isolated thylakoids by UV-light. Zeitschrift für Naturforschung C-A Journal of Biosciences **45**, 765-771.

Vass, I., Sass, L., Spetea, C., Bakou, A., Ganothakis, D.F. and Petrouleas, V. 1996. UV-B induced inhibition of photosystem II electron transport studied by epr and chlorophyll fluorescence. Impairment of donor and acceptor side components. Biochemistry **35**, 8964-8973.

Vass, I. 1997. Adverse effects of UV-B light on the structure and function of the photosynthetic apparatus. In: Handbook of photosynthesis, edited by M. Pessarakli (Marcel Dekker Inc., New York, the Netherlands), p. 931-949.

Vass, I., Kirilovsky, D. and Etienne, A.L. 1999. UV-B radiation-induced donor- and acceptor-side modifications of photosystem II in the cyanobacterium *Synechocystis* sp. PCC 6803. Biochemistry **38**, 12786-12794.

Zhao, D., Reddy, K.R., Kakani, V.G., Mohammed, A.R., Read, J.J. and Gao, W. 2004. Leaf and canopy photosynthetic characteristics of cotton (*Gossypium hirsutum*) under elevated CO_2 concentration and UV-B radiation. Journal of Plant Physiology **161**, 581-590.

E Evaluation of fluorescence and remission techniques for monitoring changes in peel chlorophyll and internal fruit characteristics in sunlit and shaded sides

1 Introduction

In apple production, there is high interest in techniques for determination of optimal harvest date and for the automation of commercial fruit sorting and grading. Modern quality management and safety practices in fruit marketing require strict documentation and traceability of fruit data in whole supply chains from the production to the consumer site (Kramer, 2005). This also creates a need for fast monitoring methods for the prediction of fruit quality and storability under controlled atmosphere conditions, during transport and in the trade under shelf life conditions. The common practice for fruit quality and maturity evaluation involves destructive estimation of fruit firmness, starch breakdown, analyses of soluble solids and titratable acids content in flesh (Streif, 1996). This is, however, labour and time consuming.

The apple maturity processes involve changes in content and composition of peel pigments (Solovchenko et al., 2006). A major alteration in apple peel during on-tree ripening and post harvest life is the degradation of the chloroplast structure with a loss in chlorophyll content (Knee, 1972; Kingston, 1992). In red coloured apple cultivars, on-tree ripening is additionally characterised by anthocyanin accumulation in the fruit epidermis (Saure, 1990; Merzlyak et al., 2002).

Due to unequal irradiation, sunlit and shaded apple fruit sides often differ in their colour and flesh characteristics. Last findings on ripening-associated pigment changes in apple fruit also showed significant differences in pigment dynamics between both apple sides on and off tree (Solovchenko et al., 2006). It has also been shown that in red-coloured apple fruit, peel may contain more chlorophyll under screening anthocyanin pigmentation (Merzlyak et al., 2002). For the non-destructive detection of chlorophyll content in the apple peel, light remission (Zude-Sasse et al., 2002; Merzlyak et al., 2003) and fluorescence techniques have been proposed (Sowinska et al., 1998; Noh and Lu, 2005). With fluorescence, however, the majority of the studies on apple fruit quality has been done employing time resolved Pulse-Amplitude-Modulated (PAM) (Song et al., 1997; De Long et al., 2004; Quartin et al., 2004) or Laser-Induced Fluorescence (LIF) technique (Noh and Lu, 2005) and focused on the parameters related to photosynthetic efficiency. In most of such studies, the previous dark adaptation of samples is usually required thus extending time for measurement. Recently developed LIF technique allows mapping of heterogeneities in crop canopy

nitrogen status under ambient light conditions. This approach is not based on the chlorophyll fluorescence kinetic analysis, but on the rapid (in the range of milliseconds) detection of red and near-infra-red fluorescence intensities in the scanning mode (Limbrunner and Maidl, 2007). The principle behind the method is a strong negative correlation between chlorophyll concentration and chlorophyll fluorescence ratio F690/F730 in leaves (Lichtenthaler and Babani, 2004; Tartachnyk et al., 2006). In general, chlorophyll fluorescence spectrum of apple peel is similar to that of leaves (Noh and Lu, 2005). The capability of such a system for the estimation of pigment content in fruit peel has not been tested yet.

To our knowledge, the heterogeneity in fruit coloration and internal attributes was neglected in previous reports on non-destructive fruit quality prediction (Peng and Lu, 2006; Zude et al., 2006). Thus, the key objective of our study was to assess the potential of LIF and remission techniques for detection of senescence based fruit quality changes considering the differences in apple peel pigment content and main flesh parameters on the sunlit and shaded sides. An additional question of our study was whether the blush anthocyanin pigmentation might affect fluorescence-based chlorophyll detection. In contrast to UV-A or blue excitation light, red beam passes upper flavonoid and anthocyanin containing layers of apple peel unabsorbed before being captured by chlorophylls (Hagen et al., 2006). For this reason we hypothesised that with ‘multipoint’ scanning measurements, patches with anthocyanin pigmentation and higher chlorophyll content underneath (Merzlyak et al., 2002) will display different fluorescence intensities and lower F690/F730 ratios as compared to apparently green areas.

2 Material and Methods

2.1 Plant material and experimental design

Apple fruit of ‘Golden Delicious’ and ‘Jonagold’ cultivars were harvested in the Experimental Station Klein-Altendorf, University of Bonn, Germany, on October 4, 2006 and stored for 2 weeks in a cold chamber at 4 °C and 80±10% relative humidity. On October 18, 2006, healthy and undamaged fruit of each cultivar were selected and transferred to a laboratory room (20±2 °C) for simulating shelf life conditions. From October 19 to November 13, ten apples of each cultivar were taken at a 3-4 day interval for the measurements. For all destructive and non-destructive analyses, a circle of approximately 12 cm^2 was marked on the sunlit and shaded fruit sides. The

sunlit as compared to shaded sides were characterised by a more pronounced yellow surface colour in 'Golden Delicious' and a more intense red colour in 'Jonagold'.

2.2 Laser-induced chlorophyll fluorescence (LIF)

LIF measurements were done with a portable fluorometer (MiniVegN, Fritzmeier Systems GmbH & Co KG - Großhelfendorf, Germany). Chlorophyll fluorescence was induced with a red (662 nm) light emitting diode laser with full width at half maximum (FWHM) of 3 nm with a pulse energy of 200 mW and laser pulse frequency of 5 kHz. The intensity of the excitation light at the level of object was about 1300 µmol PAR m^{-2} s^{-1}. The fluorescence signals were detected with two photomultipliers at 692$\pm$2 nm (F690) and 730$\pm$2 nm (F730) at a sensor viewing area of about 0.5 mm^2 for each measuring point. Fluorescence intensity is strongly dependent on geometry and, in particular, on angles of exiting light and emitted fluorescence. In order to keep the same geometry for the fluorescence recording and to minimise the impact of the induction kinetics on fluorescence intensity, the sensor head was placed on the marked circle and the apple, being in contact with the sensor, was moved around at a nearly constant velocity for 6 s to provide 'multipoint' fluorescence measurement in the defined area of interest. However, readings taken in the first and sixth second were not considered for mean value calculation because of the non-uniform velocity at the beginning and the end of the fluorescence recordings.

2.3 Pulse amplitude modulated fluorescence (PAM)

Imaging PAM-Chlorophyll fluorometer (Imaging-PAM, Heinz Walz, Effeltrich, Germany) was used to take the fluorescence images of apple fruit peel. Following the method of Schreiber (1986), a blue (470 nm) saturation pulse of 2400 µmol m^{-2} s^{-1} PAR for 0.6 s was applied to induce maximum fluorescence Fm. The Fm images were taken on the external and internal peel sides to visualise chlorophyll fluorescence intensity in the regions of the peel lenticels.

2.4 Light remission

A hand-held photodiode array spectrophotometer (Pigment Analyzer 1101, CP, Falkensee, Germany) was employed for remission measurement in apple fruit. Five light emitting diodes (max peaks = 460, 550, 660 nm with FWHM = 30-60 nm) placed in the periphery of the light cup provided illumination of the sample. The remission spectra were detected with the receiving fibre, installed in the centre of the light cup,

in the wavelength range of 500-1100 nm with a resolution of 3.3 nm. The geometry and set up of remission recording were equal to those described by Chen and Nattuvetty (1980) and Zude et al. (2007). It has been shown that such type of recording, which includes a considerable transmittance component (Chen and Nattuvetty, 1980), may provide more relevant information for apple pigment analysis than diffusive reflectance (Zude-Sasse et al., 2002). Remission was assessed at 570 (R570), 660 (R660) and 780 (R780) nm (1 reading per sample) with calculation of Normalised-Differenced-Vegetation-Index (NDVI = $(R_{780}-R_{660})/(R_{780}+R_{660})$) and Normalised-Anthocyanin-Index (NAI = $(R_{780}-R_{570})/(R_{780}+R_{570})$) for the *in vivo* evaluation of apple peel chlorophyll and anthocyanin content, respectively (Solomakhin and Blanke, 2007). Readings were referenced to white barium sulphate standard (Analytical Spectral Devices ASD, USA).

2.5 Fruit firmness, total soluble solids, titratable acids, starch and Streif index

Fruit firmness (FF) was measured destructively with a hand penetrometer (FT 327, Agritec Griesser AG, Kleinandelfingen, Germany) after peel was removed from the marked surface. The penetration depth was 8 mm and the stamp area was 1 cm. One drop of the fruit sap leachate was taken to determine the concentration of total soluble solids (SS) with a refractometer (Opton 128254, Zeiss, Jena, Germany). For titratable acid (TA) analysis, apples were cut in half in the equator zone and the juice was extracted from the whole upper fruit half without discriminating between sunlit and shaded sides. Three ml of fruit sap were transferred to a volumetric flask and 27 ml of distilled water added. The solution was titrated with 0.1 M NaOH until pH of 8.1 was reached. The concentration of titratable acid was calculated as: TA [%] = (ml NaOH used x 40)/3 x 100. The lower parts of half-cut apples were treated with Lugol solution (0.33% iodine + 0.66% potassium iodide), and starch breakdown (SB) was estimated using the European starch breakdown scale. The maturity index (SI) according to Streif (1996) was calculated as: SI = FF/ (SS x SB).

2.6 Chlorophyll content in apple peel

Apple peel removed for fruit firmness evaluation was used for chlorophyll analysis. Discs of 2.1 cm² were excised and stored in plastic bottles at –20 °C. The peel chlorophyll was extracted with dimethyl sulfoxide according to Blanke (1992). The absorbances of extracts were recorded at 647 nm (A_{647}) and 665 nm (A_{665}) with a UV-VIS spectrophotometer (Lambda 5, Perkin Elmer, USA), and chlorophyll a (C_a), and b

(C_b) concentrations were calculated according to the following equations (Moran, 1982; Blanke, 1992):

$C_a = 12.7 \times A_{665} - 2.79 \times A_{647}$ and $C_b = 20.7 \times A_{647} - 4.64 \times A_{665}$.

2.7 Microscopic investigations

Cross-sections of apple peel (cv. 'Golden Delicious') were studied by means of light fluorescence microscopy (Leitz DMR photomicroscope, Leica, Solms, Germany). Fluorescence of apple peel was induced and detected using filter cube (BP 340-380, Chromatic beam splitter FT 400, LP 430). Images were captured with the integrated Wild MPS 489 camera and further processed with Discus software (Discus, Technisches Büro Hilgers, Koenigswinter, Germany).

2.8 Statistics

The experimental data were subjected to ANOVA with the SPSS statistical package 12.0 for Windows (SPSS Inc., Chicago, USA). The 95 % probability level was taken to indicate significant differences. Means were compared by Tukey HSD multiple range test after data were checked for normal distribution and variance homogeneity. In addition, Pearson's correlation analyses for measured parameters were conducted. Data presented in Figs. 1-3 were averaged from replicating measurements on 10 fruit each (1 reading per each fruit side).

3 Results

3.1 Chlorophyll content

Sunlit and shaded apple sides of both cultivars differed significantly in their chlorophyll content (Fig. 1). During the first 16 days of the experiment, sunlit red coloured areas of 'Jonagold' fruit contained 55-116% more chlorophyll than shaded ones. In contrast, 'Golden Delicious' showed 15-40% lower chlorophyll content on sunlit compared to shaded sides. Within this period, chlorophyll content in 'Golden Delicious' decreased by almost 80% on both sides, e.g. from 5.2 to 1.1 µg cm^{-2} on the green and from 4.4 to 0.9 µg cm^{-2} on the yellow parts. These results indicate similar rates of chlorophyll breakdown for both fruit sides (0.26 µg cm^{-2} d^{-1} for the shaded and 0.22 µg cm^{-2} d^{-1} for the sunlit side).

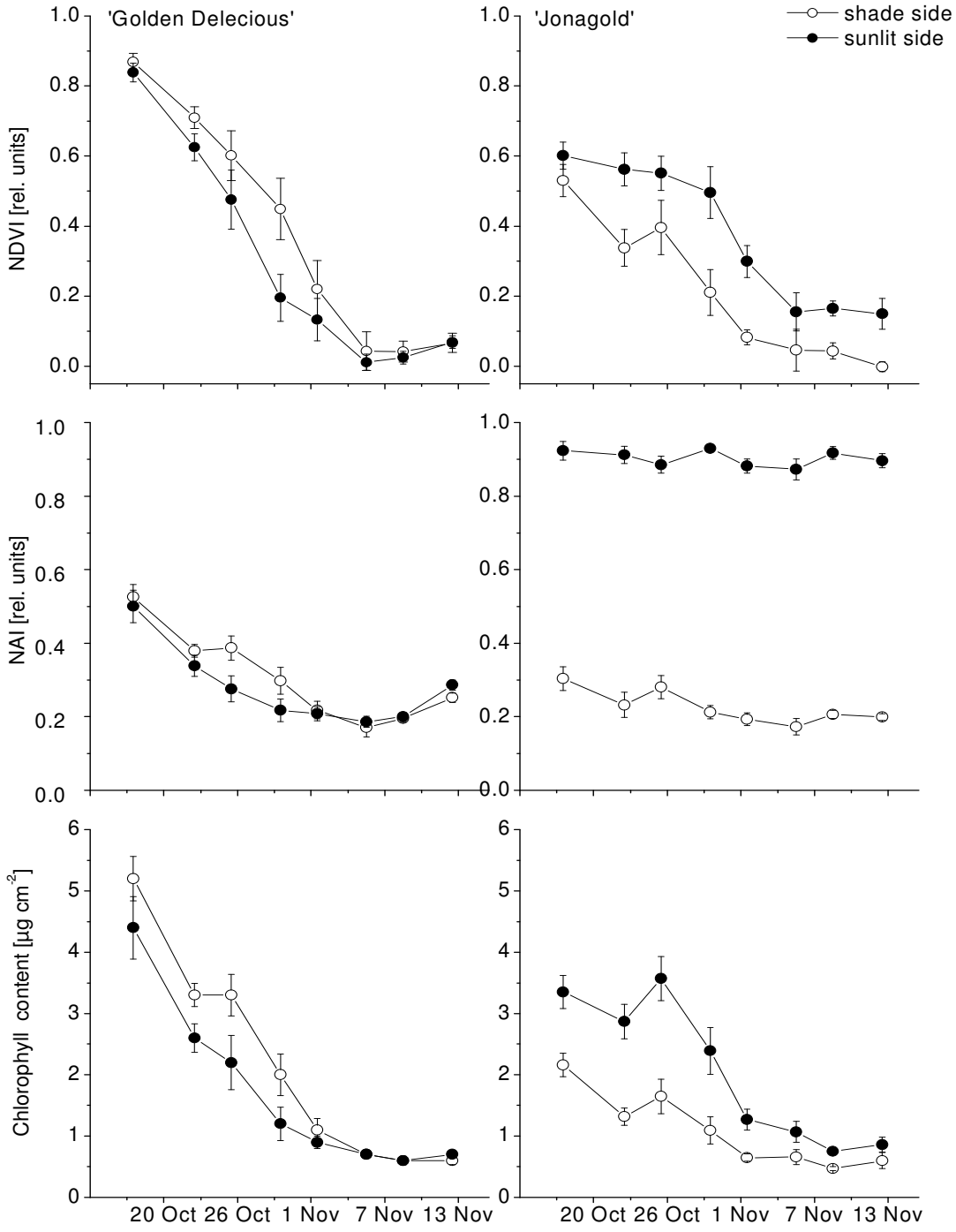

Fig. 1: NDVI, NAI and chlorophyll content of the apple peel on sunlit (closed symbols) and shaded (open symbols) sides of 'Golden Delicious' and 'Jonagold' fruit during shelf life. Vertical bars indicate ± standard error of ten replicates.

Thereafter, at the last three sampling dates, both apple sides of this cultivar displayed 0.6-0.7 µg cm^{-2} chlorophyll. Chlorophyll breakdown in the peel of 'Jonagold' apples proceeded more slowly, e.g. 62% (from 3.4 to 1.3) on sun-exposed and 32% (from 2.2

to 0.7) on shaded apple sides during the first 16 days of shelf life. This is equivalent to a daily chlorophyll reduction of 0.13 and 0.10 µg cm^{-2} on average. In contrast to 'Golden Delicious' apple, which did not differ significantly in chlorophyll content of sunlit and shaded fruit peel, at the last three sampling dates, the red sunlit parts of 'Jonagold' fruit contained 44-63% more chlorophyll compared to shaded sides.

3.2 Fruit firmness, total soluble solids, titratable acids, starch and Streif index

The fruit of both cultivars did not differ significantly in firmness on the sunlit and shaded sides (Fig. 2). Within the first 16 days of the experiment, fruit firmness of 'Golden Delicious' decreased from about 75 to 41 N with the most pronounced decline during the first 4 days of shelf life. In 'Jonagold', a strong and steady firmness decrease from 72 to 32 N was noted until Nov. 1. For the following 12 days, fruit firmness remained almost at the same level.

Throughout the whole experimental period, sunlit sides of 'Jonagold' had 5-13% higher soluble solid content in the fruit flesh than the shaded parts (Fig. 2). Such pronounced differences, however, were not found for the 'Golden Delicious' fruit. Here, only during the last 15 days of experiment, a slightly (3-6%) higher content of soluble solids was measured in sunlit fruit sides. The considerable decrease in fruit firmness of 'Golden Delicious' on the second sampling date was accompanied by an increase of soluble solids from 11 to 12.7%.

Within a month of shelf life, the amount of titratable acids decreased in both cultivars from 0.43 to 0.32% in 'Golden Delicious' and from 0.49 to 0.33% in 'Jonagold' (data not shown) probably resulting from carbon respiration losses. In the beginning of the experiment, apple fruit of both cultivars displayed an almost complete starch breakdown as indicated by 9.5-10 points according to starch breakdown scale. At the second sampling date, starch was already completely degraded (data not shown).

Streif index did not reveal significant differences between sunlit and shaded fruit sides in 'Golden Delicious' (Fig. 2). During the first 4 days of shelf life, values strongly decreased from 0.07 to 0.04 units reflecting sharp changes in fruit firmness and soluble solids content. Thereafter, apples showed a slow gradual decrease to 0.03 units until the end of experiment. In 'Jonagold', sunlit areas displayed a 9-21% higher Streif index than shaded ones. Within 4 weeks of shelf life, the maturity index gradually decreased from 0.054 to 0.029 on sunlit and from 0.059 to 0.032 units on shaded fruit areas.

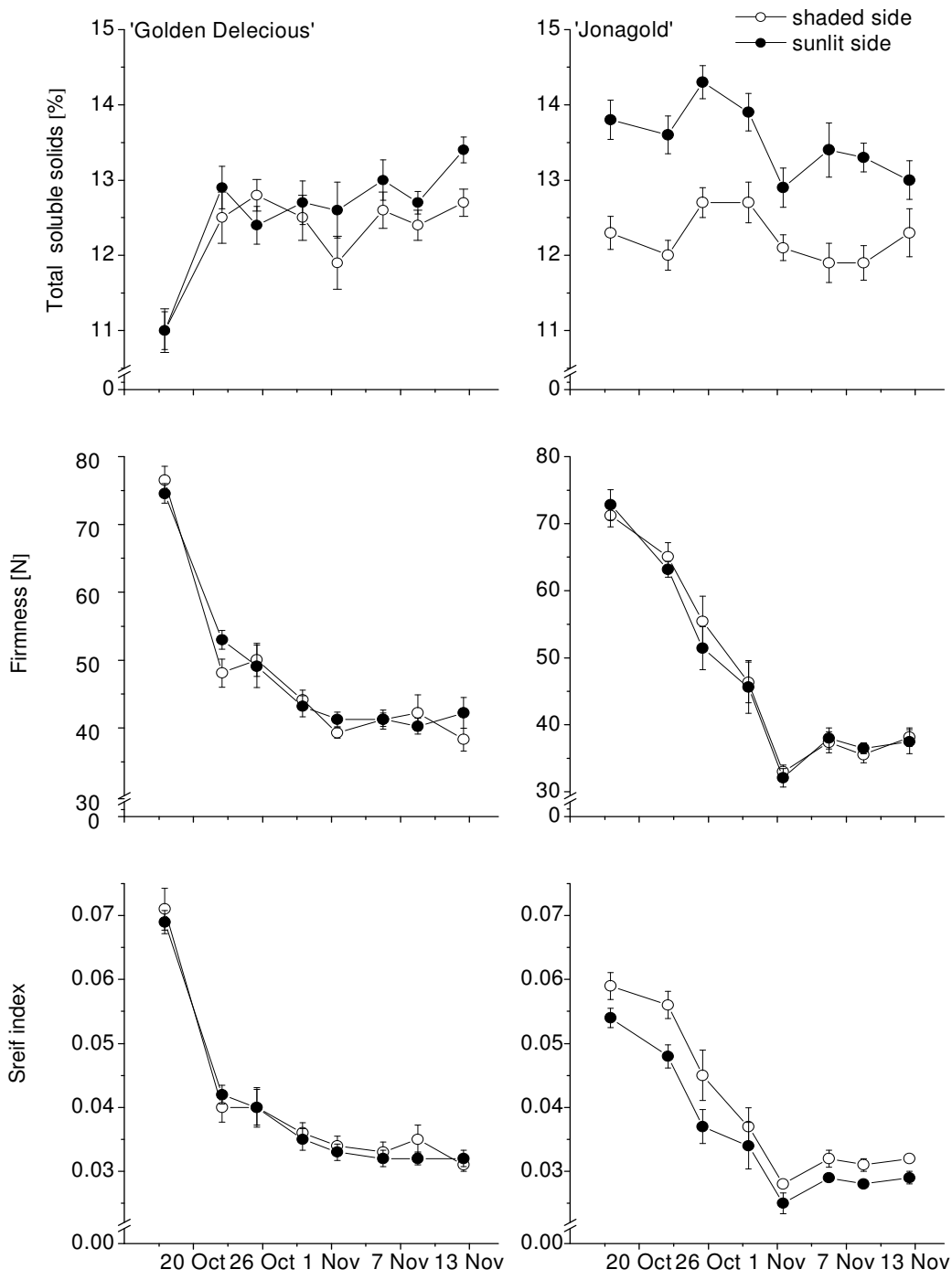

Fig. 2: Total soluble solids, fruit firmness and Streif index of 'Golden Delicious' and 'Jonagold' apples on the sunlit (closed symbols) and shaded (open symbols) fruit sides during shelf life. Vertical bars indicate ± standard errors of ten replicates.

3.3 Chlorophyll fluorescence

Throughout the experiment, the red sunlit sides of 'Jonagold' with higher chlorophyll content showed distinctly higher intensities of chlorophyll fluorescence at 690 nm and

730 nm, compared to the shaded sides (Fig. 3), while the fluorescence ratio F690/F730 was 2-9% lower on sunlit compared to shaded sides.

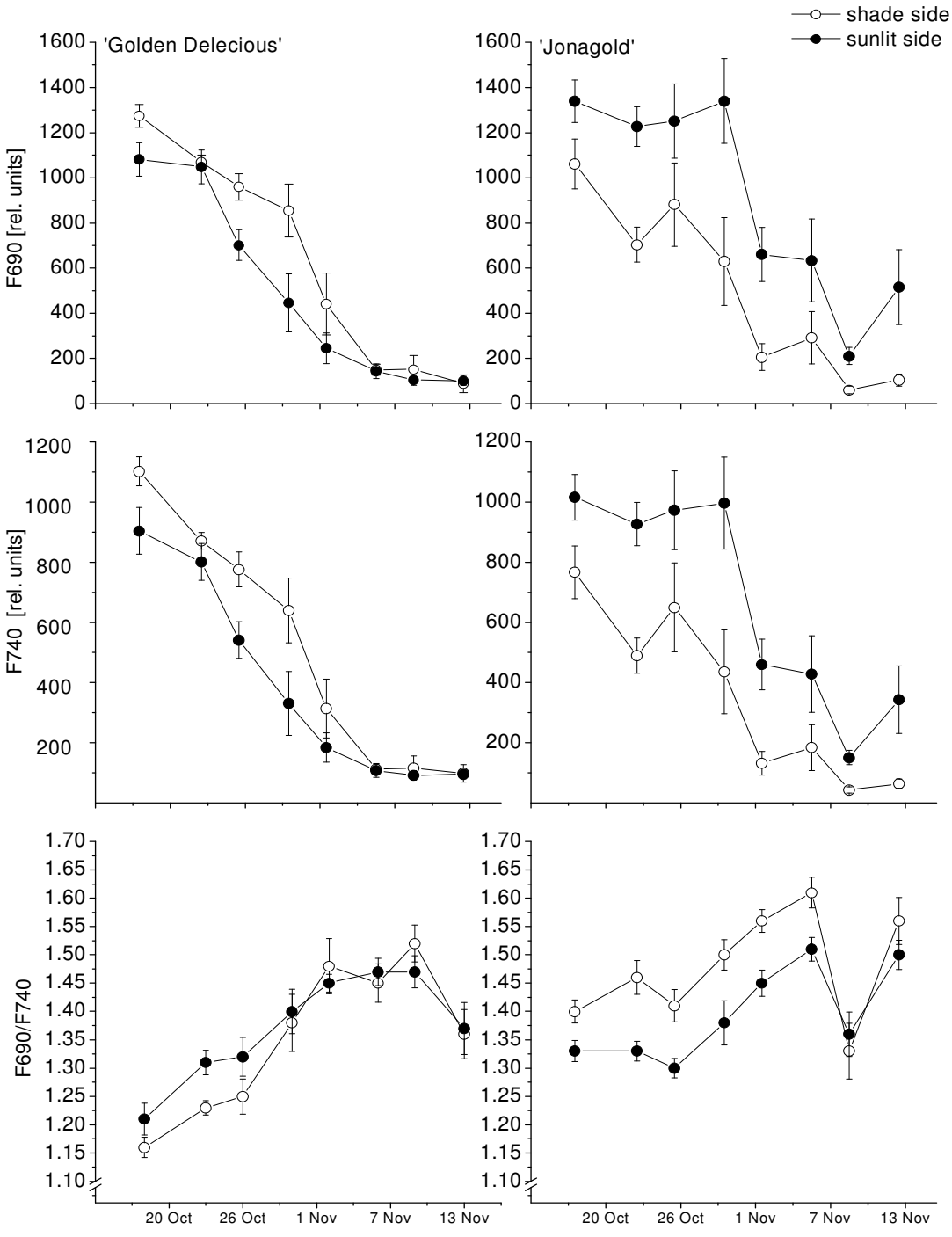

Fig. 3: Chlorophyll fluorescence intensities at 690 (F690), 730 (F730) nm and F690/F730 ratio on sunlit (closed symbols) and shaded (open symbols) sides of 'Golden Delicious' and 'Jonagold' fruit during shelf life. Vertical bars indicate $\pm$ standard errors of ten replicates.

Sunlit sides of ‘Golden Delicious’ displayed lower F690 and F730 values compared to shaded ones during the 4 weeks of shelf life. At the last 3 sampling dates of experiment, apples of this cultivar did not differ in their fluorescence intensities reflecting the same low level of peel chlorophyll content on both apple sides. As for F690/F730 ratio, higher values on the sunlit sides were observed only during the first 12 days of the experiment. In parallel to chlorophyll loss in the course of fruit senescence, F690 and F730 decreased and F690/F730 ratio increased. However, at the last sampling date, as chlorophyll in the apple peel fell below 0.8 µg cm^{-2}, fluorescence ratio displayed an enormous variation (Fig. 3) due to the extremely low (around zero) fluorescence intensities.

3.4 NDVI and NAI

Similar to fluorescence intensities, NDVI gradually decreased with chlorophyll breakdown under shelf life conditions in both cultivars and remained nearly constant at the last three sampling dates (Fig. 1). In ‘Jonagold’, the sunlit sides displayed NDVI between 0.60 and 0.15 throughout the experiment, representing 0.07-0.29 higher units compared to those of the shaded fruit surface areas. The sunlit sides of ‘Golden Delicious’ that had lower chlorophyll content showed NDVI ranging from 0.84 to 0.01, which were by 0-0.25 units lower compared to shaded areas.

The blush colouration of ‘Jonagold’ apples resulted in significantly, by 0.62-0.72 units, higher NAI on sunlit than on shaded sides (Fig. 1). In the course of the experiment, NAI was in the range of 0.92-0.90 units on sunlit and of 0.30-0.20 units on shaded sides of ‘Jonagold’ apples. In ‘Golden Delicious’, NAI did not differ on both fruit sides and gradually decreased from 0.51 to 0.27 units in the course of the experiment.

3.5 Correlation analysis

The results of correlation analysis for the data obtained during fruit senescence under shelf life conditions revealed linear relationship between fruit firmness and chlorophyll content in apple peel with the Pearson’s coefficients of 0.65-0.78 for both tested cultivars (Tab.1). For ‘Golden Delicious’, there were no differences in the rate of correlation for the analyses employing data from sunlit, shaded or both sides. For ‘Jonagold’, in contrast, Pearson’s coefficients calculated from the data from both sides appeared much lower ($r = 0.65$) compared to those from sunlit ($r = 0.74$) or shaded ($r = 0.76$) sides. This resulted from the higher chlorophyll concentration in the sun

exposed sides of apple fruit with the same firmness values on both apple sides. For other fruit quality parameters, the correlation with chlorophyll content was lower with r = 0.04-0.56 for soluble solids, r = 0.52-0.57 for titratable acids and r = 0.51-0.82 for Streif index (Tab. 1).

Tab. 1: Pearson´s correlation coefficients between chlorophyll content in the fruit peel and non-destructively or destructively estimated apple quality parameters. Correlation analyses were performed with the values from sunlit, shaded or both sides for 'Golden Delicious' and 'Jonagold' apples ($^{**}p<0.01$).

	'Golden Delicious'			'Jonagold'		
Parameter/ Fruit side	sunlit (n=80)	shaded (n=80)	both (n=160)	sunlit (n=80)	shaded (n=80)	both (n=160)
NDVI	0.92**	0.89**	0.90**	0.92**	0.91**	0.90**
NAI	0.91**	0.91**	0.91**	0.11	0.72**	0.46**
F690	0.88**	0.88**	0.88**	0.84**	0.92**	0.87**
F730	0.91**	0.93**	0.92**	0.87**	0.92**	0.89**
F690/F730	- 0.74**	- 0.76**	- 0.75**	- 0.61**	- 0.40**	- 0.56**
Fruit firmness	0.78**	0.77**	0.77**	0.74**	0.76**	0.65**
Total soluble solids	- 0.56**	- 0.35**	- 0.46**	0.41**	0.04	0.45**
Titratable acids	-	-	0.57**	-	-	0.52**
Streif index	0.82**	0.72**	0.76**	0.65**	0.75**	0.51**

Among fluorescence and remission parameters, F730 and NDVI displayed highest correlation with chlorophyll content (r = 0.89-0.92) in both investigated cultivars (Tab. 1). Irrespective of data taken for the correlation analysis, r = 0.91 was found for NAI and chlorophyll content in 'Golden Delicious'. 'Jonagold', in contrast, displayed strong discrepancy in the Pearson's coefficients calculated for the data recorded on sunlit and shaded sides. LIF parameters F690 and F730 correlated well with chlorophyll content (r = 0.84-0.93). Lower coefficients (r = 0.4-0.76) were established for F690/F730 ratio.

Regarding correlation between fruit firmness and non-destructively evaluated parameters, analyses based on the values from sunlit and shaded sides of 'Golden Delicious' resulted in r = 0.71 for NDVI, r = 0.70 for NAI, r = 0.69 for F730 or r = 0.66 for F690. The correlation coefficients between fruit firmness and these

parameters were generally lower for ‘Jonagold’ compared to ‘Golden Delicious’ when considering combined values of both fruit sides.

Tab. 2: Pearson´s correlation coefficients between fruit firmness or Streif index and non-destructively estimated light remission (NDVI, NAI) and laser-induced fluorescence (F690, F730, F690/F730) parameters. Correlation analyses were performed with the values from sunlit, shaded or both sides for ‘Golden Delicious’ and ‘Jonagold’ apples ($^{**}p<0.01$).

	‘Golden Delicious’			‘Jonagold’		
Parameter/ Fruit side	sunlit (n=80)	shaded (n=80)	both (n=160)	sunlit (n=80)	shaded (n=80)	both (n=160)
Fruit firmness						
NDVI	0.79**	0.65**	0.71**	0.71**	0.79**	0.70**
NAI	0.69**	0.73**	0.70**	0.11	0.50**	0.05
F690	0.69**	0.64**	0.66**	0.63**	0.69**	0.61**
F730	0.72**	0.69**	0.69**	0.65**	0.68**	0.61**
F690/F730	- 0.57**	- 0.54**	- 0.55**	- 0.49**	- 0.30**	- 0.36**
Streif index						
NDVI	0.80**	0.62**	0.70**	0.63**	0.77**	0.60**
NAI	0.72**	0.71**	0.71**	0.04	0.46**	- 0.10
F690	0.70**	0.59**	0.64**	0.54**	0.67**	0.49**
F730	0.73**	0.64**	0.67**	0.56**	0.66**	0.49**
F690/F730	- 0.57**	- 0.50**	- 0.53**	- 0.46**	- 0.29**	- 0.28**

4 Discussion

A key objective of our study was to assess the potential of non-destructive techniques for detection of senescence based fruit quality changes considering the differences in apple peel pigment content and main fruit quality parameters on the sunlit and shaded sides. Our data clearly show that sunlit and shaded fruit sides of both red and green coloured apple cultivars significantly differ in their chlorophyll content (Fig. 1). Similar results were reported by Merzlyak et al. (2002), who observed a higher amount of chlorophyll in sunlit than in shaded peel of red ‘Zhigulevskoye’ apple, and the opposite tendency in the green apples of ‘Antonovka’. These differences in chlorophyll content distribution on sunlit and shaded sides in red and green coloured

cultivars may be explained by the stronger chlorophyll breakdown on the sunlit sides of the green cultivars. In the red cultivars, anthocyanins, located in the epidermal cells, protect chlorophyll molecules by absorbing a significant amount of the excessive light (Merzlyak and Chivkunova, 2000). It has also been supposed that higher chlorophyll content in sunlit compared to shaded peel of red cultivars is necessary to maintain a sufficient level of photosynthesis under shielding anthocyanins lowering the amount of PAR reaching the chloroplasts (Merzlyak et al., 2002).

Among the internal fruit quality characteristics, fruit firmness showed the most noticeable correlation with chlorophyll content (Tab. 1). Interestingly, fruit firmness was not dependent on the fruit side in both tested cultivars, whereas sunlit and shaded sides differed in their chlorophyll content. The extent of this difference was much more pronounced in 'Jonagold' fruit. For this reason, Pearson's correlation between chlorophyll content and fruit firmness in this cultivar was lower when using the data from both fruit sides compared to that calculated either for sunlit or shaded side (Tab. 1). The same tendency was also found for the relationships between Streif index and chlorophyll content in apple peel calculated for sunlit, shaded or both side data in the two cultivars. These variations therefore should be considered in the models when predicting fruit maturity or quality changes with pigment-based evaluation techniques.

In respect to parameters of the non-destructive chlorophyll detection, the strongest correlation for both cultivars was found between chlorophyll content and NDVI or F730 (Tab. 1). In the green 'Golden Delicious' apples, also NAI displayed a close correlation with chlorophyll content ($r = 0.91$) independent of evaluated fruit side. A less pronounced relationship between NAI and peel chlorophyll was found for the shaded sides of the 'Jonagold' fruit ($r = 0.72$), and no correlation was observed in this variety on the sunlit sides. This is in agreement with the findings of Merzlyak et al. (2003) who reported strong linear relationship between reflectance (R) at 550 and 700 nm in the green-yellow apples, whereas in red coloured fruit, correlation between R550 and R700 was disturbed due to the re-absorption of green light by anthocyanins.

With LIF parameters, fluorescence intensities F690 and F730 proved to be more sensitive to apple peel chlorophyll content than F690/F730 ratio in the tested varieties. This resembles the situation found in the leaf tissues, where F690/F730 index shows a high correlation with the chlorophyll content at chlorophyll levels between 4 (Lichtenthaler and Rinderle, 1988) and 30 $\mu g\ cm^{-2}$ (Gitelson et al., 1998; Tartachnyk and Rademacher, 2003). In leaves with chlorophyll content below 4 $\mu g\ cm^{-2}$, the chlorophyll fluorescence spectra are not influenced by re-absorption of emitted fluorescence (Lichtenthaler and Rinderle, 1988). Therefore, higher Pearson's

coefficients found in our experiment for the absolute fluorescence intensities F690 and F730 may result from the advanced disintegration of chloroplast membranes impairing fluorescence re-absorption by chlorophyll pigment complexes in the apple peel of the tested fruit. The strongest correlation established between F730 and chlorophyll content for fluorescence parameters can be also explained by the fact that the effect of fluorescence re-absorption by chlorophylls at 730 nm is very weak as compared to that at 690 nm (Ramos and Lagorio, 2006).

Non-invasively evaluated parameters showed moderate to strong correlation with fruit firmness and maturity degree of fruit (Tab. 2). The correlation coefficients between the non-destructively evaluated indices of apple peel chlorophyll content and Streif fruit maturity index could be significantly improved in both tested cultivars by taking into respect differences in pigment content and flesh characteristics on the sunlit and shaded apple sides. However, even the best correlation of $r = 0.8$ established in our studies seems to be insufficient for a reliable non-destructive determination of fruit firmness and maturity. In addition, relationship between chlorophyll content and fruit firmness is cultivar-specific and may depend on management practices as well as environmental conditions during the growing season. For this reason, an adequate non-invasive assessment of internal fruit quality may be difficult when using only techniques based on pigment content detection. On the other hand, recent findings indicate that estimation of rates of changes of specific fruit quality parameters often provides more information on advancement of fruit maturity than their absolute values (personal communications, Christian Peereboom Voller S., 2007). Our results clearly show that under shelf life conditions, rate of changes in fruit firmness and maturity are generally consistent with the rates of chlorophyll breakdown in apple peel. The major advantage of the methods employed in our study is the very rapid and non-invasive mode of monitoring.

One of the specific questions addressed in this study was whether the anthocyanin pigmentation affects the chlorophyll fluorescence signals. In our experiment, blush areas of ‘Jonagold’ displayed higher NDVI and LIF values resulting from higher chlorophyll content under super-imposed anthocyanin pigmentation (Fig. 1). Furthermore, the correlation coefficients between chlorophyll content and NDVI or LIF parameters were at the same level if calculated for sunlit, shaded and both sides (Tab. 1). Thus, evaluation of chlorophyll content by LIF with red excitation light appeared not to be affected by super-imposed red coloration. This is consistent with the findings of Merzlyak et al. (2003) who reported for the apples with up to 50 nmol cm^{-2} anthocyanin in the peel a very weak or no anthocyanin absorption at the

wavelengths between 650 and 750 nm. Our results, therefore, extend previous studies on chlorophyll detection (Zude-Sasse et al., 2002) and clearly document that in red coloured apple cultivars, in which visual estimation of changes in ground coloration is difficult, senescence induced chlorophyll breakdown can be detected by both remission and fluorescence techniques.

Figure 4, presenting fluorescence recording along the equatorial line of 'Jonagold' apple, clearly visualises higher chlorophyll content in the patches with anthocyanin pigmentation.

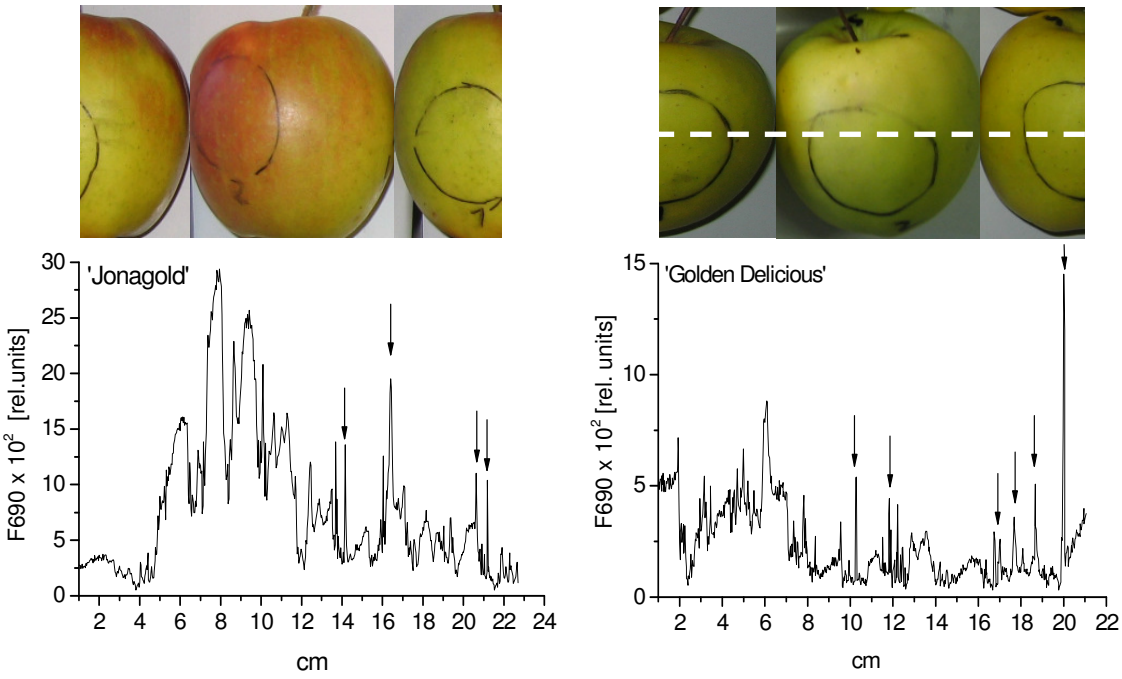

Fig. 4: Chlorophyll fluorescence at 690 nm (F690) as recorded along the equatorial line of representative 'Jonagold' (sampling date: 23.10.06) and 'Golden Delicious' (sampling date: 02.11.06) apple fruit. The dynamic high frequency (5 kHz) fluorescence measurements were started on the shaded and completed on the sunlit fruit sides as shown in the photographs above. Arrows indicate fluorescence peaks originating from the peel lenticels.

In red cultivars, such technique could be an option for automatic estimation of the proportion of red surface colour, an important classification criterion in fruit marketing. The capability of such measurements for assessing this attribute has to be proven in further studies also with fruit of other cultivars varying in their anthocyanin and chlorophyll content.

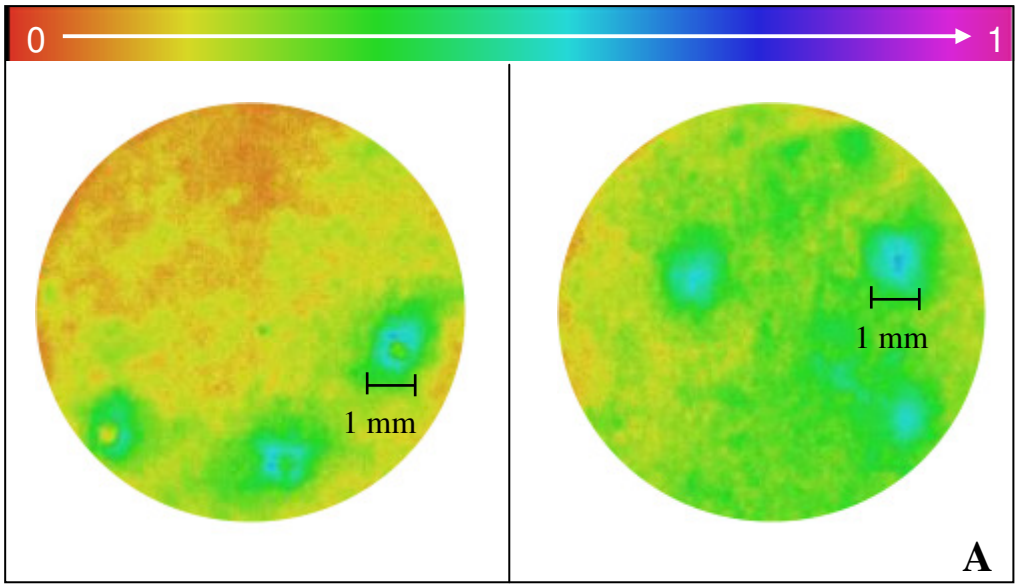

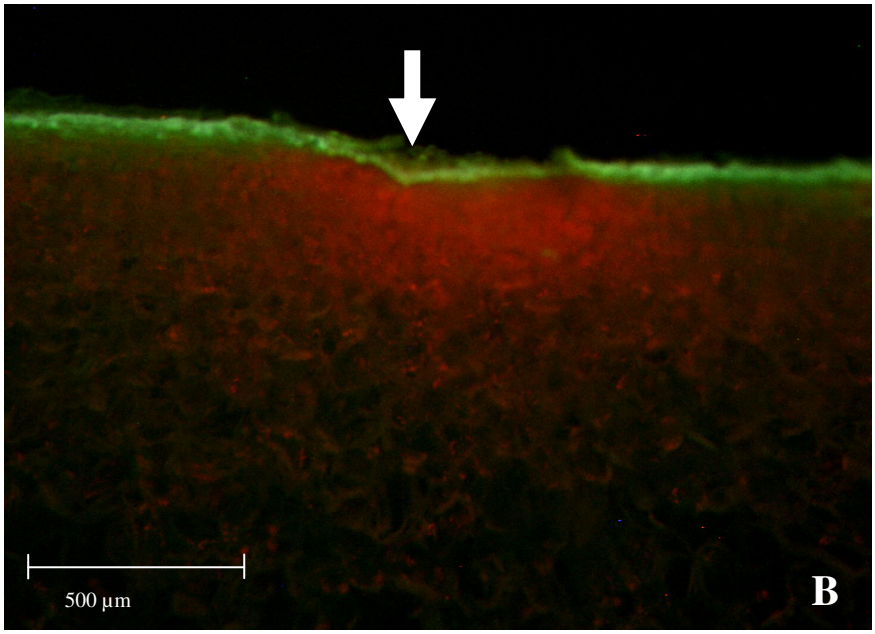

Fig. 5

A: Maximum fluorescence (Fm) images captured on the physiological upper (left) and lower (right) sides of apple peel discs punched out of 'Golden Delicious' fruit. Regions underneath and around lenticels display stronger fluorescence reflecting higher chlorophyll content in these areas.

B: Light microscope fluorescence image of apple peel cross-section (cv. 'Golden Delicious') in the lenticel area. Arrow shows a lenticel centre. The red chlorophyll fluorescence is concentrated underneath the peel lenticel, whereas in the surrounding area chlorophyll is degraded.

Interestingly, spatial resolution of dynamic fluorescence recordings revealed extremely high chlorophyll fluorescence intensities in the millimetre dimension of lenticel spots in both cultivars (Fig. 4). These distinct fluorescence peaks were attributed to higher chlorophyll content in these areas.

PAM fluorescence images of the apple peel also displayed higher Fm in the lenticel areas under blue (470 nm) excitation light (Fig. 5A) confirming enhanced chlorophyll contents in regions around these structures. The fluorescence microscope images of peel cross-sections revealed distinctly more chloroplast containing tissue underneath the lenticels (Fig. 5B). Such enhanced formation of chloroplasts may provide more effective photosynthetic assimilation in the parenchyma surrounding lenticels as the sites of CO_2 supply to fruit at the early stages of fruit development. Another reason of chlorophyll accumulation under lenticels may be delayed chloroplast breakdown underneath screening corky structures in the advanced stages of fruit ripening or senescence. Thus, 'multipoint' scanning fluorescence recording represents a highly sensitive tool for the detection of fruit spatial heterogeneity.

5 References

Blanke, M.M. 1992. Determination of chlorophyll using DMSO. Wein-Wissenschaft **47**, 32-35.

Chen, P. and Nattuvetty, V.R. 1980. Light transmittance through a region of an intact fruit. Transaction of the ASAE **23**, 519-522.

De Long, J.M., Prange, R.K., Leyte, J.C. and Harrison, P.A. 2004. A new technology that determines low-oxygen thresholds in controlled-atmosphere-stored apples. HortTechnology **14**, 262-266.

Gitelson, A.A., Buschmann, C. and Lichtenthaler, H.K. 1998. Leaf chlorophyll fluorescence corrected for re-absorption by means of absorption and reflectance measurements. Journal of Plant Physiology **152**, 283-296.

Hagen, S.F., Solhaug K.A., Bengtsson, G.B., Borge, G.I.A. and Bilger, W. 2006. Chlorophyll fluorescence as a tool for non-destructive estimation of anthocyanins and total flavonoids in apples. Postharvest Biology and Technology **41**, 156-163.

Kingston, C.M. 1992. Maturity indices for apple and pear. Horticulture Reviews **13**, 407-432.

Knee, M. 1972. Anthocyanin, carotenoid, and chlorophyll changes in the peel of Cox`s Orange Pippin apples during ripening on and off the tree. Journal of Experimental Botany **23**, 184-196.

Kramer, E. 2005. Risk management in the supply chain for fresh fruit and vegetables. In: Improving the safety of fresh fruit and vegetables, edited by W. Jongen (Abington Cambridge: Woodhead Publishing Ltd), pp. 179-228.

Lichtenthaler, H.K. and Rinderle, U. 1988. The role of chlorophyll-fluorescence in the detection of stress conditions in plants. CRC Critical Reviews in Analytical Chemistry **19**, 29-85.

Lichtenthaler, H.K. and Babani, F. 2004. Light adaptation and senescence of the photosynthetic apparatus. Changes in pigment composition, chlorophyll fluorescence parameters and photosynthetic activity. In: Chlorophyll a Fluorescence: A Signature of Photosynthesis, edited by G.C. Papageorgiou and Govindjee (Springer, The Netherlands), pp.713-736.

Limbrunner, B. and Maidl, F.-X. 2007. Non-contact measurement of the actual nitrogen status of winter wheat canopies by laser-induced chlorophyll fluorescence. In: Precision Agriculture ´07: Proceedings of the 6th European Conference on Precision Agriculture, edited by J.V. Stafford (Wageningen Academic Publishers, Netherlands), pp. 173-179.

Merzlyak, M.N. and Chivkunova, O.B. 2000. Light-stress-induced pigment changes and evidence for anthocyanin photoprotection in apples. Journal of Photochemistry and Photobiology B-Biology **55**, 155-163.

Merzlyak, M.N., Solovchenko, A.E. and Chivkunova, O.B. 2002. Patterns of pigment changes in apple fruit during adaptation to high sunlight and sunscald development. Plant Physiology and Biochemistry **40**, 679-684.

Merzlyak, M.N., Solovchenko, A.E. and Gitelson A.A. 2003. Reflectance spectral features and non-destructive estimation of chlorophyll, carotenoid and anthocyanin content in apple fruit. Postharvest Biology and Technology **27**, 197-211.

Moran, R. 1982. Formulae for determination of chlorophyllous pigments extracted with N,N-Dimethylformamide. Plant Physiology **69**, 1376-1381.

Noh, H.K. and Lu, R. 2005. Hyperspectral reflectance and fluorescence for assessing apple quality. ASAE Paper No. 053069.

Peng, Y. and Lu, R. 2006. Improving apple fruit firmness predictions by effective correction of multispectral scattering images. Postharvest Biology and Technology **41**, 266-274.

Quartin, V., Ramalho, J.C., Ramos, A.P. and Barreiro, M.G. 2004. Chlorophyll fluorescence as a non-destructive indicator for optimal harvest date of "Bravo de Esmolfe" apples. In: Livro de Actas do IV Simpósio Ibérico I Nacional VII Espanol de Maturação e Pós-Col eita, Oeiras Portugal Outubro 7-9 2004, edited by M.G. Barreiro, pp. 121-125.

Ramos, M.E. and Lagorio, M.G. 2006. A model considering light reabsorption processes to correct *in vivo* chlorophyll fluorescence spectra in apples. Photochemical and Photobiology Sciences **5**, 508-512.

Saure, M.C. 1990. External control of anthocyanin formation in apple. Scientia Horticulturae **42**, 181-218.

Schreiber, W. 1986. Continuous recording of photochemical and non-photochemical chlorophyll fluorescence quenching with a new type of modulation fluorometer. Photosynthesis Research **10**, 51-62.

Solomakhin, A.A. and Blanke, M.M. 2007. Overcoming adverse effects of hailnets on fruit quality and microclimate in an apple orchard. Journal of the Science of Food and Agriculture **87**, 2625-2637.

Solovchenko, A.E., Avertcheva, O.V. and Merzlyak, M.N. 2006. Elevated sunlight promotes ripening-associated pigment changes in apple fruit. Postharvest Biology and Technology **40**, 183-189.

Song, J., Deng, W., Beaudry, R.M. and Armstrong, P.R. 1997. Changes in chlorophyll fluorescence of apple fruit during maturation, ripening and senescence. HortScience **32**, 891-896.

Sowinska, M., Deckers, T., Eckert, C., Heisel, F., Valcke, R. and Miehe, J.-A. 1998. Evaluation of nitrogen fertilization effect on apple-tree leaves and fruit by fluorescence imaging. In: Advances in Laser Remote Sensing for Terrestrial and Hydrographic Applications: Proceedings of the SPIE Vol. 3382, edited by R.M. Narayanan and J.E. Kalshoven, pp. 100-110.

Streif, J. 1996. Optimum harvest date for different apple cultivars in the 'Bodensee' area. In: The Postharvest Treatment of Fruit and Vegetables: Determination and Prediction of Optimum Harvest date of Apple and Pears, ECSC-EC-EAEC, 1996 (Brussels), edited by A. de Jager, D. Johnson and E, Hohn, pp. 15-20.

Tartachnyk, I. and Rademacher, I. 2003. Estimation of nitrogen deficiency of sugar beet and wheat using parameters of laser induced and pulse amplitude modulated chlorophyll fluorescence. Journal of Applied Botany **77**, 61-67.

Tartachnyk I., Rademacher I. and Kühbauch W. 2006. Distinguishing nitrogen deficiency and fungal infection of winter wheat by laser-induced fluorescence. Precision Agriculture **7**, 281-293.

Zude, M., Herold, B., Roger, J-M., Bellon-Maurel, V. and Landahl, S. 2006. Non-destructive tests on the prediction of apple fruit flesh firmness and soluble solids content on tree and in shelf life. Journal of Food Engineering **77**, 254-260.

Zude, M., Birlouez-Aragon, I., Paschold, P-J. and Rutledge, D.N. 2007. Non-invasive spectrometric sensing of carrot quality from harvest to consumption. Postharvest Biology and Technology **45**, 30-37.

Zude-Sasse, M., Truppel, I. and Herold, B. 2002. An approach to non-destructive apple fruit chlorophyll determination. Postharvest Biology and Technology **25**, 123-133.

F Summary and conclusion

The key objective of this work was to assess the potential of selected chlorophyll fluorescence techniques for detection of temporal and spatial changes in leaf and plant response to economically important stress factors as a basis for implementing these techniques in 'Precision Farming'. Early detection and visualisation of fluorescence patterns upon infection with leaf rust (*Puccinia triticina*) and powdery mildew (*Blumeria graminis*) was studied at the single leaf level on wheat (*Triticum aestivum* L.) by means of Pulse-Amplitude-Modulated (PAM) fluorescence imaging. The necessity of previous dark-adaptation of plant material for reliable stress detection was investigated. The approach of 'multipoint' scanning laser-induced fluorescence (LIF) was applied for detection and discrimination of biotic (leaf rust and powdery mildew*)* and abiotic (nitrogen deficiency) stress factors in the light at wheat leaf and canopy level. In order to avoid misinterpretation of fluorescence signals in 'Precision Farming', the effect of enhanced UV-B radiation on LIF and PAM parameters was studied in detail in apple (*Malus domestica* Borkh.) leaves. An additional objective of this thesis was to investigate the capability of LIF and light-remission techniques for detecting senescence-induced heterogeneities in apple (cvs 'Jonagold' and 'Golden Delicious') peel chlorophyll content and internal fruit quality characteristics under shelf life conditions.

1. PAM fluorescence imaging enabled pre-symptomal pathogen detection and visualisation of spatial differences during proceeding *Blumeria graminis* and *Puccinia triticina* infections at the individual leaf level. The early detection was possible 2-3 days before visual symptoms and significant changes in NDVI became apparent. The initial infection of both fungi caused an increase in Fo and decreases in Fv/Fo and Fv/Fm. The appearance and development of fungal pustules was accompanied by reduction in Fo and Fm. This resulted mainly from lower absorption of fluorescence exciting light by the leaf mesophyll due to the shielding effect of fungal mycelium, and to lesser extent from the chlorophyll breakdown underneath pustules. Among the evaluated fluorescence parameters, Fv/Fo displayed the most pronounced response to both kinds of infection. Mildew infection influenced chlorophyll fluorescence neither in the direct vicinity of mycelium, nor in the apparently healthy leaf regions. Rust infected plants, in contrast, displayed significantly reduced photochemical efficiency Fv/Fm and Fv/Fo in chlorotic tissue around pustules. The same, but less pronounced tendency was found in the apparently healthy regions of rust infected leaves in the last days

of experiment. Dark adaptation of leaves proved to be necessary for accurate detection of both pathogen infections by means of fluorescence imaging. Additional experiments are needed to estimate the potential of this technique for 'Precision Farming'.

2. The 'multipoint' scanning LIF technique reveals spatial differences in fluorescence values at leaf and canopy level. F690/F730 was tendentiously lower on the abaxial leaf sides in all treatments. Throughout the experiment, N-deficient wheat plants displayed lower chlorophyll content and increased F690/F730 ratio. Pathogen infected plants showed a significantly enhanced fluorescence ratio associated with chlorophyll degradation in the infected areas only after appearance of visual symptoms. The results of cross-validation analysis indicated that with LIF measurements, samples with pathogen infections may be miss-recognised as N-deficiency and vice versa. However, considering standard deviations of F690 and F730 recordings in addition to their mean values significantly improved the identification accuracy of N-deficiency and leaf rust infection at both leaf and canopy level. Further studies are still needed to develop the LIF technique for early detection and discrimination of biotic and abiotic stresses.

3. The exposure of apple leaves to UV-B doses in the range of 10-26 W m^{-2} for 180 minutes (*UV-B_{BE}* dose = *5.4-14 kJ m^{-2}*) affected neither chlorophyll content nor leaf reflection. Although UV-B damage was not visually evident 2 hours after irradiation, it could be detected by PAM and LIF fluorescence techniques with equivalent success. The intensity of LIF, estimated as the integral of fluorescence spectrum, was reduced after UV-B irradiation by 19-30%. A stronger decrease in F686 compared to F740 fluorescence resulted in significantly lower F686/F740 values in all UV-B treatments. Apple leaves displayed a strong and significant reduction in maximum fluorescence (Fm) and a slightly increase in ground fluorescence (Fo) 2 hours after UV-B treatment, as documented by PAM fluorescence measurement. Negative linear regressions between investigated UV-B doses and selected PAM parameters were found. Among the PAM and LIF parameters tested, the Fv/Fo ratio appeared most sensitive for detection of UV-B induced damages displaying greatest changes and strongest correlation with the applied UV-B doses. PAM fluorescence images of apple leaves visualised an enhanced spatial heterogeneity of photosynthetic activity with increasing UV-B dose. The disturbance in photosynthetic functionality was followed by a continuous recovery process as indicated by restoring Fo and Fm parameters. A decline in

maximum photochemical efficiency Fv/Fm from 0.80 to 0.72 and 0.43 after exposure to 20 W m^{-2} for 240 and 360 minutes (*UV-B_{BE} = 14.4 and 21.6 kJ m^{-2})*, respectively, was followed by recovery at 7 x 10^{-4} and 5 x 10^{-3} units per hour during the first 48 hours after UV-B treatment. The recovery curves of Fm, Fv, Fv/Fm and Fv/Fo parameters during a week after UV-B irradiation were well fitted with exponential rise to maximum function, such as: $y = y_o + a\,(1 - e^{-bx})$. However, within 7 days after exposure to UV-B light, apple leaves displayed 14% or 4% lower Fm, and 5% or 1% lower Fv/Fm values compared with control plants, indicating only a partial recovery from photoinhibition and irreversible damages in PS II. These findings have to be taken into account for applying these techniques in 'Precision Farming'.

4. Changes in ground colour of apple fruit could be successfully monitored by LIF and light-remission techniques, whereas among the investigated parameters Normalised-Differenced-Vegetation-Index (NDVI) and fluorescence emission at 730nm showed the strongest correlation with peel chlorophyll content (r= 0.87-0.93). The intensity of red pigmentation of apples could be estimated by light remission Normalised-Anthocyanin-Index (NAI). Since the occurrence of anthocyanin pigmentation was accompanied by increased concentration of underlying chlorophyll, red patches of 'Jonagold' displayed higher NDVI, F690 or F730 and lower F690/F730 values than those apparently green. The 'multipoint' scanning mode of LIF provides information on fruit colour heterogeneity. Among internal fruit quality parameters, the strongest correlation with the apple peel chlorophyll content was found for fruit firmness. For the green 'Golden Delicious', there were no differences in the Pearson's coefficients calculated for the data from sunlit (r = 0.78), shaded (r = 0.77) or both sides (r = 0.77). For 'Jonagold', in contrast, r calculated for the data from both fruit sides was lower (r = 0.65) as compared to those from sunlit (r = 0.74) or shaded (r = 0.76) sides due to the different chlorophyll content and same firmness values on the sunlit and shaded sides of this cultivar. The correlation coefficients between the non-destructively evaluated indices of apple peel chlorophyll content and Streif fruit maturity index could be significantly improved in both tested cultivars by considering differences in pigment content and flesh characteristics on the sunlit and shaded apple sides. Thus, the investigated methods are ideal for sensitive and rapid monitoring of senescence-induced changes in peel chlorophyll and may enhance the accuracy of non-invasive external and internal fruit quality evaluation.

Acknowledgements

I wish to express my gratitude to Prof. Dr. G. Noga given me the chance to work on this interesting topic and integrating me in his research group. Moreover, many thanks for his support and guidance during my studies and for allowing my research trip to the 'Centro de Pomáceas' at the University of Talca (Chile).

I am grateful to PD Dr. E.-C. Oerke for his willingness to act as my co-supervisor and for his outstanding readiness as the speaker of the DFG research training group 722.

Many thanks to Dr. I. Tartachnyk for her advice and assistance and for critical reviewing the manuscripts.

Special thanks to PD Dr. M Schmitz-Eiberger for her advice and help at any time.

I am greatly thankful to all my colleagues particularly T. Kraemer and Dr. M. Hunsche for the close and friendly collaboration and their assistance during the preparation of this thesis.

I thank all the staff members of the Department of Horticulture of the University of Bonn for their cooperation and help in conducting the experiments.

Many thanks to the German Research Foundation (DFG-Graduiertenkolleg 722) for their financial support and to Fritzmeier GmbH & Co KG for providing the MiniVegN fluorescence system for my studies.

Finally, I would like to thank my family for their continuous support and encouragement.